UNIVERSITY OF BIRMINGHAM

# $NH_3$ Exhaust Gas Fuel Reforming for Diesel Engine Decarbonisation & Lean NOx Abatement over Silver/Alumina Catalyst

**By**

**Wentao Wang**




A thesis submitted to

The University of Birmingham for the degree of:

**DOCTOR OF PHILOSOPHY**

Department of Mechanical and
Manufacturing Engineering
School of Engineering
University of Birmingham
April 2014

# ABSTRACT

The following thesis focuses on the potential roles and applications of ammonia in transportation area, where ammonia is applied i) as a hydrogen carrier involved in a catalytic reforming process for $H_2$ production, ii) in its reformed form i.e. $H_2$ – $NH_3$ mixture for improved $NH_3$ combustion in CI engines (as a carbon – free energy carrier), and iii) as a reductant in engine emission abatement under the incorporation of the NH3 reforming mechanism and catalytic aftertreatment systems.

To implement the study, $NH_3$ was firstly applied in a system of exhaust gas reforming under diesel engine operation. The use of thermochemical recovery of the exhaust waste heat through autothermal reforming mechanism with ammonia decomposition produced $H_2$ – $NH_3$ contented reformate that is free of carbon.

Different amounts of $NH_3$ reformate, either produced or simulated, were sent back to the engine to replace part of the hydrocarbon fuel. The results showed that, under an intensive combustion of the $H_2$ content, the $NH_3$ combustion could be thermally promoted and contribute to significant reductions in $CO_2$, CO, THC and PM.

Following the above, the $H_2$ – $NH_3$ reformate's ignition, combustion and their effectiveness in carbon removal were further strengthened by a liquid ignition improver i.e. diethyl glycol diethyl ether (DGE), using the DGE's superior ignition properties and high oxygenation. While the enhanced $NH_3$ and $H_2$ oxidations inevitably formed NOx, the use of DGE's was even shown to suppress the engine NOx formation via its featured low temperature combustion.

Due to the fact that the reformate combustion could result in unburned $NH_3$ and $H_2$, a potential of associating these exhaust reformate with the engine emission such as NOx in a diesel aftertreatment system was revealed. Therefore, both of the produced and simulated $NH_3$ reformate were applied with real diesel exhaust over an $Ag/Al_2O_3$ – Selective Catalytic Reduction (SCR) unit. This resulted in simultaneous $NH_3$ – SCR and HC – SCR under $H_2$ assistance. Over 90 % of NOx reduction was obtained at low temperature and lean burn condition.

Finally, to prove the $H_2$ assisted $NH_3$ - SCR over $Ag/Al_2O_3$ is associated with and improved by a $NO_2$ initiated intermediate mechanism i.e. $NH_3/NO_2/NO$ – or "Fast" – SCR, increased $NO_2$ in the SCR catalyst was achieved using the $NH_3$ and $H_2$ mixture (in the form of $NH_3$ reformate) and/or a use of Diesel Oxidation Catalyst (DOC) before the SCR catalyst. The results confirmed the $NO_2$ was essential over the $Ag/Al_2O_3$ for low temperature NOx abatement, where part of the "$H_2$ effect" was to promote the silver catalyst's on – site $NO_2$ formation, which in turn strengthened the $NH_3$'s performance in the SCR process.

# Acknowledgement

I would like to express my deep sense of gratitude to my supervisors Dr. Athanasios Tsolakis and Dr. Karl Dearn, for their guidance, experience and encouragement during my PhD study, without them, a lot would be unachievable.

I'm also grateful to Dr. Jose Martin Herreros for his advice, patience and technical assistance to my research. The same is for all of the colleagues (friends) in the Future Power System Group.

The University of Birmingham and Department of Mechanical and Manufacturing Engineering are acknowledged for the provision of a PhD scholarship for the duration of my study

A lot of thanks are given to Dr. Andrew York and our colleagues at Johnson Matthey Technology Centre, Reading – UK, for the supply of the catalysts used in this research and for their useful suggestions, advice and technical expertise throughout the experimental work. Shell Global Solutions UK is acknowledged as well for the fuels used in this research.

At last but not least, I would like to give my sincere thanks to my wife Xiaoxi Zhang and my parents Junmin Wang and Li Miao, for their yeas of invaluable support, care and love, without these, this thesis would have been impossible.

**Wentao Wang**

**April 2014**

# CONTENTS


CHAPTER 1: INTRODUCTION ..... 1
1.1 Background ..... 1
1.2 Research objectives ..... 5
1.3 Thesis outline ..... 6
CHAPTER 2: LITERATURE REVIEW ..... 10
2.1 Diesel engine operation ..... 10
2.2 Diesel emissions ..... 13
2.2.1 NOx formation ..... 13
2.2.2 Particulate Matter (PM) ..... 15
2.2.3 Hydrocarbon emission ..... 17
2.2.4 CO and $CO_2$ emission ..... 18
2.3 Emission Control Technologies ..... 20
2.3.1 Exhaust Gas Recirculation ..... 20
2.3.2 Aftertreatment ..... 24
2.3.2.1 Diesel oxidation catalyst ..... 24
2.3.2.2 Diesel Particulate Filter ..... 26
2.3.2.3 Catalytic reduction of NOx ..... 29
2.3.2.4 Ammonia and Urea SCR ..... 30
2.3.2.5 Hydrocarbon SCR ..... 32
2.3.2.6 $H_2$ assisted $NH_3$ – SCR over $Ag/Al_2O_3$ ..... 35
2.4 Alternative fuel/fuel substitution and dual fuel mode in diesel combustion ..... 37
2.4.1 Biodiesel and oxygenated fuels ..... 38
2.4.2 Hydrogen ..... 41
2.4.2.1 Hydrogen combustion ..... 41
2.4.2.2 Hydrogen storage ..... 43
2.4.2.3 Hydrogen on – board production ..... 44
2.4.3 $NH_3$ and its potential vehicular applications ..... 47
2.4.4 Ammonia production and carbon/energy balance ..... 53
2.4.4.1 $NH_3$ production from biomass ..... 54
2.4.4.2 Ammonium ($NH_3$ + $NH_4^+$) recovery from human and animal waste ..... 56
2.5 Summary ..... 60
CHAMPTER 3: EXPERIMENTAL SETUP ..... 62
3.1 Test engine instrumentation ..... 62
3.2 Data Processing ..... 63
3.3 Catalysts ..... 65
3.4 Mini Reactor Setup ..... 66
3.5 Diesel Fuel ..... 69
3.6 Exhaust Gas Analysis and Measuring Equipment ..... 69
CHAPTER 4: AMMONIA AS A HYDROGEN CARRIER FOR TRANSPORTATION; INVESTIGATION OF THE AMMONIA EXHUAST GAS FUEL REFORMING ..... 73

4.1 Introduction ..... 73
4.2 $NH_3$ decomposition over Ru – $Al_2O_3$ catalyst ..... 76
4.3 Combined $NH_3$ oxidation and decomposition: $NH_3$ – ATR and $NH_3$ exhaust gas reforming 79
4.3.1 Temperature profiles ..... 79
4.3.2 $NH_3$ conversion and $H_2$ production. ..... 81
4.4 Reforming efficiencies ..... 83
4.5 Summary ..... 85
CHAPTER 5: COMBUSION OF $NH_3$ REFORMATE ON DIESEL OPERATION; THE IMPACTS IN ENGINE PERFORMANCE AND EMISSIONS ..... 87
5.1 Introduction ..... 87
5.2 The impact of small amount of reformate on engine combustion and emission ..... 89
5.3 Effects on engine combustion and emission using reformate simulated at larger amounts ..... 95
5.3.1 Engine combustions under large amount of reformate additions ..... 95
5.3.2 Engine emissions under high amount of reformate addition ..... 102
5.4 Summaries: ..... 108
CHAPTER 6: IMPROVED $H_2$ – $NH_3$ REFORMATE COMBUSTION FOR EFFECTIVE DIESEL ENGINE DECARBONISATION THROUGH USE OF DGE AS AN IGNITION ENHANCER ..... 110
6.1 Introduction ..... 110
6.2 Liquid fuel replacement ..... 113
6.3 Combustion characteristics ..... 114
6.4 Unburned gaseous additions and brake thermal efficiency ..... 118
6.5 Gaseous emissions ..... 120
6.6 Particulate matter emissions ..... 123
6.7 Summaries ..... 126
CHAPTER 7: $H_2$ – $NH_3$ REFORMATE ASSISTED LEAN NOx ABATEMENT OVER SILVER/ALUMINA CATALYST ..... 127
7.1 Introduction ..... 127
7.2 $H_2$ assisted $NH_3$ – HC – SCR ..... 130
7.3 Influence of $NH_3$:NOx ratio on the SCR reactions ..... 133
7.4 Influence of the $C_1$:NOx ratio on the SCR reactions ..... 137
7.5 Influence of NOx concentration in the SCR reactions ..... 141
7.6 Summaries ..... 144
CHAPTER 8: INCREASED $NO_2$ CONCENTRATION IN THE DIESEL ENGINE EXHAUST FOR IMPROVED $H_2$ – $NH_3$ – SCR ACTIVITY OVER $Ag/Al_2O_3$ CATALYST ..... 147
8.1 Introduction ..... 147
8.2 NO to $NO_2$ conversion through $H_2$ addition over DOC ($Pt/Al_2O_3$) ..... 151
8.3 NO to $NO_2$ conversion through $H_2$ addition over $Ag/Al_2O_3$ for $NH_3$ – SCR reaction ..... 153
8.4 SCR activity at low reaction temperature (< 200 ℃) with increased $NO_2$ concentration ..... 155
8.5 SCR activity at high reaction temperature with increased $NO_2$ concentration ..... 159
8.6 Summaries ..... 162
8.7 Appendix ..... 164
CHAPTER 9: CONCLUSIONS ..... 166

LIST OF AUTHOR'S PUBLICATIONS AND AWARDS.....173

REFERENCE.....174

# LIST OF FIGURES

**Figure 1.1:** European emission standards for passenger cars (EEC, 1993; EC, 1994; EC, 1996; EC, 1998a; EC, 1998b; EC, 2002; EC, 2007)……..2

**Figure 2.1:** The phases of combustion of direct injection compression ignition engine……..…..11

**Figure 2.2:** EU $CO_2$ emissions: (a) EU overall GHG emissions against the transport emissions, (b) $CO_2$ emissions in various sectors and (c) sources of $CO_2$ in transportation sectors……...19

**Figure 2.3:** Equivalence ratio – temperature region of diesel soot precursor formation……23

**Figure 2.4:** Diesel particulate filter…….....26

**Figure 2.5:** Reaction mechanisms for $H_2$ assisted HC – SCR and $NH_3$ – SCR over $Ag/Al_2O_3$……..37

**Figure 2.6:** Exchanging the glycerol compounds of the triglycerides molecules for lighter compounds from the lighter alcohols……..38

**Figure 2.7:** Combined urea storage and $NH_3$ – $H_2$ generator/separator system……..51

**Figure 2.8:** $CO_2$ emission life cycle assessment of ammonia and petroleum being used in vehicular application. Adapted from: S. Ishimatsu, T. Saika and T. Nohara; Ammonia Fueled Fuel Cell Vehicle: The New Concept of a Hydrogen Supply System; SAE International, 2004 – 01 – 1925…….…53

**Figure 2.9:** The flat membrane system adopted in poultry house for ammonium recovery; adapted from M. J. Rothrock Jr., A. A. Szogi and M. B. Vanotti; Recovery of ammonia from poultry litter using flat gas permeable membranes; Waste Management, 2013. 33(6): p. 1531 – 1538……58

**Figure 2.10:** Microbial fuel cell (MFC) system for ammonium recovery and energy production from urine; adapted form P. Kuntke et al, Ammonium recovery and energy production from urine by a microbial fuel cell; Water Research, 2012. 46: p. 2627 – 2636…….….59

**Figure 3.1:** Engine instrumentation……...…….…....62

**Figure 3.2:** Detailed reactor/reformer setup and its schematic diagram……..….....67

**Figure 4.1:** Experimental setup for $NH_3$ exhaust gas reforming……..…...…….....75

**Figure 4.2:** $NH_3$ decomposition over $Ru – Al_2O_3$ catalyst: (a) 2 l/min (GHSV = 18000 $h^{-1}$) of pure ammonia decomposed at different temperatures, (b) 2 – 4 l/min of pure ammonia

decomposition at different GHSV, and (c) ammonia conversion at different $NH_3$ concentrations in the $NH_3 – N_2$ mixtures and temperatures……76

**Figure 4.3:** Temperature profiles: (a) and (b) temperature profiles of $NH_3$ - ATR over 8g and 16g catalyst beds (c) temperature profiles of $NH_3$ exhaust gas reforming over 16g catalyst bed…....79

**Figure 4.4:** (a) $NH_3$ conversion in $NH_3$ – ATR at different $O_2/NH_3$ ratios over 8g and 16g catalysts; dotted line: 16g catalyst, solid line: 8g catalyst. (b) – (d): $H_2$ production as a function of $NH_3$ concentration and $O_2/NH_3$ ratio; (b) $NH_3$ – ATR over 8g catalyst, (c) $NH_3$ –ATR over 16g catalyst and (d) $NH_3$ exhaust gas reforming over 16g catalyst……..…81

**Figure 4.5:** $NH_3$ exhaust gas reforming Process efficiencies…….....……84

**Figure 5.1:** Experimental setup for large amount of simulated $NH_3$ reformate applied in diesel combustion……...…89

**Figure 5.2:** Engine in-cylinder pressure and rate of heat release at different reformate (produced) additions……..….90

**Figure.5.3:** Engine performance and emissions under different $NH_3$ reformate (produced) additions: (a) engine brake thermal efficiency, (b) diesel fuel replacement, (c) $CO_2$ emissions, (d) total hydrocarbon emission, (e) CO emissions…….…..……..91

**Figure 5.4:** Engine NOx emissions under produced reformate additions: (a) $NO_2$ and NO emissions, (b) $N_2O$ emission…….……..92

**Figure 5.5:** Diesel fuel replacement by different $H_2$ and $NH_3$ additions…….....…..….95

**Figure 5.6:** Coefficient of variation of IMEP under the $H_2$ and $NH_3$ additions at engine load condition of (a) 5 bar IMEP and (b) 3 bar IMEP……..96

**Figure 5.7**: In – cylinder pressure and ROHR of the combustions with different additions of $H_2$ and $NH_3$: (a) at 5 Bar IMEP and (b) at 3 Bar IMEP……98

**Figure 5.8:** Engine brake thermal efficiencies and different combined additions of $H_2$ and $NH_3$……100

**Figure 5.9:** Unburned $H_2$ and $NH_3$ with different combined additions of $H_2$ and $NH_3$: (a) $H_2$ and (b)
$NH_3$…….....101

**Figure 5.10:** NOx emissions obtained at different combined $H_2$ and $NH_3$ additions: (a) NO, (b) $NO_2$ and (c) $N_2O$……102

**Figure 5.11:** Carbonaceous emissions with different combined $H_2$ and $NH_3$ additions: (a) $CO_2$, (b) CO and (c) THC……104

**Figure 5.12:** Particulate size distributions for the selected combinations of $H_2$-$NH_3$-diesel combustion (a) number concentration at 5bar IMEP, (b) mass concentration at 5bar IMEP, (c) number concentration at 3bar IMEP, (d) mass concentration at 3bar IMEP…….106

**Figure 5.13:** PM emissions at selected combined $H_2$ and $NH_3$ additions…….107

**Figure 6.1**: Liquid fuel replacement by different $H_2$ and $NH_3$ additions……..113

**Figure 6.2**: In – cylinder pressure and ROHR of the combustions of diesel and DGE blends with (a) separate additions of $NH_3$ and $H_2$ and (b) simultaneous addition of $NH_3$ and $H_2$, the flow rates for $NH_3$ and $H_2$ are 14 and 15 l/min respectively……..…114

**Figure 6.3:** coefficient of variation of IMEP obtained from the combustions with different combinations $H_2$ and $NH_3$; (a) diesel and (b) DGE20……..…….117

**Figure 6.4:** Unburned gaseous additions (exhaust emissions) of (a) $NH_3$ and (b) $H_2$ at different fuelling conditions…….…118

**Figure 6.5:** Engine brake thermal efficiency for the different fuelling……...….……119

**Figure 6.6:** Proposed combustion pattern enhanced $NH_3$ and $H_2$ combustion with DGE…….…...119

**Figure 6.7**: (a) NOx (NO + $NO_2$) emission of diesel and DGE blends with $NH_3$ addition; (b) NOx (NO + $NO_2$) emission of diesel and DGE blends with $NH_3$ and $H_2$ additions……..120

**Figure 6.8:** Engine carbonaceous emissions under different fuelling; (a) $CO_2$, (b) CO and (c) unburned total hydrocarbons (THC)……..121

**Figure 6.9**: (a) – (c) PM mass concentrations of standard diesel and DGE blend with different $H_2$ and $NH_3$ additions: (a) diesel, (b) DGE20 and (c) DGE40. (d) – (f) PM number distributions…123

**Figure 6.10:** PM emissions of standard diesel and DGE blends with different $H_2$ and $NH_3$ additions…….124

**Figure 7.1:** Equipment configuration for combined $NH_3$ reformer and $Ag/Al_2O_3$ SCR system..129

**Figure 7.2:** Conversion of NOx (730 ppm exhaust NOx fixed at catalyst inlet), $NH_3$ and THC (constant engine exhaust THC produced at 430 ppm) in the SCR process: (a) with engine exhaust only; (b) with engine exhaust and 8000 ppm $H_2$; (c) with engine exhaust and 720ppm simulated $NH_3$ reformate, $NH_3$:NOx =1; (d) engine exhaust and produced reformate $NH_3$ (720 ppm) and $H_2$ (8000 ppm)……131

**Figure 7.3:** (a) NOx (730 ppm exhaust NOx fixed at catalyst inlet, and constant engine exhaust HC produced at 430 ppm) and $NH_3$ conversions at different levels of simulated $NH_3$reformate ($NH_3$/NOx ratios); (b) THC conversions at different levels of simulated $NH_3$ reformate……134

**Figure 7.4:** Effect of different levels of $NH_3$ reformate (both simulated and produced, where 8000 ppm of $H_2$ reformate was fixed) on the SCR process, a) $NO_2$ production and b) concentration of the unconverted $NH_3$ at each $NH_3$ feed level……135

**Figure 7.5:** $NH_3$ and THC concentration effects on: (a) NOx conversion, (b) CO production, (c) $NH_3$ conversion and (d) THC conversions……138

**Figure 7.6:** NOx reduction and exhaust components during the start – stop hydrocarbon transient injection: (a) NO reduction, (b) CO concentration, (c) $NO_2$ concentration and (d) $NH_3$ concentration……139

**Figure 7.7:** Transient (a) NOx conversion (engine exhaust NOx fixed at 730 ppm), (b) CO detection and (c) converted THC during passive HC – SCR, with use of 20 % EGR (increased $C_1$:NOx ratio), with use of EGR and simulated $H_2$ reformate (fixed at 8000 ppm) and the use of EGR and simulated $NH_3$ (200 ppm) – $H_2$ (8000 ppm) reformate……142

**Figure 8.1:** Experimental setup for combined reformer and SCR rector in diesel exhaust loop……149

**Figure 8.2:** Effect of hydrogen addition over the DOC on (a) outlet temperature; (b) HC conversion and (c) NO to $NO_2$ conversion and the changes to the overall $NO_2$/NO ratio at the DOC outlet……152

**Figure 8.3:** Concentration after the SCR catalyst under various $H_2$ additions without $NH_3$ (a) $NO_2$ and (b) CO……153

**Figure 8.4:** Concentration after the SCR under various NH3 additions with a fixed H2 addition (a) $NO_2$ and (b) $NH_3$……154

**Figure 8.5**: Emissions at 3 Bar IMEP, (a) NOx conversions with and without the increased $NO_2$ concentration (b) $NO_2$ detected downstream the SCR vs. the $NO_2$ being available at the SCR inlet, and (c) the experimentally observed NO and total NOx reduction vs. the calculated (based on Fast – SCR stoichiometry) NOx reduction……...156

**Figure 8.6:** NOx conversion at 2 Bar IMEP at SCR catalyst inlet temperature of 180 ˚C (a) 2000, 4000 and 8000 ppm $H_2$ addition upstream SCR; (b) experimental and calculated (based on Fast – SCR stoichiometry) NOx conversion at 2000 and 4000 ppm $H_2$ addition……...159

**Figure 8.7** (a) and (b): with different temperature and $NO_2$ level (inlet) over the SCR catalyst, the NOx conversions at (a) 3 Bar IMEP and (b) 2 Bar IMEP; (c) experimental and calculated (based on Fast – SCR stoichiometry) NOx conversion at 3 Bar IMEP, (d) NOx conversion at 4 Bar IMEP……160

**Figure 8.8:** $NH_3$ detected after the SCR catalyst at 2 Bar IMEP load condition……162

**Figure A8.1:** NOx and exhaust HC conversions over the temperature ramp with and without the DOC being placed in front of the SCR catalyst ……164

# LIST OF TABLES

**Table 2.1:** General overview of EGR effects on engine NOx and PM emission……...22

**Table 2.2:** Comparison of ammonia with other fuels including hydrogen (adapted from C. Zamfirescu and I. Dincer, Ammonia as a green fuel and hydrogen source for vehicular applications. Fuel Processing Technology, 2009. 90(5): p. 729-737)……51

**Table 2.3:** Further comparison of ammonia with other fuels based on the data listed in Table 2.2.....51

**Table 2.4:** Net energy use and $CO_2$ emission for ammonia production via biomass gasification and conventional Haber – Bosch process……..……..55

**Table 3.1:** Test ULSD composition……69

**Table 3.2:** Specifications of MKS MultiGas 2030 FTIR analyser……...……..70

**Table 3.3:** Detection limits of MKS MultiGas 2030 FTIR analyser……...……...…70

**Table 3.4:** Measurement range and resolution of AVL DIGAS 440 – non dispersive IR……..71

**Table 4.1:** Test conditions for $NH_3$ – ATR and $NH_3$ exhaust gas reforming……74

**Table 4.2:** Test conditions for $NH_3$ decomposition……75

**Table 5.1:** Reformate flow rates under different reactor conditions and their compositions in the engine intake……87

**Table 5.2:** Reformate flow rates under different reactor conditions and their compositions in the engine intake……...88

**Table 5.3:** Key properties of the gaseous additions……...…….88

**Table 6.1:** Fuel properties of the tested liquid fuel/blend……..……...112

**Table 7.1:** Average engine exhaust composition at 60% full engine load and 1500 rpm……129

**Table A7.1:** Test matrix using different reformate……...…146

**Table A8.1:** Engine conditions and average emissions……...….164

**Table A8.2:** Summaries of conditions in each experimental run……..165

# LIST OF NOTATIONS

| Symbol | Unit | |
|---|---|---|
| $\dot{m}_p$ | kg/s | Mass flow rate of the combustion products |
| $\dot{m}_{fuel}$ | kg/s | Mass flow rate of the combustion fuel supplies |
| $\dot{V}_E$ | $cm^3/s$ | Intake air volumetric flow rate under EGR induction |
| $\dot{V}_O$ | $cm^3/s$ | Intake air volumetric flow rate with no EGR induction |
| $LCV_{fuel}$ | MJ/kg | Lower calorific value of the combustion fuel |
| $LCV_p$ | MJ/kg | Lower calorific value of the combustion products |
| $P_b$ | kW | Engine brake power |
| $P_{Ind}$ | kW | Engine Indicated Power |
| GHSV | $h^{-1}$ | Gas Hourly Space Velocity |
| $V_d$ | $m^3$ | Displaced Cylinder Volume |
| N | rps | Engine Speed |
| $\eta_c$ | % | Engine combustion efficiency |
| $\eta_{th}$ | % | Engine brake thermal efficiency |

# LIST OF ABBREVIATIONS

| | |
|---|---|
| A/F | Air to Fuel Ratio |
| $Ag/Al_2O_3$ | Silver Supported on Alumina |
| $AgNO_3$ | Silver Nitrate |
| ATR | Auto – Thermal Reforming |
| BTDC | Before Top Dead Centre |
| BDC | Bottom Dead Centre |
| BOC | British Oxygen Company |
| BSFC | Brake Specific Fuel Consumption |
| BTE | Brake Thermal Efficiency |
| C | Atomic Carbon |
| CAD | Crank Angle Degree |
| cDPF | Catalysed Diesel Particulate Filter |
| $CH_3COO$- | Acetate Anion |
| $CH_3NO_2$ | Nitromethanes |
| CH4 | Methane |

| | |
|---|---|
| CI | Compression Ignition |
| CN | Cetane Number |
| CO | Carbon Monoxide |
| CO2 | Carbon Dioxide |
| $CO(NH_2)_2$ | Urea |
| COV | Coefficient of Variation |
| CPSI | Cells per Square Inch |
| CRT® | Continuously Regenerating Trap |
| Cu-ZSM5 | Copper Supported on Zeolite |
| DGE | Diethyl glycol diethyl ether |
| DI | Direct Injection |
| DMA | Differential Mobility Analyser |
| DOC | Diesel Oxidation Catalyst |
| DPF | Diesel Particulate Filter |
| EGR | Exhaust Gas Recirculation |
| EOC | End of Combustion |

| | |
|---|---|
| EOI | End of Injection |
| EU | European Union |
| FAME | Fatty Acid Methyl Ester |
| FID | Flame Ionisation Detection |
| GC | Gas Chromatograph |
| GHG | Greenhouse Gas |
| $H_2$ | Hydrogen |
| $H_2O$ | Water |
| HC | Hydrocarbon |
| HC:NOx | Hydrocarbon to NOx ratio |
| HC – SCR | Hydrocarbon Selective Catalytic Reduction |
| IC | Internal Combustion |
| IMEP | Indicated Mean Effective Pressure |
| ISFC | Indicated Specific Fuel Consumption |
| MK1 | Swedish Low Sulphur Environmental Classified Diesel Fuel |
| $N_2$ | Nitrogen |

| | |
|---|---|
| $N_2O$ | Nitrous Oxide |
| NDIR | Non-Dispersive Infra-Red |
| $NH_3$ | Ammonia |
| $NH_3$ – SCR | Ammonia Selective Catalytic Reduction |
| NO | Nitric Oxide or Nitrogen Monoxide |
| $NO_2$ | Nitrogen Dioxide |
| NOx | Nitrogen Oxides |
| O | Atomic Oxygen |
| $O_2$ | Oxygen |
| $O^{2-}$ | Oxygen Species |
| $OH^-$ | Hydroxyl Radicals |
| PAH | Polycyclic Aromatic Hydrocarbon |
| PM | Particulate Matter |
| POx | Partial Oxidation |
| ppm | Parts Per Million |
| Pt | Platinum |

| | |
|---|---|
| $Pt - Al_2O_3$ | Platinum Supported on Alumina |
| REGR | Reformed Exhaust Gas Recirculation |
| Rh | Rhodium |
| ROHR | Rate of Heat Release |
| SCR | Selective Catalytic Reduction |
| SI | Spark Ignition |
| SMPS | Scanning Mobility Particle Sizer |
| $SO_2$ | Sulphur Dioxide |
| SOC | Start of Combustion |
| SOF | Soluble Organic Fraction |
| SOI | Start of Injection |
| SRR | Steam Reforming |
| TCD | Thermal Conductivity Detector |
| TDC | Top Dead Centre |
| THC | Total Hydrocarbon |
| ULSD | Ultra Low Sulphur Diesel |

| | |
|---|---|
| $V_2O_5$ | Vanadium Oxide |
| VOF | Volatile Organic Fraction |
| WGS | Water Gas Shift |

# CHAPTER 1: INTRODUCTION

## 1.1 Background

Current energy consumption relies mostly on fossil fuels, yet depletion of oilfields and detrimental emissions to the environment became worldwide issues. One major example is the use of internal combustion (IC) engines. While the IC engines are regarded commonly as the most efficient and applicable power production technology for the worlds' energy demand, its rapid application has been recognised as one of the reasons that caused the current oil crisis and raised a concern of global warming due their $CO_2$ emissions (Atadashi, Aroua et al. 2010, Wang, Ge et al. 2013). Therefore, IC engines equipped with fuel – efficient technologies to achieve better fuel economy and less $CO_2$ emission is of the primary interest and calling for a large amount of research strength.

Having the merits of good fuel – efficiency, high torque output and long work durability, the use of diesel operation in recent years has become increasingly popular in both commercial and passenger services. Furthermore, as coupled with modern engine technologies such as turbo – charging (Siwale, Kristóf et al. 2013), variable valve timing (VVT) and advanced injection strategy (Li, Xu et al. 2014, Zhuang, Qiao et al. 2014), the demand for diesel passenger cars has increased significantly over the past decade.

However, the diesel engine featured lean combustion in excess oxygen drives the formation of nitrogen oxides ($NO_x$) (Jiménez-Espadafor, Torres et al. 2012). Apart from that, carbonaceous particle materials (PM) are also produced due to the nature of the combustion process (Tan, Hu et

al. 2007). These emissions and their negative impacts on human health and environment excite the ever stringent emission standards (e.g. EURO, FTP and Japan emission standards). As shown in Fig. 1.1, the trend of cutting down the major emissions from the passenger cars has increased enormously in the European standards over the last two decades.

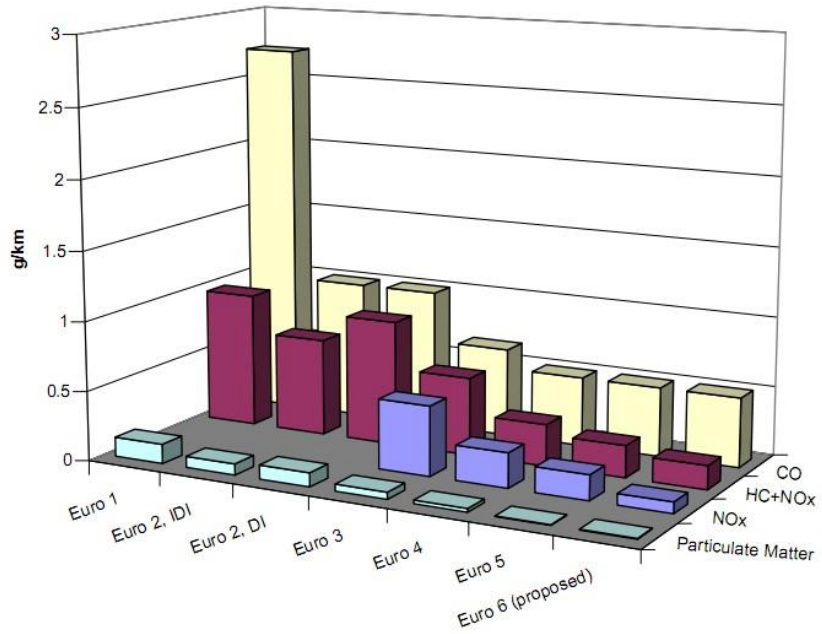


**Figure 1.1:** European emission standards for passenger cars (EEC, 1993; EC, 1994; EC, 1996; EC, 1998a; EC, 1998b; EC, 2002; EC, 2007)

In addition, although the individual fuel consumption is able to be reduced per unit car by the newly equipped technologies, the increased demand of the total vehicle units, especially in those developing countries such as China and India, can be inferred to render the technologies' fuel benefit on saving the net fossil fuel in a global scale.

Hence, fuel alternatives that are provided with less carbon content (or not at all), not derived from the fossil feedstock and proved to maintain a similar engine performance can be deduced to be one of the most appropriate materials to help in resolving the energy and environment problems.

For the above reasons, $NH_3$ could be regarded as a potential alternative in vehicular applications and its combustion in IC engine can be referred back to 1940's, during the World War II (Zamfirescu and Dincer 2008). Nevertheless, without specially modified engine designs, the $NH_3$'s combustion is often flawed with lack of efficiency and high ammonia emission/slippage, especially in the compression ignition engines (Zamfirescu and Dincer 2009).

From another point of view, $NH_3$ is provided with large hydrogen content, whose gaseous form has long been demonstrated as a potential fuel alternative for IC engines for the purposes of combustion improvement and emission control i.e. reductions in HC, CO, $CO_2$, Particulate Matter and NOx (Senthil Kumar, Ramesh et al. 2003, Tsolakis, Megaritis et al. 2005). In addition, hydrogen has also been proven to enhance the performance of some engine aftertreatment systems, such as SCR, DOC and diesel particulate filter (DPF). However, while the $H_2$'s beneficial impacts are increasingly observed, its vehicular applications are barricaded by the problems that arise from hydrogen's less developed delivery and handling infrastructure and ineffective on – board storage method (Ahmed and Krumpelt 2001) In contrast, $NH_3$ has been used as a fertilizer in the agricultural industry for more than a century, whose distribution network was fully matured (Zamfirescu and Dincer 2008). In addition to that, $NH_3$'s on – board application on today's heavy

duty vehicle is already adopted in a form of urea for diesel engine's lean NOx control i.e. $NH_3$/urea – SCR (Zamfirescu and Dincer 2011).

Therefore, a vehicle on – board $H_2$ production that uses $NH_3$ as a source could be a viable approach to solve the above $H_2$ production and storage problems. Nonetheless, the currently adopted method for extracting gaseous $H_2$ from $NH_3$ is ammonia thermal decomposition reaction, whose sustainable activity happens at a temperature often higher than 500 ℃ and with a capable catalyst. Hence regarding the exhaust waste heat as the only convenient heat source in a vehicle, then the reaction may not be sustained in diesel operation as the exhaust temperature is usually ranged from 150 – 400 ℃. Apart from that, although separate studies on $NH_3$ and $H_2$ combustions were largely recorded for CI engine applications, less information was acquired on the combustion of the combined $NH_3$ and $H_2$ (as a possible form of the $NH_3$ reforming product). The interplay between the $H_2$ and $NH_3$ and the corresponding effects in a CI type of combustion is rarely studied. The same is also true for the diesel aftertreatment, where the impacts of the reformed $NH_3$ such as on the SCR catalyst for reaction's conversion efficiency, selectivity and low temperature performance are all of interest to be found out.

## 1.2 Research objectives

The aim of this research is to, first of all, find a feasible approach to run the catalytic $NH_3$ decomposition in a thermally self – sustainable way, which is able to be applied on a vehicle to fulfill the vehicle's on – board $H_2$ demand. Secondly, the reformed ammonia (expected to be a $H_2$ – $NH_3$ mixture) is to be applied as a carbon – free fuel alternative in CI combustion with partial diesel substitution. Thirdly, an investigation of the $NH_3$ reformate used in diesel aftertreatment i.e. silver ($Ag/Al_2O_3$) SCR catalyst will be conducted for engine lean NOx control. Hence with such an arrangement, the potential roles of $NH_3$ in vehicular applications, namely, a hydrogen carrier (for fuel reforming), a fossil fuel alternative and energy carrier (for combustion) and a catalytic reductant (for aftertreatment) can be assessed in a comparative and systematic way.

The research's main objectives and approaches are listed as the following:

1. To implement the ammonia decomposition for engine applications, the research work examines the feasibility of combining an endothermic $NH_3$ decomposition reaction with an exothermic $NH_3$ oxidation using engine exhaust as the primary source of oxygen and reaction heat. Hence with the thermochemical heat recovery and the oxidative mechanism of $NH_3$, the overall reaction is expected to have a similar feature to that of an autothermal reforming reaction. Any influential reaction parameters will be identified; their impacts on the product composition (i.e. $H_2$ purity) and the reforming efficiencies will be analysed.

2. To study the engine performance, combustion characteristics and emissions from the combustion of $NH_3$ reformate; identifying any interaction or synergic effect between the $H_2$ and $NH_3$ combustions.

3. To study the application of $NH_3$ reformate (e.g. $H_2$ and unconverted $NH_3$) used as a reductant or enhancer in catalytic reduction of emissions. In the presented work the influence of actual and simulated reformates ($H_2$ and $NH_3$) is studied in enhancing the $Ag/Al_2O_3$ SCR catalyst in reducing $NO_x$ emissions through the promotion of a "Fast – SCR" like mechanism. This is to be achieved by increasing $NO_2$ availability in the SCR catalyst with the application of reformate directly onto the SCR catalyst and/or by the use of a DOC catalyst that is introduced upstream the SCR catalyst.

## 1.3 Thesis outline

The thesis consists of nine chapters. A brief description of every chapter is given below:

- **Chapter 2 Literature Review:**

In this chapter, a background of diesel engine operation, engine exhaust emissions and emissions control strategies are briefly introduced. Two alternative fuels and energy carriers, namely $H_2$ and $NH_3$ are considered. In addition, their sources, production methods and associations with vehicular application are discussed as well

- **Chapter 3 Experimental Setup:**

The diesel engine, experimental facilities, gas (exhaust) analysers and catalysts used in the research are detailed

- **Chapter 4 Ammonia as hydrogen carrier for transportation; investigation of ammonia exhaust gas reforming for $H_2$ production**

In this chapter, the exhaust gas reforming of $NH_3$ for producing gaseous hydrogen is conducted over $Ru/Al_2O_3$ pellets inside a prototype reformer (reactor). The $NH_3$ decomposition and oxidation are combined under different $O_2/NH_3$ ratio and gas – hourly – space – velocity (GHSV), determined by the amount of exhaust gas induction. The reaction's thermal behavior, i.e. an autothermal reaction pattern is demonstrated and proved by means of taking temperature records of the catalyst bed. All these parameters can be associated to give a systematic analysis of the reformate compositions and correspondingly the reforming efficiencies.

- **Chapter 5 Combustion of $NH_3$ reformate in diesel engines; the impacts on engine performance and emissions:**

In this chapter, the $NH_3$ reformate produced or simulated by means of bottled gas is sent back to the engine at various engine conditions for partial diesel replacement. The influence of the reformate on engine combustion and emissions are recorded and analysed, and are compared to those of the standard diesel, pure $H_2$ and $NH_3$.

- **Chapter 6: Improved $H_2$ – $NH_3$ reformate combustion for effective diesel engine decarbonisation through use of DGE as an ignition enhancer**

For the purpose of enhancing the reformate combustion, diethyl glycol diethyl ether (DGE) is applied as an ignition and combustion improver due its large oxygenation and superior ignition properties. Different levels of DGE are blended into the diesel to accompany the various amounts of $NH_3$ reformate (simulated with different compositions) during the combustion process.

- **Chapter 7: $H_2$ – $NH_3$ reformate assisted lean NOx abatement over Silver/Alumina catalyst**

An integrated system of $NH_3$ exhaust gas reforming and $Ag/Al_2O_3$ SCR is applied for lean NOx reduction. The $NH_3$ – $H_2$ contented reformate is supplied to the SCR catalyst as the reductant/co – reactant for the $H_2$ – assisted $NH_3$ SCR reaction. Since the simultaneous presences of $H_2$ and HCs are in the engine exhaust as well, a parallel reaction of HC – SCR is obtained. The association between both of the SCR reactions and their combined effect on affecting the NOx reductions are investigated.

- **Chapter 8: Increased $NO_2$ concentration in diesel engine exhaust for improved $H_2$ – $NH_3$ – SCR activity over $Ag/Al_2O_3$**

The $H_2$ assisted $NH_3$ – SCR reaction is revealed to perform partially in a route of fast SCR i.e. $NO_2/NO$ – SCR, where the NO oxidative activation to $NO_2$ over the $Ag/Al_2O_3$ is revealed as an essential reaction step. However, the low temperature $NO_2$ formation on $Ag/Al_2O_3$ is shown to be restricted. Hence, a platinum loaded diesel oxidation catalyst (DOC) is employed and combined into the exhaust system to externally enhance the $NO_2$ concentration that is needed in the SCR

reaction. The results show improved SCR performance (NOx conversion) is achieved at lower temperature and with reduced $H_2$ addition over the $Ag/Al_2O_3$ catalyst.

- **Chapter 9: Conclusions**

A conclusion of the core findings in above sections is presented. Further recommendations on the research work are also given.

# CHAPTER 2: LITERATURE REVIEW

## 2.1 Diesel engine operation

Being provided with high compression ratio and lean fuel operation, diesel engines are inherently given more thermodynamic advantages over their rivals, namely the spark ignition engines.

In a direct – injection (DI) diesel engine, only air is taken during the intake stroke. This is until the air is compressed during the compression stroke, which ensures the engine can utilise an increased compression ratio, whilst the fuel is introduced into the cylinder at almost the exact point (i.e. auto – ignition temperature) at which it is required to ignite. The injected diesel travels downwards and undergoes the processes of fuel atomisation, entraining the intake air, and rapid fuel vaporisation to form a sheath – like air/fuel mixture layer along the sides of the jet. High compression ratio tends to improve the fuel evaporation and air – fuel mixing in a considerably reduced space along with the adiabatic heat of compression. Since the compressed air is at a temperature higher than that needed for the fuel's ignition, the fuel with air contact starts to oxidise spontaneously after a short period of ignition delay. With additional hot air kept entraining into the mixture, the rate of oxidation (combustion) increases and reaction products under partial oxidation are formed. Around the cloud of the products, a subsequent diffusion flame sheath is formed at a temperature reaching over 2700 K. The entrained air during the premixed combustion will be depleted eventually and the mixing – controlled combustion in a quasi – steady flame will continue to proceed till the end. The excess $O_2$ taken into the cylinder helps the combustion to be

more complete, whilst the higher compression ratio enables the engine to extract more mechanical energy during the expansion stroke (Heywood 1988, Flynn, Durrett et al. 1999, Stone 1999).

To describe and analyse the above combustion process, the rate of heat release (ROHR) calculated from the in – cylinder pressure is employed. Since the ROHR represents the rate at which chemical energy (heat) is extracted from the fuel, therefore from a chemical point of view the ROHR can be regarded as the rate of reaction. One typical rate of heat release diagram for a direct injection engine is illustrated in Fig. 2.1.

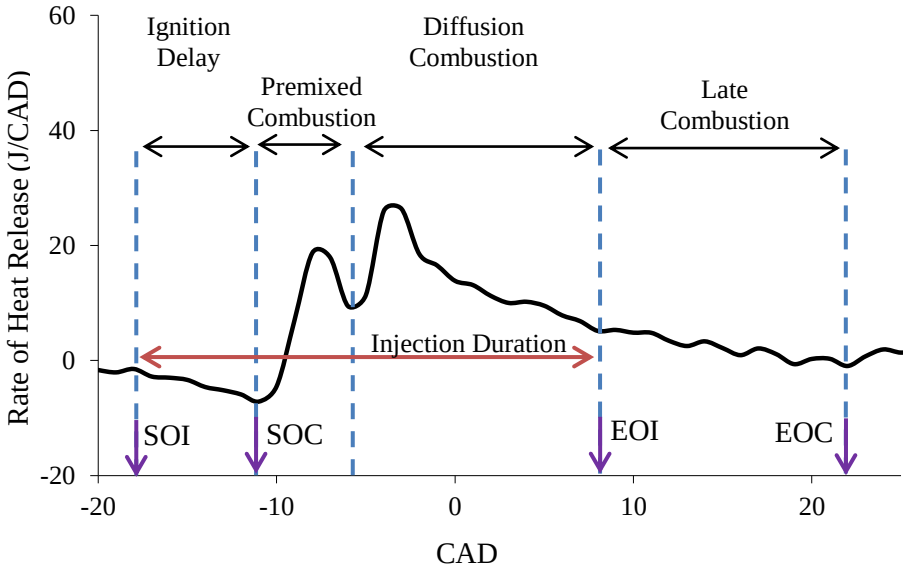


**Figure 2.1:** the phases of combustion of DI CI engine

Shown by Fig. 2.1, there are four main stages in the combustion process, which are:

1) Ignition delay: this stage occurs at fuel vaporisation (appearance of the negative ROHR i.e. heat adsorption), presenting the period between the start of fuel injection (SOI) and the start of combustion (SOC). The SOC is indicated by the first positive ROHR
2) Premixed combustion stage: after the ignition delay, the fuel mixed with air burns rapidly. This is as a result of the injected fuel had time to be mixed with air, so that the air – fuel mixture reaches its flammability limit and burns within a few crank angle degree (CAD). The premixed combustion proceeds while the fuel injection is still ongoing, so the injected fuel is entering the hot burning mixture and being combined to release the heat. This contributes to the characterised sharp ROHR increase in this typical combustion phase.
3) Mixing controlled/diffusion combustion phase: at this stage, bulk fuel burning commences. As being different to the premixed combustion, where fuel burns instantaneously, the heat release rate here in this stage is controlled when the mixtures becoming ready to burn. The diffusion phase finishes when the ROHR is approximately zero during the expansion stroke i.e. end of injection (EOI).
4) Late combustion phase: this combustion stage extends to the expansion stroke, demonstrating the heat released by small portion of fuel that is remained unburned or from the combustion products (e.g. CO) that is further oxidising.

## 2.2 Diesel emissions

When oxidation reaction proceeds within the diesel operation, the combustion process not only produces substance such as $CO_2$, $H_2O$ and $H_2$, but also forms other unwanted species that generally known as pollutants. These undesired species are categorised into three phases, which consist of solid (dry carbon or soot or namely particulate matters), liquid (unburned hydrocarbons and lubricating oils) and gas matters (CO, $CO_2$ gaseous HCs, NOx and sulphur oxides) (Heck and Farrauto 2001).

### 2.2.1 NOx formation

Nitrogen oxides are featured gaseous species in diesel engine exhaust, which are formed by nitric oxide (NO) and nitrogen dioxide ($NO_2$), and are perhaps the most important engine out emission because of their intrinsic toxicity and difficulty in abatement.

The formation of NO occurs when nitrogen (relatively small amount) in air reacts with oxygen at high temperature (>1800 K) (Bacha, Blondies et al. 1998). This thermal mechanism was established by Zeldovich (Stone 1999)(expressed by Eq. 2.1 – 2.3) and is regarded as the dominant process responsible for the majority of NOx formation in CI engine, as peak temperature in this type of combustion can be greater than 2000 K.

$$O + N_2 \leftrightarrow NO + N \qquad (2.1)$$

$$N + O_2 \leftrightarrow NO + O \qquad (2.2)$$

$$N + OH \leftrightarrow NO + H \qquad (2.3)$$

Except the thermal mechanism, NO can be produced through the fuel mechanism when oxygenated fuel is applied: the fuel – borne oxygen is equally effective in nitrogen oxidation (Nichols, Thompson et al. 1993).

When temperature falls beneath 1200 K, $NO_2$ is produced from NO by the reaction:

$$NO + HO_2 \leftrightarrow NO_2 + OH \qquad (2.4)$$

Nevertheless, at higher temperature such as those typical of the flame zone, the $NO_2$ is converted back through the reaction:

$$NO_2 + O \leftrightarrow NO + O_2 \qquad (2.5)$$

During the engine combustion, high formation of NO can be found between the ignition and the appearance of peak in – cylinder temperature, where both of the pressure and temperature are high due to the compression of the early burn mixture. When the combustion mixture expands, temperature of the burnt gas decreases. This subsequently reduces the temperature of the fuel – air mixture through burnt gas dilution, resulting in freezing of NO chemistry. This effect proceeds more rapidly in CI engine than in SI engine with much less decomposition of NO occurring.

In addition to the reaction mechanism, it is found the NOx formation is strongly tied up with the flame temperature. Highest NOx concentration is found in slightly rich mixture, where highest flame temperature can be resulted during the oxidation. Apart from that, flame speed is also

revealed as a pivotal factor for NOx production: longer time is allowed for the NOx to form within the lean mixtures, of which lower flame speed is usually provided (Stone 1999).

As reported in the literature (Bosch and Janssen 1988), NOx exert negative impacts to human health. Inhalation of such oxides causes poisonous for the respiratory system, provoking both lung infection and respiratory allergies. In terms of the environmental impacts, NOx is reported to be responsible for the formation of acid rain and the resultant acidification of aquatic systems, ground level ozone (smog), and general atmospheric visibility degradation (Seinfeld and Pandis 1998) .

### 2.2.2 Particulate Matter (PM)

In general, PM is defined as the black smoke trapped when exhaust gases are passed through a sampling or filter medium below 52 ℃ (EPA) or 47 ℃ (EC). Collectively, the particulates (or the black smoke) are composed of soot and other liquid or solid phase matters that are separated in 3 main categories, namely the solid fraction (carbonaceous soot and ash), soluble organic fraction and water particulates.

Soot is mostly in a form of solid carbon particle clusters originated form unburned fuel, which nucleates from the vapour to solid phases in the fuel – rich region (due to the fuel droplet not vapourising and burning) and contributes to more new particles through fragmentation (Ganesan 2008). Recent research on PM reveals the production of soot started from the decomposition of fuel molecule to urge the formation of the first aromatic ring structure (Richter

and Howard 2000). This is followed by a growth of polycyclic aromatic hydrocarbon (PAH) in a particle nucleation stage. Later, the unburned gas phase hydrocarbons i.e. acetylene and PAH are condensed at the soot surface to form soluble liquid or solid phase materials, contributing to an increase of the particulate size. In addition to the unburned fuel, the heavier fractions of the liquid HC are also derived from the engine lubricating oil, forming the soluble organic fraction (SOF) or volatile organic compounds (VOF) that presented in the PM (Tree and Svensson 2007).

Mass analysis of typical particulate from a heavy duty diesel engine shows the composition is: 41 % soot, 14 % sulphate and water, 13 % Ash (from metal compounds of the hydrocarbons) and 32 % SOF that consists of 25 % unburned oil and 7 % unburned fuel with high boiling point (Kittelson 1998).

Based on the aerodynamic diameters, the size and mass distribution of particles can be separated into 3 categories i.e. nuclei – mode (5 – 50 nm diameter range), accumulation mode (50 – 1000 nm) and coarse mode ( > 1000 nm) (Kittelson 1998). Most of the PM generated by the diesel engine is featured with a diameter less than 100 nm (PM10); the formed spherules mostly vary between 15 and 30 nm in diameter. The size/mass of the PM can be changed during combustion. Apart from the aforementioned HC condensation and adsorption onto the soot surface, the PM size and mass can be also increased through coalescence and coagulation of the PMs (when two soot particles collide with one another and coalesce to form one particulate), which serve as well to reduce in PM number (Stone 1999). Furthermore, the growth of PM size can be attributed to agglomeration of several particles. This occurs when a particle stops its

surface growth and starts to contact with other particles. The particles in contact do not coalesce and remain as separate particulate.

Increased nanoparticle emissions are harmful to human health. PM with diameter greater than 10 μm can be filtered by the nasal passages. Any smaller PM can penetrate in to the pulmonary and bronchial system and be retained. PM below 2.5μm is able to penetrate into the lungs, endangering greatly the human health via potential respiratory and cardiovascular diseases (Stone 1999).

### 2.2.3 Hydrocarbon emission

Unburned hydrocarbon can be caused during the combustion from the region where the mixture is too lean, thus oxidation of HC is not proceeding, especially during the ignition delay process (Yu and Shahed 1981). The locally over – lean mixture (thus no auto – ignition) will not support the flame propagation in the cycle. Hence the longer the delayed period, the greater amount of HC will be left. Nonetheless, there is a delayed period below which no more hydrocarbons can be increased. Then, the formation of HC will primarily originate from the fuels retained at the injector nozzle, or due to the flame quenching at the cylinder walls (low temperature) that makes the hydrocarbon to be kept at the crevices regions such as the top of the piston edge and rings.

On the other hand, the locally over – rich mixture (by under mixing the fuel and air) also upsets the combustion, which happens primarily in the late combustion stage when the fuel is

leaving the injector nozzle at very slow velocity. This makes the unburned HC to increase as well (Heywood 1988).

In general, the diesel engine featured lean burn combustion tends to emit low levels of HCs. Nevertheless, increased emission of hydrocarbons become problematic as they are the precursors of photochemical smog and ozone level when reacted with the NOx (Khair and Majewski 2006).

### 2.2.4 CO and $CO_2$ emission

The emission of carbon monoxide (CO) from an IC engine is usually associated with the deficient oxidation of the hydrocarbon material (incomplete combustions) and is mostly derived from the fuel – rich region. Therefore, its formation is determined closely by the fuel/air ratio (Heywood 1988). Diesel combustion is lean with excessive oxygen supply, so that the CO emission is often small and negligible. However, because the mixture during combustion is highly heterogeneous, CO can be produced locally in the combustion chamber.

Since CO is odorless, colorless, noncorrosive and highly toxic, its emission is hardly noticeable and is therefore regarded as extremely dangerous to human health.

In terms of $CO_2$ emission, it is recognised as the major component contributing to the increased "greenhouse gas" level in a global scale. According to a recent report given by the European Commission (Hill, Hazeldine et al. 2009), while $CO_2$ emission is being reduced in sectors such as industry and households, the $CO_2$ emitted from the transportation sector has increased continuously from 1990s (Fig. 2.2a). If this increase is kept going without interference, $CO_2$ in the transport section will surpass all the other sectors' combined to become the major

source of greenhouse gases by 2050 (Fig. 2.2b). From a quantitative analysis (Fig. 2.2c), it is found the road sector, namely the automobiles, accounts for more than 70 % of the $CO_2$ emission in the transportation.

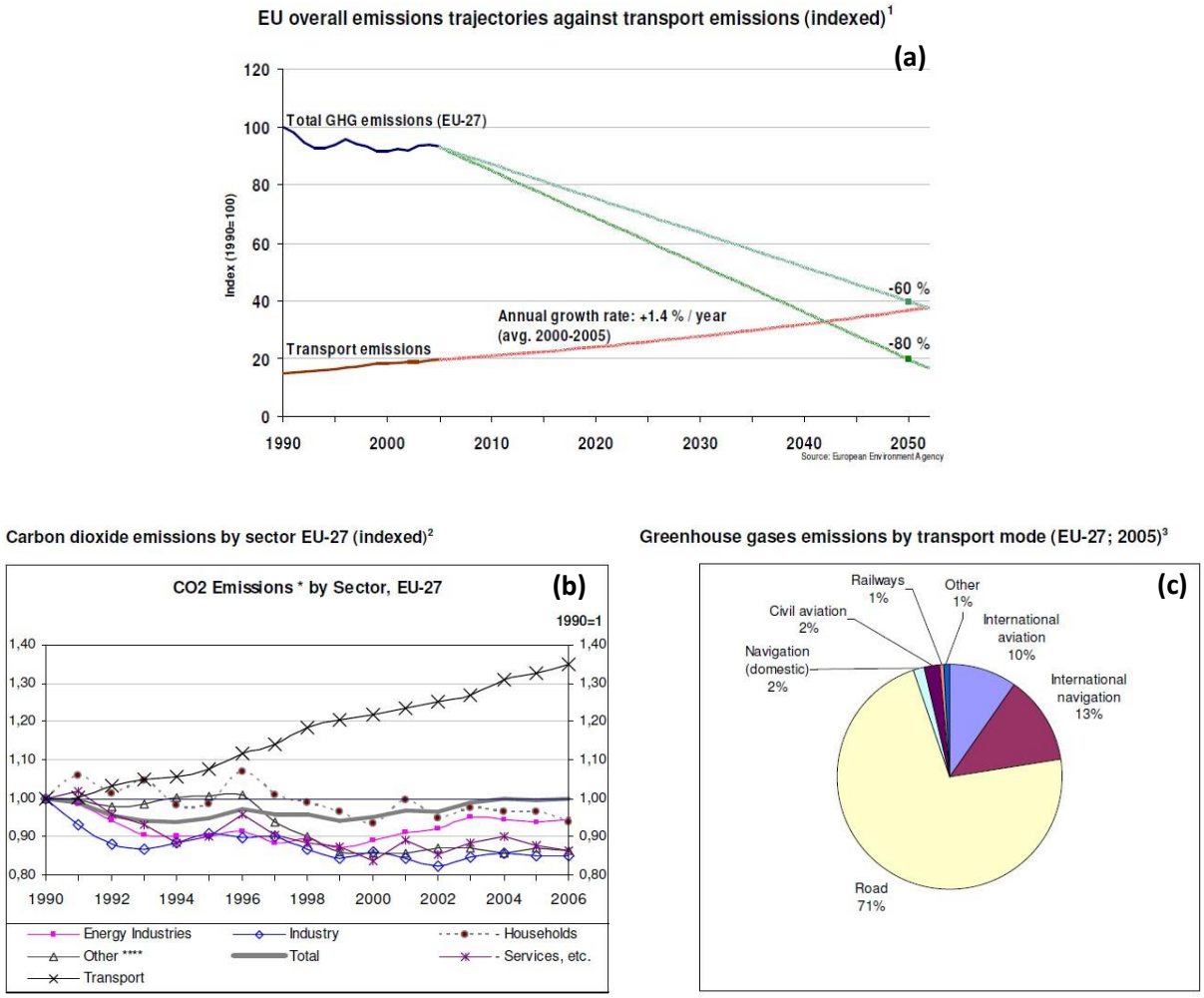


**Figure 2.2:** EU $CO_2$ emissions: (a) EU overall GHG emissions against the transport emissions, (b) $CO_2$ emissions in various sectors and (c) sources of $CO_2$ in transportation sectors

In theory, emission and adsorption of $CO_2$ can be cycled continuously in the ecosystem, used as a compound in photosynthesis for the growth of plants. Nonetheless, the removal of large amounts of natural forest has rendered the strength of natural $CO_2$ adsorption. Therefore, urgent $CO_2$ cut down from the artificial source is of great importance before the climate change deteriorates further.

## 2.3 Emission Control Technologies

In order to fulfill the ever stringent emission legislations, several technologies were developed accordingly for the purpose of emission control. These include exhaust gas recirculation (EGR), soot traps/filters and catalytic vehicle aftertreatment, to serve the engine emission reduction.

### 2.3.1 Exhaust Gas Recirculation

Exhaust gas recirculation is one technology developed for IC engine NOx reduction and has long been proved as a viable and efficient method in commercial practices. The technology uses a fraction of the engine exhaust redirected to the engine intake system through a control valve design. The key strategy was to alternate the thermodynamic properties and the in – cylinder oxygen availability (reduced) of the intake charge whilst maintaining similar engine power and efficiency. With reduced total oxygen concentration per cycle, the formation of NOx is greatly suppressed (Zheng, Reader et al. 2004). The decrease in flame temperature as a result of the large amount of diluents (heat absorbers) induction i.e. $CO_2$, $H_2O$ (water vapour) and $N_2$ from the earlier cycle, also contributes to an overall reduction of the in – cylinder temperature. Therefore,

the presence of EGR restricts the temperature rise from the same amount of heat released. As to keep the constant engine condition (torque and power output), the same fuel quantity must be demanded despite the truth that the temperature and oxygen conditions are both degraded. Thus the induction of EGR often causes emission problems.

On the other hand, it was shown in the literature (Ladommatos, Adelhalim et al. 1998), the lack of oxygen after EGR implementation resulted in retarded ignition delay, which allows a longer delayed period that shifts the whole combustion process more to the engine expansion stroke. This leads to reduced period of time to be spent on the combustion stage that are both provided with high temperature and pressure. In addition to that, the prolonged ignition delay is supposed to increase the amount of fuel being consumed in the premixed combustion stage. Nonetheless, due to the restricted oxygen concentration, the combustion rate of the mixture was reduced instead, contributing to incomplete combustion. Also with the early quenching of the flame on the chamber wall, more incomplete combustion products will be yielded, accompanied by increased fuel consumption.

To summarise the EGR effects, an earlier work of Ladomamatos (1998) separated the EGR influence into three main categories, including the dilution, chemical and thermal effects that come from different components of the EGR influent. Table 2.1 gives a general review of these effects.

**Table 2.1:** General overview of EGR effects on engine NOx and PM emission

| Effect of EGR | Effective EGR components | Main influence of the effective components | Effect on NOx | Effect on PM |
|---|---|---|---|---|
| **Dilution** | $O_2$ | Restricted $O_2$ concentration | 80 – 90 % reduction | 80 – 90% increase |
| **Chemical** | $CO_2$ | Thermal dissociation and participation in the combustion | 5 – 10 % reduction | 5 – 10 % reduction |
| | $H_2O$ | | | 5 – 10 % increase |
| **Thermal** | $CO_2$ | Acting as heat absorbers due to high specific heat capacity | Less than 5 % reduction | Small |
| | $H_2O$ | | | |
| **Inlet Temperature (Hot EGR)** | NA | Increased inlet charge temperature and reduced volumetric efficiency | Increase (proportional to inlet charge temperature) | Increase (proportional to inlet charge temperature) |

According to the results presented in Table 2.1, primary reduction of NOx from EGR incorporation is from the dilution effect via reduced oxygen mass fraction. Minor contributions are received from the chemical and thermal effect.

The results shown in Table 2.1 reveal an important side – effect brought by the use of EGR, namely the NOx/PM trade – off. This is mainly caused by the lack of oxygen, especially when the engine is operated under high load condition. The bulk fuel spray created fuel – rich area, where the hydrocarbon is struggling in finding oxygen to react with (Zheng, Reader et al. 2004). The uncharged radicals and molecules serve as the nucleation precursors, and the soot formation takes place in the diffusion flame, followed by size growth and particle coagulation (Hall-Roberts, Hayhurst et al. 2000).

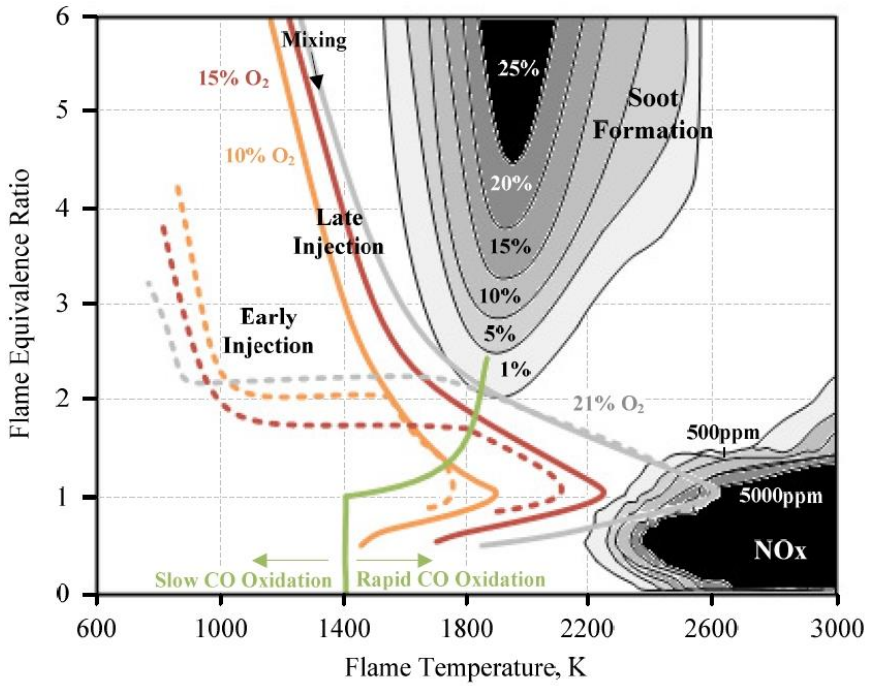


**Figure 2.3:** Equivalence ratio – temperature region of diesel soot precursor formation

Fig. 2.3 details (Johnson 2008) the NOx – soot emissions map against the equivalence ratio and the temperature. Theoretically, clean combustion is achievable through incorporation of high level EGR and both of early and late fuel injections. In the case of advanced injection, condition of soot formation is avoided as much of the fuel charge is mixed with gas before ignition, i.e. eliminating the fuel rich area. In terms of late injection, the charge mixing is accompanied by simultaneous mixture combustion. Therefore, the prolonged mixing and high levels of EGR suppress both of the formation of NOx and soot.

### 2.3.2 Aftertreatment

Aftertreament technologies are mainly applied after the engine (combustion), to reduce the unwanted emissions from the exhaust tailpipe. Common aftertreatment systems include diesel oxidation catalyst (DOC), selective catalytic reduction (SCR) catalyst and diesel particulate filter (DPF). As most of the aftertreatment system is dedicated to one type of emission control, e.g. DOC for carbonaceous removal, SCR for NOx abatement and DPF for PM reduction, a combination of these technologies would be required for multi – task emission control.

The catalyst or filters made for vehicles are usually in a form of ceramic monolith honeycomb with a coated channel walls that contain catalytically active material. The ceramic material is usually made from cordierite ($2MgO.2Al_2O_3.5SiO_2$) that is known to have a low coefficient of thermal expansion, which helps the structure to withstand the high heating rates of the exhaust gas (York, Tsolakis et al. 2010).

#### 2.3.2.1 Diesel oxidation catalyst

Diesel oxidation catalyst plays an important role in diesel engine combustion for control of HC, CO and PM that consists of SOF and volatile organic fraction (VOF). The main reactions proceed over the DOC are usually:

$$CO + \frac{1}{2}O_2 \rightarrow CO_2 \qquad (2.6)$$

$$C_nH_m + \left(n + \frac{m}{4}\right)O_2 \rightarrow nCO_2 + \frac{m}{2}H_2O \qquad (2.7)$$

In addition to the carbonaceous emission reduction, it is also known that oxidation of NO can equally occur over the DOC for a production of $NO_2$ (Eq. 2.8). The $NO_2$ is recognised as a strong low temperature oxidation agent, which is positive for efficient solid soot removal in a subsequent DPF system or for performance enhancement in some SCR system.

$$NO + \frac{1}{2}O_2 \rightarrow NO_2 \qquad (2.8)$$

Since both of the HCs and CO are provided with low light – off temperature, their oxidation are suggested to be achieved under lean air/fuel ratio (Zelenka, Ostgathe et al. 1990). However, at high load operation, the engine tends to reduce the total number of PM but increase the proportion of dry soot, thus increasing the soot/SOF ratio, which is recognised as unfavorable for the oxidation catalyst. On the other hand, increased SOF oxidation can promote the $SO_2$ to $SO_3$ conversion that leads to formation of sulphate, which contributes to sulphur poisoning the catalyst (Heck, Farrauto et al. 2002). Apart from sulphur, Blackman et al. (Blakeman, Andersen et al. 2003) also reported catalyst poisoning can occur through deposit of HC and other carbonaceous species at low exhaust temperature. Hence catalyst designed with high durability and extended resistance to species' poisoning (surface coverage) at low exhaust temperature are required.

The catalytically active materials coated on the DOC are usually noble metal platinum (Pt) or base metal palladium (Pd) layer. The Pt – based DOC catalyst usually expresses higher HC and CO conversion than the later, and it shows resistance to sulphur poising while maintaining good low temperature activity for HC and reasonable SOF conversions (Watanabe, Kawashima et al. 2007). However, as platinum is categorised as a noble metal, its cost is considerably high. For

commercial purpose, Johnson Matthey recently (Watanabe, Kawashima et al. 2007) proposed a combined coating of Pt/Pd that not only enhances the oxidation of unburned HCs and simultaneous sulphur tolerance, but also keeps the catalyst's cost at lower level.

### 2.3.2.2 Diesel Particulate Filter

The technique used to reduce the emission of PM is usually based on a physical filtration system. Currently, the mostly adopted trapping device is in a type of wall flow filter, known as DPF. The device is typically build from aluminum titanate ($Al_2TiO_5$), cordierite or silicon carbide (SiC) (York, Tsolakis et al. 2010), which is made into a honeycomb structure with channels being blocked at alternate ends, as shown in Fig. 2.4.

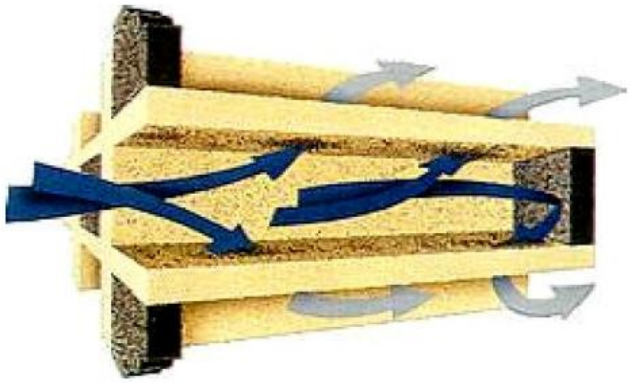

**Figure 2.4:** Diesel particulate filter

To filter the PM, exhaust gas is forcibly passed through the walls, trapping the soot particles within the porous wall and over the inlet channel surfaces (Matti Maricq 2007). Hence the DPF is both effective for reducing the mass and number of the emitted particles

Since the device retains physically the trapped soot, the continuous soot packing and blockage increases the engine backpressure, leading to reduced engine fuel economy. Hence, periodical DPF regeneration is required to remove the filtered soot. The solid carbon species generally require temperatures of approximately 500 to 600 ℃ to oxidise.

Thermal regeneration of the DPF can be done in an exhaust environment with excessive oxygen by burning up the solid soot. However, under high load operation (richer combustion), the strength of the regeneration can be impaired due to reduced oxygen availability. In this case, an auxiliary system is often required to provide additional assistance in the soot regeneration process. This can be chosen from various types including full flow burner, electrical heater or selective heating by microwave technology (Khair 2003).

Alternatively, exhaust $NO_2$ that is continuously emitted from the engine can be utilised over the filter for soot oxidation. This is the basis of the Continuously Regeneration Trap (CRT), which is commonly referred to the passive regeneration. The performance of such system is highly limited by the available amount of $NO_2$ (can be additionally produced by a upstream DOC catalyst) and the temperature of the exhaust stream; ineffective soot removal will be resulted from insufficient NOx and low exhaust temperature, i.e. low engine load operation. Therefore, active regeneration is considered by adding extra heat into the system. This is often made possible by incorporating an upstream DOC with hydrocarbons injections i.e. increasing the catalyst's downstream exhaust temperature (York, Tsolakis et al. 2010). However, high risk of thermal damage to the DPF can be incurred from the high temperature uncontrolled generation of excessive soot loading and/or injected fuel. This damage is often irreversible. Hence, a low

temperature regeneration using the aforementioned $NO_2$ mechanism is usually preferred, combining in the catalytic soot oxidation.

To catalytically oxidise the solid soot, a thin layer of porous washcoat that is made from platinum is usually employed in the DPF design, which is known as the Catalysed Continuous Regeneration Trap (CCRT). The main purpose behind this design is to promote the formation of $NO_2$, as it is a stronger low temperature oxidation agent than $O_2$. Its reported higher rates performance in diesel particulate oxidation can be achieved at temperature as low as 250 ℃ (Allansson, Blakeman et al. 2002). However, deficiency of this catalysed system often occurs when there is a poor contact between the soot and the catalyst layer (loose contact), which weakens the chemical interaction between the materials and thus limits the soot reduction efficiency (Neeft, van Pruissen et al. 1997). Increased contact between the soot and the catalysed monolith channel is reported when adopting copper (Cu), potassium (K) and molybdenum (Mo).

According to Ehrburger et al. (Ehrburger, Brilhac et al. 2002), mechanisms of $O_2$ and $NO_2$ on carbonaceous (soot) oxidation are provided as the following:

$O_2$ chemisorption on the carbon surface (-C* is a carbon active site):

$$-C^* + NO_2 \rightarrow -C(O) + NO \qquad (2.9)$$

Decomposition of the intermediate C – O complex by $NO_2$ promotion:

$$-\mathrm{C(O)} + NO_2 \rightarrow -C(ONO_2) \qquad (2.10)$$

Carbon surface active sites regeneration:

$$C - C(ONO_2) \rightarrow CO_2 + NO + -C^* \quad (2.11)$$

$$C - C(ONO_2) \rightarrow CO_2 + NO_2 + -C^* \quad (2.12)$$

Overall oxidation:

$$\mathrm{C} + 2NO_2 \rightarrow CO_2 + 2NO \quad (2.13)$$

$$\mathrm{C} + NO_2 \rightarrow CO + NO \quad (2.14)$$

**2.3.2.3 Catalytic reduction of NOx**

Selective catalytic reduction of NOx is widely accepted as the most effective aftertreatment for automobile NOx removal. Over a bed of suitable catalyst, SCR reaction takes place with injection of reducing agent (usually as ammonia, hydrocarbon and hydrogen) to breakdown NO and $NO_2$ and form nitrogen, water and carbon dioxide.

The SCR reaction is very complicated and its performance is determined by various factors (Burch and Coleman 2002): 1) temperature of the exhaust stream, 2) exhaust composition, 3) type and concentration of the reducing agent, 4) reducing agent to NOx ratio, 5) type and structure of the catalyst, 6) gas hourly space velocity (GHSV) and 7) catalyst poisoning and aging.

Therefore, the type SCR is classified based on the nature of the catalyst (catalytic material) and the type of reducing agent involved in the mechanism.

### 2.3.2.4 Ammonia and Urea SCR

The ammonia or urea SCR was initially developed for stationary application such as power plants, nitric acid plants, solid waste incineration plants, reforming furnaces and industrial boilers (Larrubia, Ramis et al. 2000). Its use was later expanded to heavy duty diesel engines and was demonstrated to be highly efficient in automobile NOx removal. Common catalysts are made from supported vanadium ($V_2O_5$) and iron or copper on zeolite. Most successful $NH_3$ – SCR with large commercial breakthrough is thought to be the vanadium catalyst, whose application in heavy duty diesel engine was revealed to have good selectivity for the conversion of NO and $NO_2$ into $N_2$ with moderate formation of $N_2O$.

Several reactions were found to participate in an ammonia SCR system, Eq. 2.15 – 2.19 summarised the desirable reactions that reduce NOx to $N_2$:

$$6NO + 4NH_3 \rightarrow 5N_2 + 6H_2O \quad (2.15)$$

$$4NO + 4NH_3 + O_2 \rightarrow 4N_2 + 6H_2O \quad (2.16)$$

$$6NO_2 + 8NH_3 + \rightarrow 7N_2 + 12H_2O \quad (2.17)$$

$$2NO + 4NH_3 + O_2 \rightarrow 3N_2 + 6H_2O \quad (2.18)$$

$$NO + NO_2 + 2NH_3 \rightarrow 2N_2 + 3H_2O \quad (2.19)$$

However, ammonia (anhydrous) is toxic and corrosive and its storage often requires pressurised tanks and piping due to its high vapour pressure, these lead to concerns of its vehicle on – board safety. To solve this problem, urea as an ammonia substitution is employed due to its

much less toxicity and similar performance demonstrated in the SCR reaction. In the last decade, urea – SCR has been continuously developed for heavy – duty diesel vehicles for NOx removal to meet the increasingly stringent environmental legislations (Lambert, Hammerle et al. 2004, Tennison, Lambert et al. 2004, Walker, Blakeman et al. 2004).

There are three mechanisms included in the urea – SCR reaction process: 1) thermal decomposition and hydrolysis of the urea ($NH_2 – CO – NH_2$) to release gaseous ammonia and carbon dioxide (Eq. 2.20 – 2.21) (Willand, Teigeler et al. 1998); 2) the released ammonia will react with the NOx species according to the reactions listed from Eq. 2.15 – 2.19; 3) according to the adopted $NH_3$ : NOx ratio (reductant to reactant ratio) and the actual completeness of the reaction (based on the designed stoichiometry), both of NOx and $NH_3$ can be retained in the product stream, so that a downstream oxidation mechanism is needed to remove any slipped $NH_3$ especially in the transient operation (Koebel, Elsener et al. 2000).

$$NH_2\text{-}CO\text{-}NH_{2(l)} = NH_3 + HNCO \qquad (2.20)$$

$$HNCO + H_2O = NH_{3(g)} + CO_2 \qquad (2.21)$$

Hence the effectiveness of ammonia/urea SCR depends on a precise control of the ammonia injection rate; a too small injection suppresses NOx conversion, whereas an excessive one contributes to the unwanted $NH_3$ emission.

In general, the urea/ammonia SCR system is advantageous in terms of good performance of NOx removal, with no fuel penalty and high durability under real – world diesel engine conditions

with sulphur – containing fuels (Walker, Allansson et al. 2003, Johnson 2004, Kusaka, Sueoka et al. 2005).

#### 2.3.2.5 Hydrocarbon SCR

Apart from the ammonia/urea SCR technology reviewed in the previous section, an alternative for NOx control is HC – SCR. This method is also feasible for NOx conversion under lean exhaust condition, but it is comparatively less developed than the Ammonia/urea SCR. The hydrocarbon SCR (HC – SCR) uses HCs as the reducing agent, via a mechanism as shown in Eq. 2.22.

$$C_nH_m(g) + \left(2n + \frac{m}{2}\right)NO(g) \rightarrow \left(n + \frac{m}{4}\right)N_2(g) + nCO_2(g) + \left(\frac{m}{2}\right)H_2O(g) \qquad (2.22)$$

$$C_nH_m(g) + \left(2n + \frac{m}{4}\right)O_2(g) \rightarrow nCO_2(g) + \left(\frac{m}{2}\right)H_2O(g) \qquad (2.23)$$

Therefore, the engine emitted hydrocarbon can be involved in the above mechanism for NOx reduction. Thus the nature of the HCs is changed from an unwanted emission into a desired reductant for reduction of the other emission.

In general, diesel exhaust gas only contains small amount of unburned hydrocarbons, which may be insufficient for the emitted NOx. In addition to that, a competitive reaction of nonselective hydrocarbon oxidation (Eq. 2.23) can further restrict the system's HC availability. Hence, additional injection of hydrocarbon is often desired to complement the exhaust hydrocarbon. In

recent years, this method has gained increasing attention from researchers due to its merit of not requiring additional reductant storage.

In addition to the available HC concentration, the hydrocarbon structure is another influential factor determining the effectiveness of a HC – SCR. Shibata et al. (Shibata, Shimizu et al. 2002) made an investigation over alumina supported copper catalyst (Cu – $Al_2O_3$) by using linear and branched alkanes with different carbon numbers. The study showed increased reaction rate of NO and hydrocarbon when the number of carbon in the linear alkanes enlarged. With respect to the branched alkanes provided with the same carbon numbers, the reaction rate of NO and HC is found to be lower. According to Burch et al. (Burch, Breen et al. 2002), such greater activity at lower temperature is attributed to the longer alkanes' weaker C – H bond and larger enthalpy of adsorption.

On the other hand, light alcohols, e.g. ethanol and butanol are often found to be more active at lower temperature (250 ℃) and also give a wide temperature window for the reaction. This is believed due to their low molecular weight that enhances the diffusion rates and the reactivity of some highly polar (also water soluble) compounds in accessing the catalyst surface site against water (Thomas, Lewis et al. 2005). In contrast, alkanes convert NOx at much higher temperature whilst the alkenes' performance is at a temperature intermediate between that of the alkanes and alcohols. The number of carbon atoms in the structure of alkane, alkene and alcohol are revealed to be also important for the reaction temperature, giving better activity to longer chain hydrocarbons at reduced temperature (Burch, Sullivan et al. 1998).

In terms of the catalyst, silver – loaded alumina ($Ag/Al_2O_3$) is recognised as one of the most active and selective catalyst for this application. Its advantageous features are found as low activity for $SO_2$ oxidation, high selectivity to $N_2$ and high thermal and hydrothermal durability (Shibata, Shimizu et al. 2002, Houel, Millington et al. 2007). Nevertheless, the catalyst's self – poisoning by surface nitrates formation and carbon – rich surfaces species (transformed from the gaseous hydrocarbons) hinders the catalyst's low temperature activity (< 300 ºC) by preventing the reductants/reactants from accessing the active sites. The catalyst's surface coking was revealed to rely on the nature of the hydrocarbons and their presences as a result of the adopted HC:NOx ratio. It was recommended to keep a low HC:NOx ratio at low reaction temperature whilst a high ratio at increased temperature to compensate the loss of hydrocarbon through oxidation (Eq. 2.23) (Houel, Millington et al. 2007).

Recently, presence of hydrogen in HC – SCR was shown to strengthen the reaction's activity over silver loaded system especially at low reaction temperature. This promotional effect is often referred to 'hydrogen effect' but without a conclusive explanation on its working mechanism. Eränen et al (Eränen, Klingstedt et al. 2004) suggests there are at least two functions of the hydrogen as a promoting agent; first, hydrogen stimulates the oxidation of all involved reaction species, leading to increased rate of key intermediates formation; secondly, the introduced hydrogen helps in the formation of activated NOx species. Other researchers attribute this effect to essentially an activation of the molecular $O_2$ (Richter, Bentrup et al. 2004): hydrogen reduced the activation energy for $O_2$ converting into reactive $O_2^-$ species, which are reactive toward the C – H bonds of the hydrocarbon (Shimizu, Tsuzuki et al. 2006). Moreover, it is also suggested that

the removal of the formed nitrates over the Ag site as well as the alumina support is the role that hydrogen play in the reaction (Brosius, Arve et al. 2005). Similarly, the hydrocarbon derived carbon rich species such as the carbon deposit on the catalyst can equally block the catalyst. Hydrogen was reported to produce $NO_2$ that oxidise away these carbon species to restore the catalyst's activity (Houel, Millington et al. 2007).

It must be pointed out that $H_2$ is only suggested to be a promoting agent rather than a main reactant of the HC – SCR mechanism. Its addition over 500 ℃ is shown to accelerate the HC oxidation instead of the relative reaction to NOx reduction, resulting in hindered reaction performance (Houel, Millington et al. 2007).

#### 2.3.2.6 $H_2$ assisted $NH_3$ – SCR over $Ag/Al_2O_3$

The above sections reviewed the $NH_3$ and HCs based SCR reactions. To date, further researches even demonstrated successful $NH_3$ – SCR on the $Ag/Al_2O_3$ catalyst, as long as the reaction is assisted by $H_2$ (Richter, Fricke et al. 2004). Compared to the reaction occurring with those commercial catalysts, the $H_2$ promoted $NH_3$ -SCR on $Ag/Al_2O_3$ can start at comparatively lower temperature and achieve equally high NOx conversion (Fogel, Doronkin et al. 2012, Tamm, Fogel et al. 2013). In the literature, the role of $H_2$ in HC – SCR is proposed as a formation of Ag clusters ($Ag_n^{\delta+}$) on $Ag/Al_2O_3$ via $H_2$ reduction of $Ag^+$ ions. It was proposed that the formed Ag clusters work with $H^+$ ions in reducing $O_2$ to yield superoxide $O_2^-$, which is known as the key intermediate for the activation of radical reactions involving both hydrocarbon and NO species

that finally leads to $N_2$ production (Shimizu, Shibata et al. 2006). Other reaction schemes proposed intermediate formation of amines and ammonia for the HC – SCR along the reduction path (Pârvulescu, Grange et al. 1998, Klingstedt, Arve et al. 2006). This suggests $NH_3$ – SCR is actually part of HC – SCR on the silver catalyst.

Explained by Shimizu et al. (Shimizu, Shibata et al. 2006, Shimizu, Tsuzuki et al. 2006), HC radicals and NHx species are formed via $O_2^-$ activating respectively the C – H and N – H bound of HC and $NH_3$, whilst oxidative activation of NO is also taking place to form $NO_2$. In the case of $NH_3$ SCR reaction, the NHx species are reacted with $NO_2$ to free nitrogen and water. On the other hand, the yielded HC radicals in the HC – SCR mechanism are later converted into acetate ions, and in a further step, to form $CH_3COO^-$. The formed $NO_2$ and $CH_3COO^-$ react together to produce nitromethanes i.e. $CH_3NO_2$, which forms $NH_3$ under presence of species such as isocyanate (NCO). The reactions occurring afterward will go through the mechanism proposed for $NH_3$ SCR as the above mentioned. Further study on the same catalyst discovered the $H_2$ assisted $NH_3$ – SCR might react partially in the form of Fast – SCR (Eq. 2.19); the NO to $NO_2$ oxidation is revealed to be an essential step that activates the overall SCR reaction (Doronkin, Fogel et al. 2012).

The reaction schemes made by Shimizu et al. are adapted in Fig. 2.5 for both of the $H_2$ assisted HC and $NH_3$ SCR reactions (over $Ag/Al_2O_3$)

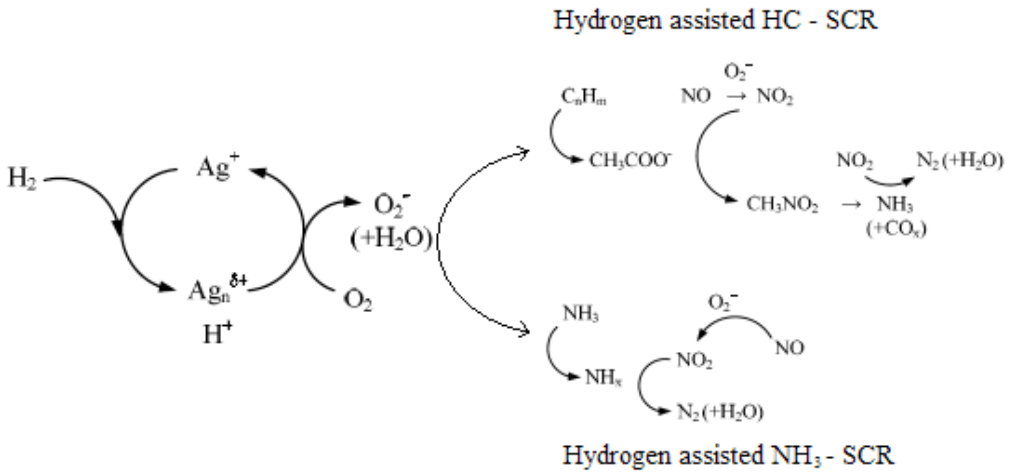


**Figure 2.5:** Reaction mechanisms for $H_2$ assisted HC – SCR and $NH_3$ – SCR over $Ag/Al_2O_3$

## 2.4 Alternative fuel/fuel substitution and dual fuel mode in diesel combustion

To further deal with the engine emission and, more importantly, find solutions to the presently confronted fuel depletion, large efforts have been devoted into the research of new energies that are affordable, reliable and environmentally sustainable. This encompasses the investigation of alternative fuels and development of alternative fuel processes on top of the engine combustion. Since CI engine is potentially capable of combusting various types of feedstock, fuels derived from biomass, e.g. biodiesel or in a form of combustible energy carriers, e.g. $H_2$ and $NH_3$ have been increasingly investigated and examined on whether they are suitable alternative fuel or fuel substitutions in diesel combustion.

### 2.4.1 Biodiesel and oxygenated fuels

Vegetable oils, as in a form of renewable feedstock, attract considerable interests in the diesel combustion and have long been used as fuel for diesel engines. However, its higher viscosity and lower volatility hinders its direct use in engines. Therefore it is needed to apply the process of transesterification (of triglycerides, e.g. oils or fats) with a use of methanol or ethanol, to exchange the glycerol compounds of the triglycerides molecules for lighter compounds from the lighter alcohols (Monyem and H. Van Gerpen 2001), Fig. 2.6

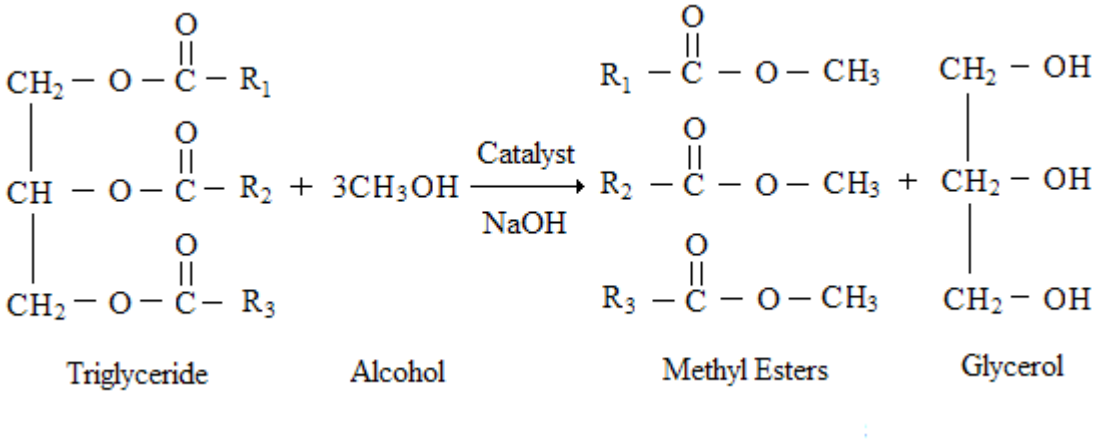


**Figure 2.6:** Exchanging the glycerol compounds of the triglycerides molecules for lighter compounds from the lighter alcohols

The end products is mainly built by fatty acid methy esters (Or ethyl esters), being composed of straight saturated and unsaturated hydrocarbon chains. Hence, the biodiesel is often oxygenated

(with fuel borne oxygen) and can be produced from a wide range of sources such as soybean, rapeseed, sunflower, palm, peanut and animal fats.

There are several features of using biodiesel in the diesel combustion (Graboski and McCormick 1998, Monyem and H. Van Gerpen 2001, Yamane, Ueta et al. 2001, Ribeiro, Pinto et al. 2007, Lapuerta, Armas et al. 2008):

1) In general, combustion of biodiesel maintains or improves engine efficiency with simultaneous reduction in harmful emissions including THC, CO and PM. Noticeably, significant reductions in sulphur oxides and PAH (soot precursors) can be obtained, which is due to the oxygen content of the biodiesel molecule that results in more complete combustion. This is considered as highly effective in the regions of fuel – rich diffusion flames, leading to more rapid oxidation of the already formed soot and its precursors.
2) Due to biodiesel's different chemical and physical properties, its combustion in an unmodified engine can cause reduction in ignition delay. The increased oxygen contents is regarded as the main reason, which increases the in – cylinder oxygen concentration and promotes the early ignition of the fuel and thus advances the overall combustion phasing. Except that, when being injected, the fuel's lower compressibility (higher bulk modulus) makes quicker the pressure rise produced in a pump – line – nozzle system, thus contributing to quick fuel propagation outwards the injector because of its higher sound velocity.
3) Use of biodiesel can cause an increased NOx emission. This could be a resultant of the advanced ignition, which results in more fuel being oxidised in the premixed combustion. It is known that the high combustion temperature and pressure in the premixed phase is favorable

for the NOx formation. The increased fuel – borne oxygen contained in the biodiesel, however, is not a main cause of the NOx emission. The flame (adiabatic) temperature and the volumetric fuel delivery are calculated to be both lower than that of the diesel under the same load operation (combustion temperature is any higher than the diesel's).

4) Due to the chemical and physical features of biodiesel, better lubricant properties are given by the biodiesel than conventional fuels. Nevertheless, this highly depends on the varying fuel quality such as glycerol content, degradability and cold flow properties

Apart from biodiesel, there are various types of biomass – derived alternatives that are potentially regarded as promising fuel or fuel additives for compression ignition engines. One example is dimethyl ether (DME), which can be produced from many renewable materials such as plants, wastes and agricultural products (Gross and Kong 2013). The DME's oxygenation and high cetane (CN=60) number makes it a good ignition improver for combustion enhancement of some less flammable components, e.g. $NH_3$ and natural gas (CNG) (Gusakov, Valjeho Maldonado et al. 2008, Gross and Kong 2013).

Other oxygenated fuel such as diethyl ether (DEE, CN >125) was shown to improve successful combustion of LPG fuel diesel engine. Under the DEE's combustion enhancement, engine efficiency was reported to increase while HC and particulate emissions were both decreased (Miller Jothi, Nagarajan et al. 2008). In addition to that, co – fueling CNG and DEE to diesel engine also yielded similar enhancement (Karabektas, Ergen et al. 2014).

### 2.4.2 Hydrogen

Hydrogen, as clean fuel and dense energy carrier in term of mass, has potential applications in automobiles, chemical industry and fuel cell power generation (Dupont 2007). Its intensive utilisation is envisaged for the mid-term future and has been spurred to become one of the methods to alleviate the current environmental pollution due to emissions of combusting fossil fuels. Various researches have been conducted in directing hydrogen into internal combustion engines. With hydrogen being at presence, NOx emissions from gasoline engines can be alleviated (Kirwan, Quader et al. 1999), diesel engines can benefit through cancelling the NOx-Particulate tradeoff (Tsolakis and Megaritis 2004, Tsolakis, Megaritis et al. 2004), and as mentioned in the earlier chapter, the SCRs in vehicle aftertreatment units for reducing NOx can be promoted.

#### 2.4.2.1 Hydrogen combustion

The addition of hydrogen in internal combustion engines has been shown can improve fuel economy or decrease the engine emissions or both together (Al-Baghdadi 2003, Tsolakis, Megaritis et al. 2005). Its high burning velocity leads to easier ignition of the hydrogen/hydrocarbon mixture, which decreases the chance of misfiring, thus improving the emission, performance and fuel economy (Senthil Kumar, Ramesh et al. 2003). Compared to regular fuels, co – fuelling hydrogen with other components extents the mixture's flammability limits and accelerates the relatively slow reaction rate of typical fuels.

The addition of hydrogen alone into diesel combustion was revealed to substantially lower the emissions of CO and HC via its fast flame propagation and temperature. The $CO_2$ concentration was also decreased to due to the simple fact that hydrogen is not carbon based (Saravanan and Nagarajan 2010). However, this pure addition incurred an increased NOx emission as a penalty of the heightened combustion temperature. Nevertheless, previous study of hydrogen addition via application of REGR ($H_2$ syn –gas produced by exhaust gas reforming and redirected to engine with EGR influent) showed combined beneficial effects of premixed combustion (for soot elimination) and EGR (NOx control) (Tsolakis and Megaritis 2004, Tsolakis, Megaritis et al. 2004). In addition to that, the presence of $H_2$ was demonstrated to increase the NO oxidation via production of $HO_2$ radicals (Chong, Tsolakis et al. 2010). This resulted in enhanced formation of $NO_2$ that is potentially beneficial for the aftertreatment like DPF and SCR, mentioned in earlier sections.

For delivering the hydrogen into the combustion chamber, either port addition in a form of port fuel injection (PFI) through the intake manifold or direct injection (DI) into the combustion chamber can be adopted. Compared to diesel fuels, $H_2$ is provided with lower density and less lower heating value (LHV) in terms of volume (Heywood 1988). Therefore, to inject hydrogen directly into chamber, a fuel injector with very large volumes flow is demanded. This also offers potential efficiency and safety advantages over the more developed premixed hydrogen engine option (Naber and Siebers 1998). On the other hand, the port injection of hydrogen, though it is provided with simplicity in terms of instrumentation, has basic thermodynamic disadvantage of its volumetric deficiency (i.e. low density and low volumetric LHV). Therefore, a net reduction in

the number of molecules involved in the chemical reactions (during the combustion) is caused. Hence, the power output cannot exceed 80 % of a regular hydrocarbon – fuelled engine of the same swept volume (Arcoumanis 1988). In addition to that, despite the fact that higher substitution of $H_2$ reduces the net carbon elements, the replacement of the intake air due to $H_2$ occupation will be on the other hand serving to restrict oxygen concentration. This tends to increase the formation of carbonaceous emissions as a result of richer stoichiometry (Lilik, Zhang et al. 2010).

#### 2.4.2.2 Hydrogen storage

Hydrogen is not provided with a natural form in the earth. Its presence can be only found as an element in various compounds with other elements, e.g. $H_2O$, $CH_4$, coal and diesel. As aforementioned, hydrogen has low volumetric energy density. This makes the hydrogen on – board storage difficult. However, there are still ways of hydrogen storage for automotive applications (Arcoumanis 1988):

1) Hydrogen can be compressed and handled in a similar way as that of the compressed natural gas. The typical pressure for storing hydrogen in a gas cylinder is usually between 200 – 300 bars, or potentially as high as 700 bars, provided the container seal is specially modified for the small molecule of hydrogen. Nevertheless, this still causes on board storage problem with the size of the container.
2) Hydrogen can be stored via the technique of cryogenic liquid. However, to convert gaseous $H_2$

into liquid requires a high energy input that makes this process become energetically inefficient.

3) Large amount of hydrogen can be stored in metal hydrides as it is capable of reacting with metallic mixtures such as FeTi. However, the weight of this system is comparatively large and causes fuel penalty when being kept on – board.

#### 2.4.2.3 Hydrogen on – board production

Previous studies have shown that $H_2$ can be produced by means of hydrocarbon reforming (Martin and Wörner 2011). This method can be also adopted for the purpose of on – board production of $H_2$ i.e. exhaust gas fuel reforming, which is considered as a potential solution to deal with the hydrogen storage issue (Tsolakis, Megaritis et al. 2005). The exhaust gas forming is in fact based on the existing reforming technologies.

To date, the developed fuel reforming technology for mass production of $H_2$ are steam reforming reaction (SRR), Partial Oxidation (POX), water gas shift reaction (WSG) and Autothermal reforming (ATR).

The SRR process provides high efficiency and reformates quality, i.e. a higher hydrogen production accompanied by lower rate of side reactions and fewer by – products (Nahar 2010). Since this reaction is highly endothermic in nature, external source to lend heat is necessary.

The main reactions for SR in reforming oxygenated fuels are as the following:

$$C_nH_mO_k + (n-k)H_2O \rightarrow nCO + (n+\frac{m}{2}-k)H_2 \quad (2.24)$$

$$CO + H_2O \leftrightarrow CO_2 + H_2 \quad (2.25)$$

$$C_nH_mO_k + (2n-k)H_2O \rightarrow nCO_2 + (2n+\frac{m}{2}-k)H_2 \quad (2.26)$$

$$CO + 3H_2 \leftrightarrow CH_4 + H_2O \quad (2.27)$$

The fuel is converted primarily with heated steam to yield carbon monoxide and hydrogen as indicated in reaction (2.24). The produced CO and $H_2$, together with the un-reacted water then participate in a Water-Gas-Shift-Reaction (WGSR, Eq. 2.25) to further enhance the hydrogen productivity. Reaction (2.24) and (2.25) thus can be combined to form reaction (2.26) that represents the highest $H_2$ yield of the SRR process (Satterfield 1991, Marquevich, Coll et al. 2000). Nonetheless, the undesirable hydrogenation of carbon monoxide as shown by reaction (4) will, at all time, compete the reforming reactions to consume the produced $H_2$ and CO, which leads to loss of overall syn – gas formation. The theoretical hydrogen production via the above reaction (2.26) is affected by the oxygen content within the fuel, i.e. higher oxygen presence numerically reduces the stoichiometric hydrogen formation per mole of the reactant fuel. The steam/carbon ratio (S/C) is another crucial factor that regulates the overall $H_2$. Higher S/C ratios than the stoichiometric are usually adopted to ensure efficient SRR (Marquevich, Farriol et al. 2001).

The POX reaction benefits from its exothermic nature and relatively short reformer contact time, hence the process is provided with a fast start-up time and has a merit in reforming heavy oil fractions (Nahar 2010). Numerous researches demonstrated successful hydrogen production of a

wide range of fuels through catalytic partial oxidation (Huff, Torniainen et al. 1994, Schmidt and Huff 1994, Traxel and Hohn 2003). For partial oxidation, the overall reaction is defined as:

$$C_nH_mO_k + \left(\frac{n-k}{2}\right)O_2 \rightarrow nCO + (\frac{m}{2})H_2 \qquad (2.28)$$

However, it has been shown that the catalytic partial oxidation, rather being as a substantive and direct reaction, could in fact be proposed as a two-step indirect mechanism. This embraces a depletion of oxygen through combusting part of the reactant fuel, reaction (2.29), and has steam reforming (2.24) and dry reforming (2.30) to follow using the produced water, carbon dioxide and the remaining fuel to form CO, $H_2$ and methane. WGSR, reaction (2.25), is also involved and is thought to be as a side reaction. Several published studies found evidence for this indirect reaction (Wang, Dewaele et al. 1996, Mallens, Hoebink et al. 1997), while others advocate for a mechanism in between (Deutschmann, Schwiedernoch et al. 2001, Lyubovsky, Roychoudhury et al. 2005)

$$C_nH_mO_k + \left(n + \frac{m}{4} - \frac{k}{2}\right)O_2 \rightarrow nCO_2 + (\frac{m}{2})H_2O \qquad (2.29)$$

$$C_nH_mO_k + \left(n + \frac{m}{2} - k\right)CO_2 \rightarrow (2n + \frac{m}{2} - k)CO + (\frac{m}{2})H_2 \qquad (2.30)$$

The ATR process combines the heat effects of the POX and SRR: part of the fuel is oxidised to provide the energy needed by a subsequent fuel reforming mechanism to produce $H_2$. If sufficient hydrocarbon oxidation takes place, the endothermic SRR can be self – sustaining using the provided heat. The main reaction for ATR is expressed as:

$$C_nH_m + xO_2 + (2n - 2x)H_2O \rightarrow nCO_2 + (2n - 2x + \frac{m}{2})H_2 \quad (2.31)$$

The industrial ATR uses air as the oxygen source for the hydrogen production. If diesel engine exhaust is used to provide the $O_2$ instead of the air, and part of the exhaust heat is recovered as a primary energy source for the reaction then the ATR process is transformed into diesel exhaust gas reforming. Thus the ATR and exhaust gas reforming are sharing the reaction equation (2.31).

### 2.4.3 $NH_3$ and its potential vehicular applications

Ammonia has been overlooked in the past for vehicular applications; both as a fuel and a hydrogen carrier. In general, its low heating value on mass basis indicates ammonia has less energy for combustion than conventional fossil fuels i.e. gasoline and diesel. However, the stoichiometric air – fuel ratio for ammonia is much lower compared to diesel fuel. This results in ammonia having a LHV of 2.64 MJ per kg of stoichiometric mixture, which is comparable to that of diesel (2.77 MJ/kg) (Reiter and Kong 2011)

Ammonia is a potential carbon – free fuel for internal combustion engine, whose combustion does not produce $CO_2$. The study on applying ammonia in vehicular uses can be dated back to 1942, used for power busses in World War II due to fuel shortage (Ryu, Zacharakis-Jutz et al. 2014). In 1960s, the US military demonstrated $NH_3$ as a substitute for hydrocarbons in spark ignition (SI) and CI engines (Pearsall and Garabedian 1967). Due to the large production pressure on the current oil wells, $NH_3$ has again drawn much attention because of the driven force in finding new fuel alternatives.

A lot of researches have been devoted into utilisation of ammonia in SI engine because of its high octane number. Engine tests were carried out with compression ratios varying from 6:1 to 10:1 (Starkman, Newhall et al. 1966). The result revealed $NH_3$ is better to be introduced in a vapour form and partly decomposed into hydrogen and nitrogen. The minimum decomposed $NH_3$ is suggested to be 4 -5 % wt of the total $NH_3$ used. This can effectively lower the ignition energy of $NH_3$ from 8 MJ to 0.018 MJ, while increasing the laminar burning velocity from 0.015 $ms^{-1}$ to 3.51 $ms^{-1}$ (Saika, Nakamura et al. 2006). In another study, simultaneous uses of $NH_3$ and gasoline was applied in SI engine (Grannell, Assanis et al. 2008). A mixture containing 70 % ammonia and 30 % gasoline (on energy basis) was shown to be appropriate for the normally aspirated, wide – open throttle conditions.

In terms of diesel engines, it was shown, with a combined combustion of directly injected diesel fuel, a maximum 95 % of energy replacement can be achieved using ammonia vapour introduced through the intake manifold (Reiter and Kong 2008). By adding high quantity of $NH_3$, the engine rated power can be exceeded. Since the carbon based primary fuel is more replaced by $NH_3$, $CO_2$ emissions can be largely reduced.

The predominant reaction of $NH_3$ in the engine forms only $N_2$ and $H_2O$ (Eq. 2.32). However, due to the fact that $NH_3$ is nitrogen bounded, NOx formation is found as the major side – reaction that always accompanies the main ammonia combustion (Eq. 2.33 and 2.34).

$$NH_3 + \frac{3}{4}\left(O_2 + \frac{79}{21}N_2\right) \rightarrow 1.5H_2O + \frac{93}{28}N_2 \quad (2.32)$$

$$4NH_3 + 5O_2 \rightarrow 6H_2O + 4NO \quad (2.33)$$

$$N_2 + O_2 \rightarrow 2NO \quad (2.34)$$

Nevertheless, recent literature shows due to $NH_3$'s relatively low flame temperature, when an addition of ammonia (in combustion) is applied at less than 40 % of the overall combustion energy, the thermal formation of NOx will in fact be suppressed, due to the overall reduced combustion temperature under the $NH_3$ fuelling (Reiter and Kong 2008, Reiter and Kong 2011).

On the other hand, it should be noticed that one mole of ammonia contains 1.5 mol of hydrogen, which is 17.8% by weight or 108 kg – $H_2/m^3$ embedded in liquid ammonia at 20 ℃. Comparing this to the most advanced hydrogen storage systems, e.g. metal hydrides, which store $H_2$ up to 25 $kg/m^3$, the advantage of ammonia in carrying hydrogen per unit volume is significant (Schlapbach and Zuttel 2001). Therefore, using hydrogen extracted from ammonia appears to be more beneficial than combusting ammonia directly in an IC engine. Zamfirescu (Zamfirescu and Dincer 2009) in a recent study compared $NH_3$ with other common fuels such as gasoline, CNG, LPG and methanol, showing that $NH_3$ is competitive to these fuels in terms of gravimetric, volumetric and energetic costs (see in Table 2.2). Based on this study, a further comparison between each fuel's molar hydrogen carrying ability per unit mass, volume and cost can be made, which indicates ammonia is a more affordable hydrogen carrier, (Table 2.3). Recently, increasing numbers of studies have shown that hydrogen production can be implemented through ammonia thermal decomposition (i.e. Eq. 2.35) for small scale fuel cell power systems (Zhang, Xu et al. 2005, Chen, Zhu et al. 2010). Decomposition of ammonia is by definition COx free, and $CO_2$ yielded during ammonia synthesis can be sequestrated on-site at the production plants (Zamfirescu and Dincer 2009, Kim and Kwon 2011). Thus using ammonia as a hydrogen source

is potentially an alternative to the conventional hydrocarbon reforming and makes the on-board hydrogen production free of COx.

$2NH_3 = 3H_2 + N_2 \qquad \Delta H_r = +46 \text{ kJ/mol}$ (2.35)

In addition to that, the storage, distribution and transportation infrastructure of ammonia is established (Christensen, Johannessen et al. 2006), with 100 million tonnes of ammonia being delivered each year. Thus the existing production and handling system of ammonia reveal a great potential in expanding its usage to vehicle applications as a sustainable fuel (Zamfirescu and Dincer 2008). Ammonia has already been applied but in the form of urea on today's heavy duty diesel vehicles for catalytic aftertreatment systems for NOx reduction. Therefore special technology and regulation for safe storage of ammonia on passenger cars should be developed or an additional step of thermo-catalytic conversion of urea to ammonia should be applied as shown in the literature (Zamfirescu and Dincer 2011): a combined urea storage and $NH_3$ – $H_2$ generator/separator system used in the vicinity of the exhaust pipes, as shown in the schematic diagram in Fig. 2.7.

**Table 2.2:** Comparison of ammonia with other fuels including hydrogen (adapted from C. Zamfirescu and I. Dincer, Ammonia as a green fuel and hydrogen source for vehicular applications. Fuel Processing Technology, 2009. 90(5): p. 729-737)

| **Fuel /storage** | **P [bar]** | **Density [kg/m$^3$]** | **HHV [MJ/kg]** | **HHV' [GJ/m$^3$]** | **c [CN$/kg]** | **C [CN$/m$^3$]** | **C/HHV' [CN$/GJ]** |
|---|---|---|---|---|---|---|---|
| **Gasoline, $C_8H_{18}$/liquid** | 1 | 736 | 46.7 | 34.4 | 1.36 | 1000 | 29.1 |
| **CNG, $CH_4$/integrated storage** | 250 | 188 | 42.5 | 10.4 | 1.20 | 226 | 28.2 |
| **LPG, $C_3H_8$/pressurised tank** | 14 | 388 | 48.9 | 19.0 | 1.41 | 548 | 28.8 |
| **Methanol, $CH_3OH$/liquid** | 1 | 786 | 14.3 | 11.2 | 0.54 | 421 | 37.5 |
| **Hydrogen, $H_2$/metal hydrides** | 14 | 25 | 142.0 | 3.60 | 4.00 | 100 | 28.2 |
| **Ammonia, $NH_3$/pressurised tank** | 10 | 603 | 22.5 | 13.6 | 0.30 | 181 | 13.3 |

HHV: higher heating value per kg HHV': higher heating value per m$^3$

c: cost per kg C: cost per m$^3$

**Table 2.3:** Further comparison of ammonia with other fuels based on the data listed in Table 2.2

| **Fuel /storage** | **Hydrogen content [kmol/m$^3$]** | **Hydrogen content [kmol/kg]** | **C$^1$[CN$/kmol]** |
|---|---|---|---|
| **Gasoline, $C_8H_{18}$/liquid** | 116.2 | 0.16 | 8.5 |
| **CNG, $CH_4$/integrated storage** | 47 | 0.25 | 4.8 |
| **LPG, $C_3H_8$/pressurised tank** | 70.5 | 0.18 | 7.8 |
| **Methanol, $CH_3OH$/liquid** | 98.3 | 0.13 | 4.2 |
| **Ammonia, $NH_3$/pressurised tank** | 106.4 | 0.18 | 1.7 |

C$^1$: Cost of per kmol of carried hydrogen regarding the fuel as hydrogen carrier

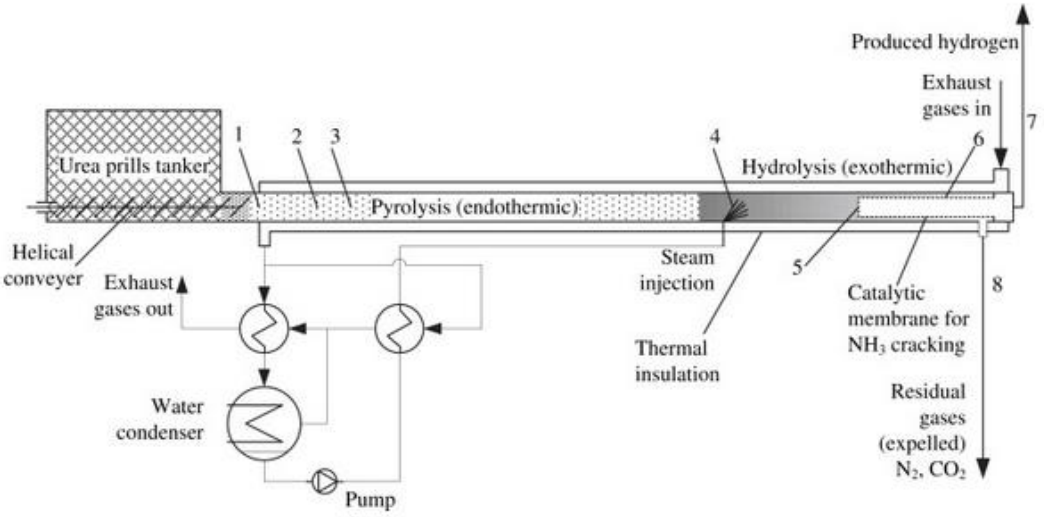


**Figure 2.7:** Combined urea storage and $NH_3 – H_2$ generator/separator system

The overall process of this device undergoes few steps (Zamfirescu and Dincer 2011):

1) Stage 1: granular urea is forced into the pyrolysis reactor at ambient temperature
2) Process 1 – 2: The temperature is heated to 133 ℃ to achieve the melting point of urea
3) Stage 2: Achieved the melting temperature at 133 ℃.
4) Process 2 – 3: Urea melts at quasi – constant temperature.
5) Stage 3: Urea was converted into liquid phase
6) Process 3 – 4: Pyrolysis of $NH_3$ occurs: $HNCO + H_2O = NH_{3(g)} + CO_2$ (Eq. 2.21), temperature keeps increasing
7) Stage 4: Both ammonia and isocyanic acid are formed when temperature reaches approximately 200 ℃ (small amount of other product can also be present in the stream)
8) Process 4 – 5: under steam injection, the isocyanic acid is hydrolysed while the system temperature keeps going up
9) Stage 5: when temperature is increased to 500 ℃, pyrolysis of $NH_3$ is completed

Up to this point, gaseous $NH_3$ is already generated and ready to be directed for the desired applications. The study (Zamfirescu and Dincer 2011) involved further steps to decompose $H_2$ from the produced $NH_3$ , as the following:

10) Process 5 – 6: Catalytic thermal decomposition takes place according to the reaction Eq. 2.35
11) Stage 6: High quantity of $H_2$ is yielded
12) Stage 7: $H_2$ is separated through membrane
13) Stage 8: Nitrogen and carbon dioxide remain in the main product

### 2.4.4 Ammonia production and carbon/energy balance

A full life cycle assessment, i.e. well – to – wheel analysis, indicates the large difference in $CO_2$ emission (75 %) between the vehicular applications of ammonia and petroleum is in fact from their end uses, e.g. combustion or reforming (Ishimatsu, Saika et al. 2004). Since $NH_3$ is free of carbon, its combustion in engines or reaction associated with hydrogen production does not form any carbonaceous emissions. However, $NH_3$ used in current agricultural and industrial sectors is mainly derived from the standard Haber – Bosch process, which uses the hydrogen produced from fossil fuels and $N_2$ from air (Andersson and Lundgren). This makes the massive $NH_3$ production rely on steam reforming of none – renewable hydrocarbons i.e. mainly natural gas that accounts for 67% of the global ammonia feed stock (IFA 2008). The direct $CO_2$ emission from this process is measured at 1.64 kg/kg $NH_3$ (Gilbert and Thornley).

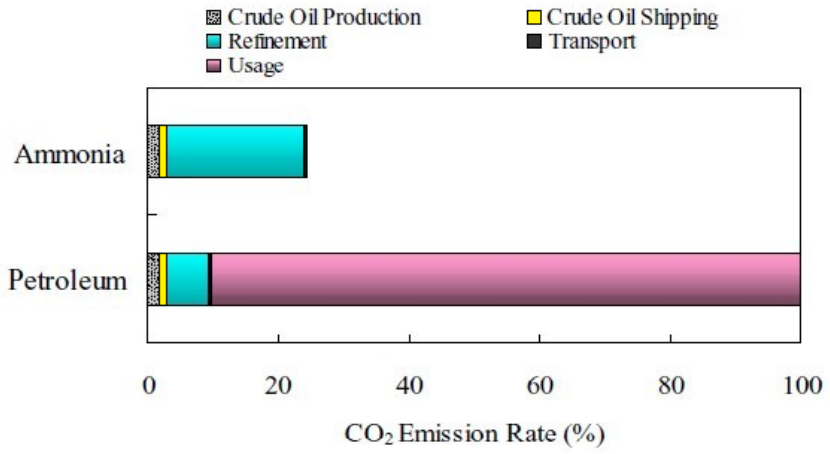


**Figure 2.8:** $CO_2$ emission life cycle assessment of ammonia and petroleum being used in vehicular application. Adapted from: S. Ishimatsu, T. Saika and T. Nohara; Ammonia Fueled Fuel Cell Vehicle: The New Concept of a Hydrogen Supply System; SAE International, 2004 – 01 – 1925.

Shown by Fig. 2.8, the $CO_2$ emitted from the production and refinement of $NH_3$ (20 %) is three times higher than that of the petroleum (6.5 %). Hence, despite the fact that the end use of ammonia helps the overall $CO_2$ reduction, its bulk production still demonstrates a large dependence on the petroleum resource. Thus, the current method of $NH_3$ production does not mitigate the global oil crisis; it is still urgent to find a renewable and sustainable way of $NH_3$ production, whose primary source is not the fossil system.

#### 2.4.4.1 $NH_3$ production from biomass

Production of $NH_3$ using thermal conversion of biomass, e.g. lignocellulosic biomass would be an environmentally friendly option. One reason for the increased interests on such industry is the established infrastructure of biomass supply, which is provided with large logistical and feedstock handling advantages (Andersson and Lundgren). Additionally, the industry is potentially suffered from the increased energy prices and stronger competition on raw materials, therefore to look for additional streams of revenue to the existing production is of importance to this industry (Klugman, Karlsson et al. 2007). In recent studies, Gilbert et al. (Gilbert, Thornley et al. 2009) demonstrated a life cycle assessment in energy and carbon balances for ammonia production from biomass gasification with respect to the conventional production method with natural gas (as mentioned above). The study was focused on the use of short rotation coppice (SRC) willow as the reference biomass and a Fast Internal Circulating Fluidised Bed gasifier

(FICFB) with $CO_2$ removal to provide $H_2$ enriched syngas for a final ammonia synthesis. The main inventory analysis, the fossil – based and biogenic energy uses and the process $CO_2$ emission (with respect to the conventional method) were adapted from the literature (Gilbert and Thornley) and listed in Table 2.4.

**Table 2.4:** Net energy use and $CO_2$ emission for ammonia production via biomass gasification and conventional Haber – Bosch process

| Energy | Unit | Natural gas, steam reforming | Biomass gasification, partial oxidation |
|---|---|---|---|
| **Biomass (30 % moisture content)** | kg/kg $NH_3$ | - | 2.97 |
| **Diesel (agricultural process)** | MJ/kg $NH_3$ | - | 0.13 |
| **Transport (Biomass)** | MJ/kg $NH_3$ | - | 0.38 |
| **Electricity for gasification** | MJ/kg $NH_3$ | - | 0.59 (2.3 % from renewable sources ) |
| **Natural gas fuel** | MJ/kg $NH_3$ | 23.4 | - |
| **Natural gas feedstock** | MJ/kg $NH_3$ | 8.10 | 2.71 |
| **Net fossil – based energy use** | MJ/kg $NH_3$ | 31.50 | 3.81 |
| **Equivalent $CO_2$ emission** | $CO_{2eq}$/kg $NH_3$ | 1.64 | 0.55 |

From the energy calculations listed in Table 2.4, the fossil based energy required by the process of biomass gasification is saved by 88 % from that of the conventional method based on the natural gas reforming. On the other hand, the $CO_2$ emission is reduced by 66 % (1/3 of that of the conventional process). Therefore, assuming such technology being widely adopted, the $CO_2$ emission within the refinery/production stage shown in the above life cycle assessment (Fig. 2.8) is supposed to drop to the same level as that of the petroleum refinery, which expands further the $CO_2$ benefit of $NH_3$ uses in the vehicular applications.

In addition to the reference SRC willow, vast forms of biomass/biomass residue such as sea plants (Kaewpanha, Guan et al. 2014), fruits shell/peel (Brachi, Chirone et al. 2014) and forestry waste (Gañan, Abdulla et al. 2005, Gañán, Al-Kassir Abdulla et al. 2006, Lapuerta, Hernández et al. 2008) were proved as feasible feedstock for process of gasification. These, if being organised in a big scale, will serve as fossil fuel substitutions for mitigating the production pressures on the oil wells.

#### 2.4.4.2 Ammonium ($NH_3$ + $NH_4^+$) recovery from human and animal waste

Ammonia in gaseous form plays an essential role in nitrogen cycle in atmosphere (Aneja, Schlesinger et al. 2006). Among the various atmospheric $NH_3$ sources, livestock production is regarded as the most dominant origin of the annual emission, contributing to 64 % of the total anthropogenic $NH_3$ emissions on a global scale (FAO 2006). Large emissions of $NH_3$ originated from animal production (poultry, meet, diary, egg product and etc.). Country with a large livestock population such as China produces 11.7 Mt of annual $NH_3$ emission in a national scale (Gao, Ma et al. 2013), while country with smaller scale like England and Wales produces roughly 0.5 Mt of gaseous $NH_3$ per annum (Webb 2001). According to a report given by the Food and Agriculture Organisation of the United Nation (FAO, 2006) (FAO 2006), the global atmospheric $NH_3$ emission had increased from 18.8 Mt since 19$^{th}$ century to 56.7 Mt in early 90s, this number kept increasing in recent years and is predicted to be 116 Mt by 2050. Based on the lower heating values of $NH_3$ and standard diesel fuel i.e. 18.6 and 43.4 MJ/kg, the energy contained by the

emitted $NH_3$ from the global food production sector will be equivalent to that of 50 Mt of diesel fuel.

To recover the ammonium ($NH_3$ and $NH_4^+$), technologies were developed accordingly for the recoveries from both of the liquid and gaseous wastes. In a recent literature (Rothrock Jr, Szögi et al. 2013), use of flat gas – permeable membranes was investigated as components of a new process to capture and recover $NH_3$ in poultry house. The process combines the passage of gaseous $NH_3$ through a microporous hydrophobic membrane, capture with a circulating dilute acid on the other side of the membrane and production of concentrated ammonium ($NH_4$) salt (Fig. 2.9) (Rothrock Jr, Szögi et al. 2013). The study is based on a typical poultry house (1800 $m^2$) that grows 20,000 broilers (42 days per flock, 6 flocks per year) with average production of 0.77 g N $bird^{-1}$ $d^{-1}$ (Smith, Ott et al. 2008) and a manure N loss of 38 % as $NH_3$ gas (Moore Jr, Daniel et al. 1995). The daily loss of N from the culture house can be calculated at 5.9 kg N $d^{-1}$. Provided the average recovery efficiency being at 96 % of the membrane system (Rothrock Jr, Szögi et al. 2013), a total annual N recovery can be made at 1427 kg N per year (5.9 kg N $d^{-1}$ x 0.96 x 42 d x 6 flocks).

On the other hand, to recover the $NH_3$ from liquid waste such as urine, a microbial fuel cell was developed in the literature (Kuntke, Śmiech et al. 2012) to simultaneously produce energy and recover ammonium. The studied microbial fuel cell was based on a design of gas diffusion cathode, Fig. 2.10.

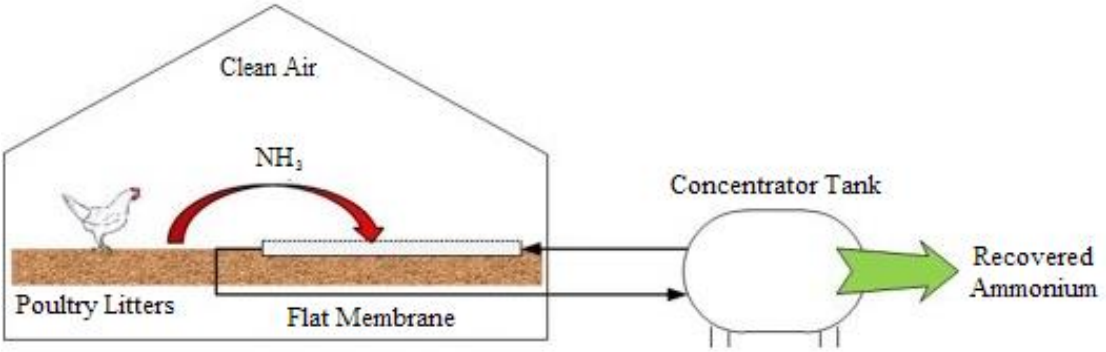


**Figure 2.9:** The flat membrane system adopted in poultry house for ammonium recovery; adapted from M. J. Rothrock Jr., A. A. Szogi and M. B. Vanotti; Recovery of ammonia from poultry litter using flat gas permeable membranes; Waste Management, 2013. 33(6): p. 1531 – 1538.

Through the migration of ammonium and diffusion of ammonia, ammonium transport to the cathode took place, which made ionic ammonium to be converted to volatile ammonia in the cathode chamber. The study shows an ammonium recovery rate of 3.29 g N $d^{-1}$ $m^{-2}$ (vs. membrane surface area) could be achieved at a current density of 0.5 A $m^{-2}$ (vs. membrane surface area), and an energy balance in the study demonstrated a surplus of energy 3.46 kJ g $N^{-1}$ (Kuntke, Śmiech et al. 2012). This means more energy was produced than demanded in the process of ammonium recovery. Hence, combining this technology with water – free urinals, the ammonia production is supposed to proceed easily in daily life.

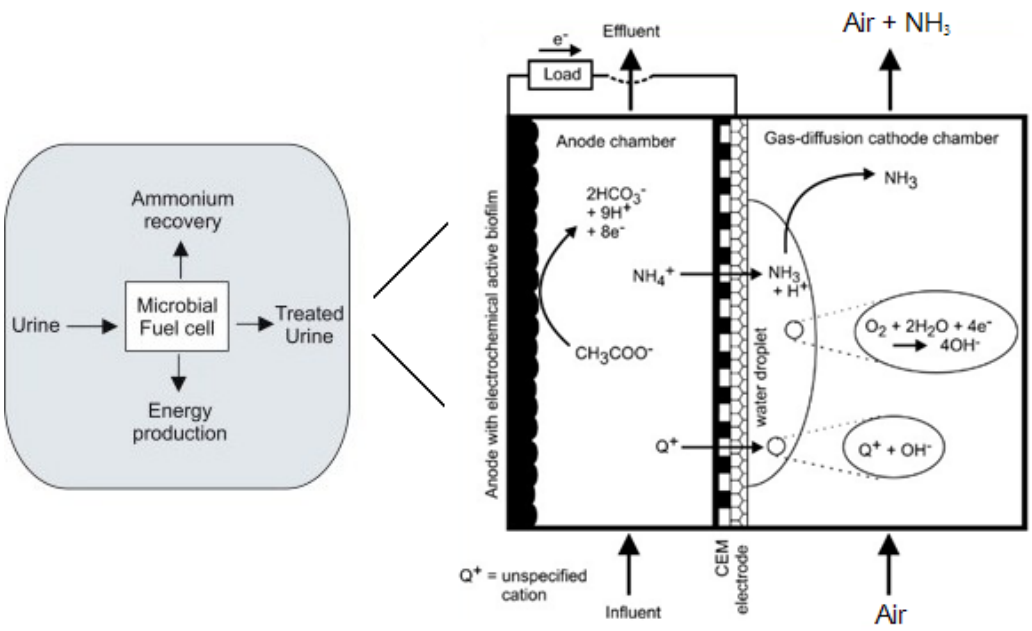


**Figure 2.10:** Microbial fuel cell (MFC) system for ammonium recovery and energy production from urine; adapted form P. Kuntke et al, Ammonium recovery and energy production from urine by a microbial fuel cell; Water Research, 2012. 46: p. 2627 – 2636.

Furthermore, the metal amine complexes such as $Mg(NH_3)_6Cl_2$ used for ammonia storage is formed simply by passing the ammonia over anhydrous magnesium chloride at room temperature; the absorption and desorption of $NH_3$ is completely reversible (Christensen, Johannessen et al. 2006).

Therefore, the above technologies for ammonium recovery could be potentially incorporated with the production of metal amine, expanding the purpose of ammonium recovery further to vehicular applications.

## 2.5 Summary

Although improvements have kept increasing for cleaner and more efficient diesel operation, the challenges in diesel engine advancement for future emission targets and legislations remain still, which are calling for long – term input of researches and developments.

It is possible that switching the fuels' origin from fossil system to renewable sources and applying chemical refining process can make the fuels "cleaner" during the production – to – combustion cycle. Nevertheless, the nature of being essentially carbon based makes the HC fuels' vehicle in site carbon emission performances to be always inferior to those of the carbon – free alternatives i.e. $H_2$ and $NH_3$. Provided the $H_2$ and $NH_3$ are also derived from renewable sources, then they are inferred to even gain the carbon emission improvement in an overall "well – to – wheel" assessment as similar to that of the upgraded/renewable hydrocarbons. However, further researches are still needed for having more efficient acquiring methods that are suitable for mass productions of these fuel alternatives. In addition, better combustion of $H_2$ and $NH_3$ will also need to be developed either individually with careful engine calibrations or combining the combustions with exhaust gas aftertreatment.

Apart from the use of carbon – free alternatives, aftertreament is another method shown to have effective control over the engine emissions. The silver loaded alumina SCR catalyst for example is currently the most researched device for diesel lean NOx control. As described in this chapter, the catalyst' low temperature reactivity could be significantly improved via a $H_2$ and $NH_3$ associated reaction mechanism. However, such reaction has not yet been applied in the real

exhaust system, or neither has it been provided with a practical on – board method to deliver the simultaneous $H_2$ and $NH_3$ that are demanded by the catalysts. These are all considered as the major obstacles preventing the catalyst become practically applicable and commercially available.

# CHAPTER 3: EXPERIMENTAL SETUP

In this chapter, the experimental facilities used in this research are detailed. These include the test engine, catalytic reactors, catalysts and emission analysers

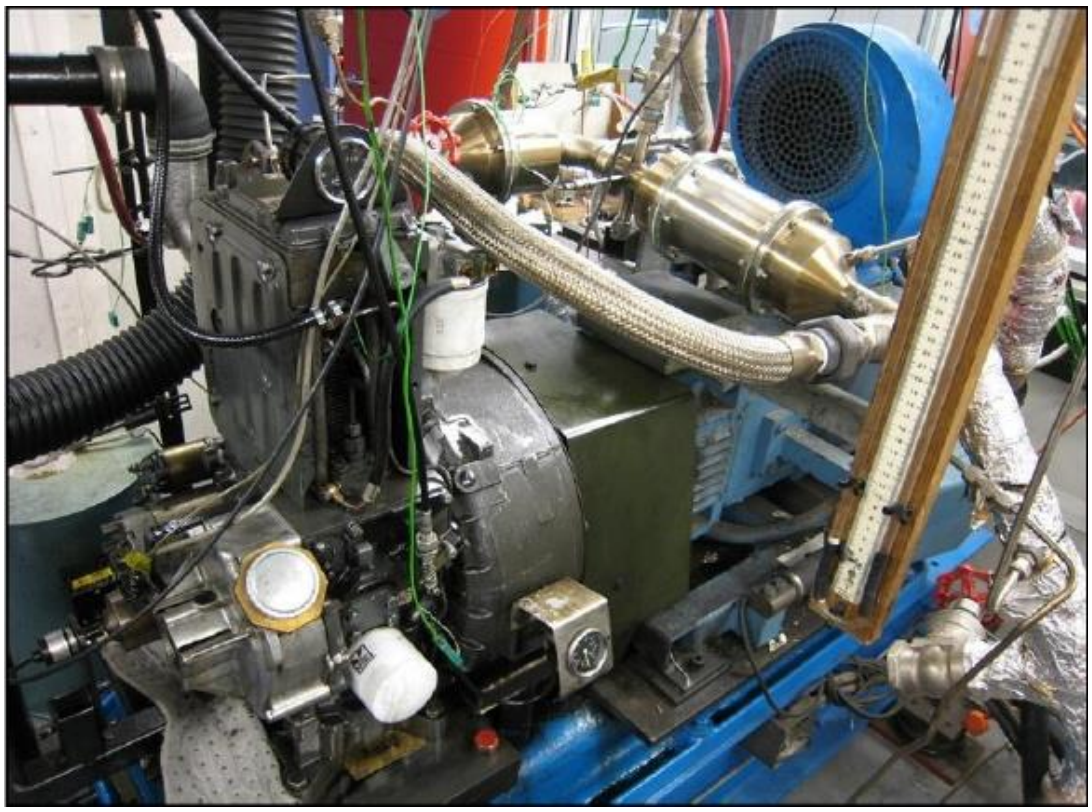

**Figure 3.1:** Engine instrumentation

## 3.1 Test engine instrumentation

The engine used in this research work is a Lister Petter model TR1 diesel engine, as shown in Fig 3.1. The engine is a single – cylinder, direct injection, naturally aspirated diesel engine. The main engine specifications are: bore 98.4 mm, stroke 101.6 mm, conrod length 165.0 mm, displacement volume 773 $cm^3$, compression ratio 15.5, maximum power 8.6 kW at 2500 rpm and

maximum torque 39.2 Nm at 1800 rpm. The standard injection timing of this engine is preset at 22 Crank Angle Degree (CAD) before the Top Dead Centre (BTDC).

The engine is motored and loaded by an electric dynamometer with a motor and a load cell. When the engine is running, the in – cylinder pressure is acquired by a KISTLER 6125B pressure transducer, mounted flush at the cylinder head and connected via a KISTLER 5011 charge amplifier to a data acquisition board. The crankshaft position was measured using a digital shaft encoder. The data acquisition and combustion analysis are carried out using an in – house (University of Birmingham) developed LabVIEW software running a National Instruments (PCI – MIO – 16E – 4) data acquisition board. Output from the engine are engine in – cylinder pressure, indicated mean effective pressure (IMEP), percentage coefficient of variation (% COV) of IMEP, average values and percentage COV of peak pressure, average crank angle for ignition delay, and other combustion information.

### 3.2 Data Processing

1) **Apparent heat release rate $\frac{dQ}{d\theta}$:** the definition given by Heywood (1998) (Heywood 1988) using the following equation:

$$\frac{dQ}{d\theta} = \frac{\gamma}{\gamma-1} p \frac{dV}{d\theta} + \frac{1}{\gamma+1} V \frac{dp}{d\theta} \qquad (3.1)$$

Where, γ is the ratio of specific heats ($C_p/C_v$), p is the instantaneous in – cylinder pressure and V is the instantaneous engine cylinder volume. The values of γ are calculated by interpolation based on the actual p – V diagrams.

2) **Indicated Mean Effective Pressure (IMEP):** calculated only from the cylinder pressure to represent the ideal average output pressure over a cycle of the engine, as expressed by the following equation:

$$\text{IMEP} = \frac{Indicated\ Work\ per\ Cycle}{Displaced\ Volume} = \frac{\oint pdV}{V_d} \qquad (3.2)$$

Where, p and V are the in – cylinder pressure and corresponding cylinder volume respectively

3) **Indicated Power $P_{ind}$ :** the indicated power is based on IMEP and expressed by the equation below:

$$P_{ind}(kW) = \frac{IMEP \times V_d \times N \times k}{1000} \qquad (3.3)$$

Where N is the engine speed in revolutions per second (rps) and k is a constant (1/2 for a 4 – stroke engine). $V_d$ ($m^3$) is the displaced volume.

4) **Displaced volume $V_d$ :** used to measure the volume swept by all the pistons inside the cylinders and is expressed as the following equation:

$$V_d = \text{A} \times \text{L} \times \text{n} \qquad (3.4)$$

Where A ($m^2$) is the piston area, L (m) is the stroke length and n is the number of cylinders

5) **Indicated specific fuel consumption (ISFC, in g/ikWh):** indicates the fuel mass flow rate ($\dot{m}_{\text{fuel}}$) per unit power output and can be expressed by:

$$\text{ISFC} = \frac{\dot{m}_{fuel}}{p_{ind}} \qquad (3.5)$$

6) **Combustion Efficiency ($\eta_C$):** indicated by the proportion that the heat produced by the combustion to the net theoretical heat potential carried by the fuel：

$$\eta_C = (\dot{m}_{fuel} \times LHV_{fuel} - \dot{m}_p \times LHV_P)/(\dot{m}_{fuel} \times LHV_{fuel}) \qquad (3.6)$$

Where the LHV values indicate the lower heat values of either the fuel the combustion

products. The products usually consider both of the complete combustion products i.e. $CO_2$ and $H_2O$ and incomplete combustion products i.e. CO, unburned HCs and soot.

7) **Engine Brake Thermal Efficiency ($\eta_{th}$):** indicating how much heat energy comes from the fuel is converted into mechanical work

$$\eta_{th} = P_{Brake}/(\dot{m}_{fuel} \times LHV_{fuel}) \qquad (3.7)$$

Where $P_{Brake}$ is the engine brake power, $\dot{m}_{fuel}$ is the fuel mass flow rate and LHV is the lower heating value

### 3.3 Catalysts

This this section details the catalyst that were provided by Johnson Matthey Plc and applied as part of this research study. One important parameter used to assess the catalysts reactivity is the gas hourly space velocity (GHSV), which is defined as the reactant's volumetric flow rate per hour over the total volume of the catalyst and with a unit $h^{-1}$:

$$GHSV\ (h^{-1}) = \frac{Gas\ flow\ rate\ over\ catalyst\ (\frac{m^3}{h})}{Catalyst\ volume\ (m^3)} \qquad (3.8)$$

Details of the catalysts are provided in the following section

**Reforming catalyst ($Ru/Al_2O_3$):** a ruthenium catalyst is chosen for ammonia reforming, given its activity in both ammonia oxidation (Schriber and Parravano 1967) and decomposition (Yin, Zhang et al. 2004, Ng, Li et al. 2007). The catalyst was

**1)** provided by Johnson Matthey and coated on 1/8 inch OD $\gamma$-$Al_2O_3$ pellet supports with a loading ratio of 2% by weight.

2) **Silver SCR catalyst ($Ag/Al_2O_3$):** The HC – SCR and $NH_3$ – SCR catalyst used was provided by Johnson Matthey; a 2 wt. % silver catalyst prepared by impregnating γ – alumina (surface area ~ 150 $m^2/g$) with aqueous $AgNO_3$ before drying and calcining in air for 2 h at 500 ℃. The catalyst was made into an aqueous suspension, which was then uniformly coated onto ceramic monolith substrates (diameter 1 inch, length 3 inches) with 600 cpsi cell density

3) **Diesel Oxidation Catalyst ($Pt/Al_2O_3$):** the DOC used was provided by Johnson Matthey, prepared by impregnation of a low loading supported Pt based catalyst coated on a cordierite honeycomb monolith substrate with diameter of 115mm and length 75mm and with high cell density (600 cpsi)

### 3.4 Mini Reactor Setup

While catalyst like the DOC detailed above can be applied in a full scale (the size commercially adopted) in the test engine exhaust manifold, smaller catalysts (e.g. extruded from the full size catalyst) are often more flexible and convenient in terms of performance evaluation and catalyst characterisation. For instance, smaller catalyst can be loaded into a specially designed reactor and put into an electric furnace for reaction temperature control, which would otherwise depend on the real engine exhaust temperature if being applied directly into the exhaust manifold. In the current research, a reactor is designed to fit the mini catalysts all measured at or below 1 inch (25.3mm); the selected catalyst i.e. pellets or monolith is loaded inside of the reactor. A schematic diagram in Fig. 3.2 is used to display the design of the mini reactor, where both of the

reactor's size and configuration can be changed using different parts to cater for different catalysts and applications.

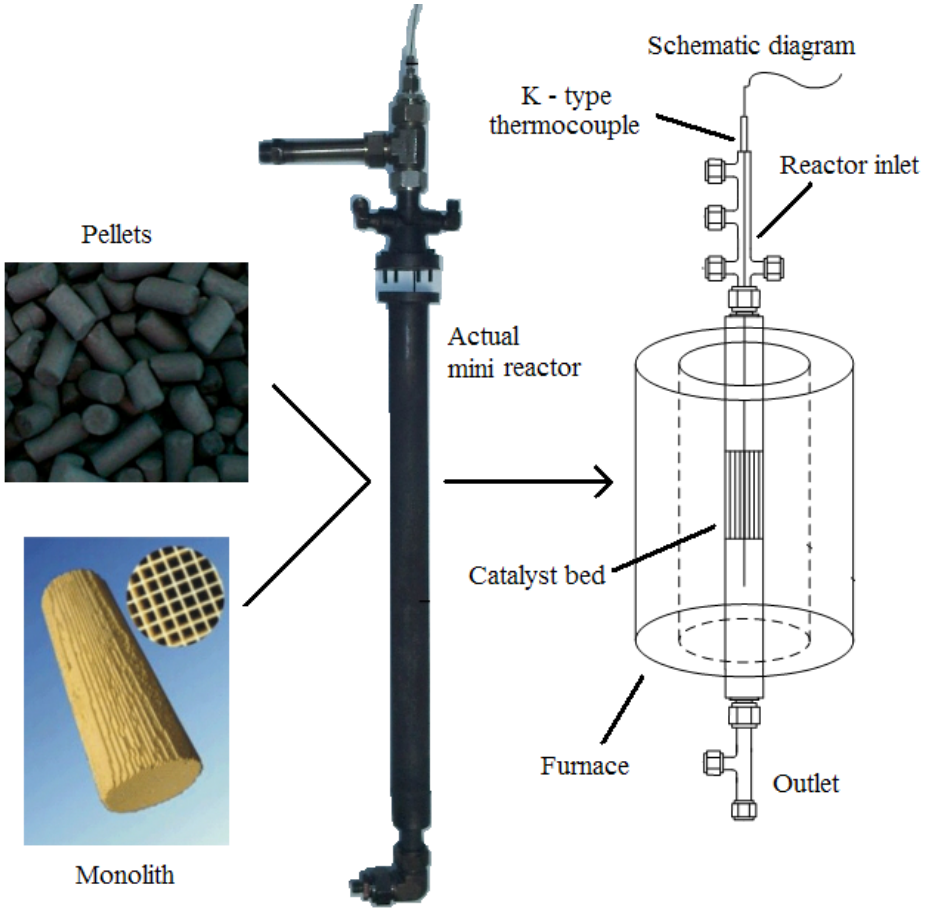


**Figure 3.2:** Detailed reactor/reformer setup and its schematic diagram

### 1) Mini $NH_3$ Reformer Setup

All reforming tests were carried out in a laboratory reforming reactor, which is configured similarly to the one shown in Fig. 3.2. The $Ru/Al_2O_3$ pellets are loaded inside a stainless steel reactor (15 mm in diameter) that is held vertically within a tube furnace. At the centre of the catalyst bed, a tubular sheath is fitted, which is made from a stainless steel tube with one end

sealed. In order to investigate the process's thermal behaviour, a k-type thermocouple is inserted into the sheath to record the reaction temperature along the catalyst bed. Ammonia is supplied by a gas bottle and injected into the reactor, controlled by a flow metre. Nitrogen and air are introduced at separate inlets of the reactor. Before each experiment, inert nitrogen is initially introduced through the reactor to make sure the temperature gradient along the catalyst bed is minimised. For ammonia exhaust gas reforming part of the diesel engine exhaust is extracted from the exhaust manifold and is introduced into the reactor. The exhaust flow rate was controlled to meet different $O_2/NH_3$ ratios.

**2) SCR Reactor Setup**

The $Ag/Al_2O_3$ monolith is loaded in a similar tubular reactor (with 25mm in diameter) as well, which is connected to the engine exhaust pipe downstream the engine outlet. Part of the exhaust gas is extracted and introduced into the reactor. The flow rate of the exhaust gas was controlled using a flow meter to keep a constant catalyst gas hourly space velocity (GHSV), and the reactor temperature is controlled by means of furnace. A K – type thermocouple was placed before SCR to record its inlet temperature. To add gaseous reactant such as $NH_3$ and $H_2$ into the SCR reactor, gases bottles or the outlet of the mini $NH_3$ reformer can be connected to the engine exhaust before the SCR reactor extraction point. The gaseous additions are all controlled by flow meters. To add hydrocarbons as reactant, the selected HC was supplied by an electric syringe pump and injected and atomised by an in-house built atomiser.

### 3.5 Diesel Fuel

The ultra – low sulphur diesel (ULSD) fuel used in this was supplied by Shell Global Solutions UK. The main physical and chemical fuel properties are shown in Table 3.1

**Table 3.1:** Test ULSD composition

| **Fuel Analysis** | **Method** | **Diesel (ULSD)** |
|---|---|---|
| **Cetane Number** | ASTM D613 | 53.9 |
| **Density at 15 ℃ (kg/m$^3$)** | ASTM D4052 | 827.1 |
| **Viscosity at 40 ℃ (cSt)** | ASTM D445 | 2.467 |
| **50% distillation ( ℃)** | ASTM D86 | 264 |
| **90% distillation ( ℃)** | ASTM D86 | 329 |
| **LCV (MJ/kg)** | | 42.7 |
| **Sulphur (mg/kg)** | ASTM D2622 | 46 |
| **Aromatics (% wt)** | | 24.4 |

### 3.6 Exhaust Gas Analysis and Measuring Equipment

- A **MKS MultiGAS 2030 FTIR analyser** (Fourier Transform Infrared Spectroscopy) is applied to analyse the gas component in the engine exhaust or at the reactor outlet. To obtain the gas information, the FTIR analyser emits at once a beam that contains several frequencies of light to measure how much of that beam is absorbed by the sample (i.e. gas components), then, the beam is modified to involve different combination of frequencies, and this process will be repeated till several data points can be generated. These data points will be used to infer what the absorption (of the sample) is at each wavelength and therefore confirm the sample species. The MKS MultiGAS 2030 FTIR analyser is capable of measuring gaseous species including NO, $NO_2$, $N_2O$, $NH_3$, HCs, CO, $CO_2$ and $H_2O$ (except for $N_2$, $H_2$ and $O_2$). Some of the major specifications of this analyser are summerised and listed in Table 3.2,

while its detection limits are shown in Table 3.3

Table 3.2 Specifications of MKS MultiGas 2030 FTIR analyser

| | |
|---|---|
| Measurement Technique | FTIR Spectrometry |
| Ranges | Concentration settings between 10 ppb and 100% full scale |
| Spectral Resolution | 0.5 – 16 $cm^{-1}$ |
| Scan Speed | 1 scan/sec @ 0.5 $cm^{-1}$ |
| Scan Time | 1 – 300 sec |
| Infrared Source | Silicon Carbide |
| Reference Laser | Helium Neon (15798.2 $cm^{-1}$) |
| Detector | $LN_2$ – cooled MCT; TE – cooled MCT |
| Purge Pressure | 20 psig (1.5 bar) max. |
| Spectrometer Purge Flow | 0.2 l/min of dry $N_2$ or $CO_2$ free clean dry air with dewpoints below – 70 ℃ |
| Optics Purge Flow | 0.2 l/min of dry $N_2$ or $CO_2$ free clean dry air with dewpoints below – 70 ℃ |
| Sample Temperature | Ambient to 191 ℃ (calibration temperature dependent) |
| Sample Flow | 0.2 – 20 l/min |
| Sample pressure | 0.01 – 4 atm ( calibration pressure dependent) |

Table 3.3 Detection limits of MKS MultiGas 2030 FTIR analyser

| Formula | Lowest detected limit with 20/20$^{TM}$ Cell and 1 sec Measurement |
|---|---|
| $NH_3$ | 0.5 ppm |
| $CO_2$ | 0.2 ppm |
| CO | 1.2 ppm |
| $H_2CO$ | 0.6 ppm |
| HCI | 1.5 ppm |
| HF | 0.2 ppm |
| $CH_4$ | 0.6 ppm |
| $NO_2$ | 0.4 ppm |
| NO | 3.6 ppm |
| $NF_3$ | 0.5 ppm |
| $SiF_4$ | 0.15 ppm |
| $SO_2$ | 0.6 ppm |
| $CF_4$ | 40 ppb |
| $C_8H_{10}$ | 1.0 ppm |

- An **AVL DIGAS 440 non – dispersive IR** analyser is used to measure $O_2$ through an electrochemical method. By utilising the fact that molecules absorb specific frequencies, the Infrared spectroscopy is capable of matching the frequency of the absorbed radiation to the transition energy of the bond or group (of the sample) that vibrates, hence determine the sampled species. The AVL DIGAS 440 non – dispersive IR used in this study also provides measurements including CO, $CO_2$ (by Non – Dispersive Infrared detector i.e. NDIR) and NOx (by chemiluminescence method). These measurements are compared to those measured by the FITR analyser. The measurement range and resolution of this IR analyser are shown in Table 3.4

Table 3.4 Measurement range and resolution of AVL DIGAS 440 – non dispersive IR

| | Measurement range: | Resolution |
|---|---|---|
| CO | 0 – 10 vol% | 0.01 vol% |
| HC | 0 – 20000 ppm | 1 ppm |
| $CO_2$ | 0 – 20 vol% | 0.1 vol% |
| $O_2$ | 0 – 22 vol% | 0.01 vol% |
| $NO_2$ | 0 – 5000 ppm | 1 ppm |
| Lambda | 0 – 9.999 | 0.001 |
| Engine Speed | 400 – 6000 $min^{-1}$ | 1 $min^{-1}$ |
| Oil Temperature | -30 – 125 ℃ | 1 ℃ |

- A **HP 5890 series II gas chromatograph** (GC) equipped with a thermal conductivity detector (TCD) is used to measure hydrogen. Argon is used as carrier gas due to its low thermal conductivity (0.024 W/m/K). This is less similar to the thermal conductivity of $H_2$ when compared to the other carrier gases. There are two columns for the sample gas. The first column was 1m long with a 1/8 – in. diameter Haysep Q, 80 – 100 mesh. The second column

was a 2m long 1/8 – in. diameter Molesieve 5Å (MS5A). The H2 chromatogram area was measured using a HP 3395 integrator. Before taking any gas samples, the device is calibrated use gas bottle that contains 30 % $H_2$ with the rest being the balance $N_2$. This allows the integrator to plot an area that represents the 30 % $H_2$ in the gas mixture. When taking the actual measurement, another plot is made. Hence the actual volumetric $H_2$ concentration is able to be extrapolated from the calibrated value.

- A **TSI scanning mobility particle sizer** (SMPS) 3080 electrostatic classifier is employed to establish the particle size distribution. This is comprised of an electrostatic classifier series 3080, a 3081 Differential Mobility Analyser (DMA) and a model 3775 Condensation Particle Counter (CPC). For measuring particle concentrations lower than 5x104 particles/$cm^3$, the CPC provides a particle count accuracy of $\pm 10\%$, whilst $\pm 20\%$ is provided for measuring particle concentrations lower than 107 particles/$cm^3$. The measurement (diameter) range is nominally either 12 – 437nm or 14 – 670nm with a dilution ratio set to 200:1 using a heated rotating disc diluter (150℃). When taking the exhaust samples, the possibility of any HC condensation and nucleation is minimized by the temperature controlled dilution process.

# CHAPTER 4: AMMONIA AS A HYDROGEN CARRIER FOR TRANSPORTATION; INVESTIGATION OF THE AMMONIA EXHUAST GAS FUEL REFORMING

## 4.1 Introduction

The main aim of this research is to study the feasibility of ammonia exhaust gas reforming for fulfilling the on – board hydrogen demand in the aspects of engine combustion (i.e. alternative to hydrocarbons) and aftertreatment systems (i.e. reactants and/or reaction promoters). As reported in earlier studies (Ganley, Seebauer et al. 2004, Yin, Zhang et al. 2004, Saito, Mitsui et al. 2009, Plana, Armenise et al. 2010), a temperature higher than 500 ℃ is usually required for catalytic $NH_3$ decomposition in order to achieve stable $NH_3$ conversion and high $H_2$ production. However, for on-board applications the exhaust gas temperature of a typical diesel engine is only in the range of 150 – 400 ℃. Thus a mechanism is required to raise the temperature of the gas stream for the purpose of on-board $NH_3$ decomposition. The new approach is to apply the same principle as that of autothermal reforming (ATR) and exhaust gas fuel reforming, where part of the fuel is oxidised to provide the energy needed by a subsequent fuel reforming mechanism to produce $H_2$. If sufficient ammonia oxidation takes place, the endothermic ammonia decomposition can be self – sustaining using the provided heat.

The expected selective catalytic oxidation of ammonia (into nitrogen and water) and $NH_3$ decomposition reactions are expressed by Eq. (4.1) and (4.2), respectively. The desired combination is shown by Eq. (4.3).

$$4NH_3 + 3O_2 = 6H_2O + 2N_2; \quad \Delta H_r = -1260 \text{ kJ/mol} \qquad (4.1)$$

$$2NH_3 = 3H_2 + N_2; \qquad \Delta H_r = +46 \text{ kJ/mol} \qquad (4.2)$$

$$NH_3 + xO_2 = 2xH_2O + (1.5\text{-}2x)\ H_2 + 0.5N_2; \qquad x < 0.75 \quad (4.3)$$

In Eq. (4.3), x represents the $O_2/NH_3$ molar ratio, a parameter which controls the intensity of the exothermic portion in the overall process, which can in turn determine the stoichiometric yield of hydrogen. In the current study, air is used to provide the oxygen needed by the reaction and is referred to $NH_3$ – ATR throughout. Furthermore, if diesel engine exhaust is used to provide the $O_2$, and part of the exhaust heat is recovered as a primary energy source for the reaction then the $NH_3$ – ATR is transformed into $NH_3$ exhaust gas reforming.

The catalyst's activity in ammonia decomposition was studied first. Test conditions including catalyst inlet temperature, gas-hourly-space-velocity (GHSV) and catalyst inlet $NH_3$ concentrations were varied (Table 4.1). Following that $NH_3$ – ATR was performed at two catalyst loadings: 8 g and 16 g, whereas $NH_3$ exhaust gas reforming was studied over the 16 g catalyst only. A $NH_3$ flow of 3 l/min was used throughout the $NH_3$ – ATR and Exhaust gas reforming. Air and engine exhaust were added into the $NH_3$ flow at varying $O_2/NH_3$ ratios and $NH_3$ concentrations (Table 4.2). A 400 ℃ reactor temperature was maintained using a furnace to simulate the diesel exhaust temperature at mid – high load operation to give the reactor the primary heat. The experimental setup is given in the Fig. 4.1, where $NH_3$ with either air or exhaust extracted from the engine are introduced.

**Table 4.1:** Test conditions for $NH_3$ – ATR and $NH_3$ exhaust gas reforming

| | **$NH_3$ (l/min)** | **$N_2$ (l/min)** | **Total flow (l/min)** | **$NH_3$ (%)** | **Cat. inlet temp (℃)** | **GHSV ($h^{-1}$)** |
|---|---|---|---|---|---|---|
| Temperature effect | 2 | - | 2 | 100 | 300 - 800 | 18000 |
| GHSV effect | 2 - 4 | - | 2 - 4 | 100 | 800 | 18000 - 36000 |
| $NH_3$ Conc. effect | 2 - 4 | 0 - 2 | 4 | 50 - 100 | 300 - 800 | 36000 |

**Table 4.2:** Test conditions for $NH_3$ decomposition

| | **8 g catalyst bed ($NH_3$ - ATR)** | | | **16 g catalyst bed ($NH_3$ - ATR)** | | | **16 g catalyst bed ($NH_3$ Exhst. Ref.)** | | |
|---|---|---|---|---|---|---|---|---|---|
| $O_2/NH_3$ | Tot. Flow (l/min) ($NH_3$ + Air) | GHSV ($h^{-1}$) | $NH_3$ Conc. (%) | Tot. Flow (l/min) ($NH_3$ + Air) | GHSV ($h^{-1}$) | $NH_3$ Conc. (%) | Tot. Flow (l/min) ($NH_3$ + Exh) | GHSV ($h^{-1}$) | $NH_3$ Conc. (%) |
| 0.04 | - | - | - | 3 + 0.67 | 13392 | 84 | 3 + 0.79 | 14230 | 79.05 |
| 0.06 | 3 + 0.86 | 28928 | 77.78 | 3 + 0.86 | 14464 | 77.78 | 3 + 1.19 | 15720 | 71.56 |
| 0.08 | 3 + 1.14 | 31071 | 72.41 | 3 + 1.14 | 15535 | 72.41 | 3 + 1.58 | 17210 | 65.37 |
| 0.09 | 3 + 1.29 | 32142 | 70.00 | 3 + 1.29 | 16071 | 70.00 | 3 + 1.78 | 17955 | 62.65 |

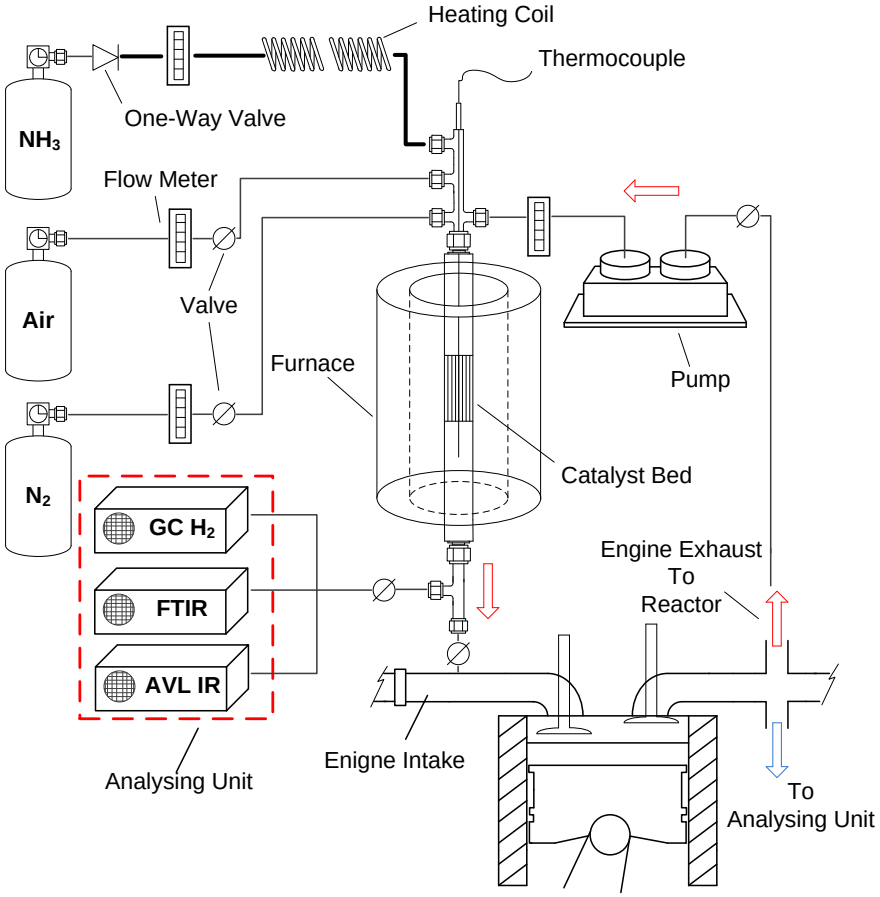


**Figure 4.1:** Experimental setup for $NH_3$ exhaust gas reforming

## 4.2 $NH_3$ decomposition over Ru – $Al_2O_3$ catalyst

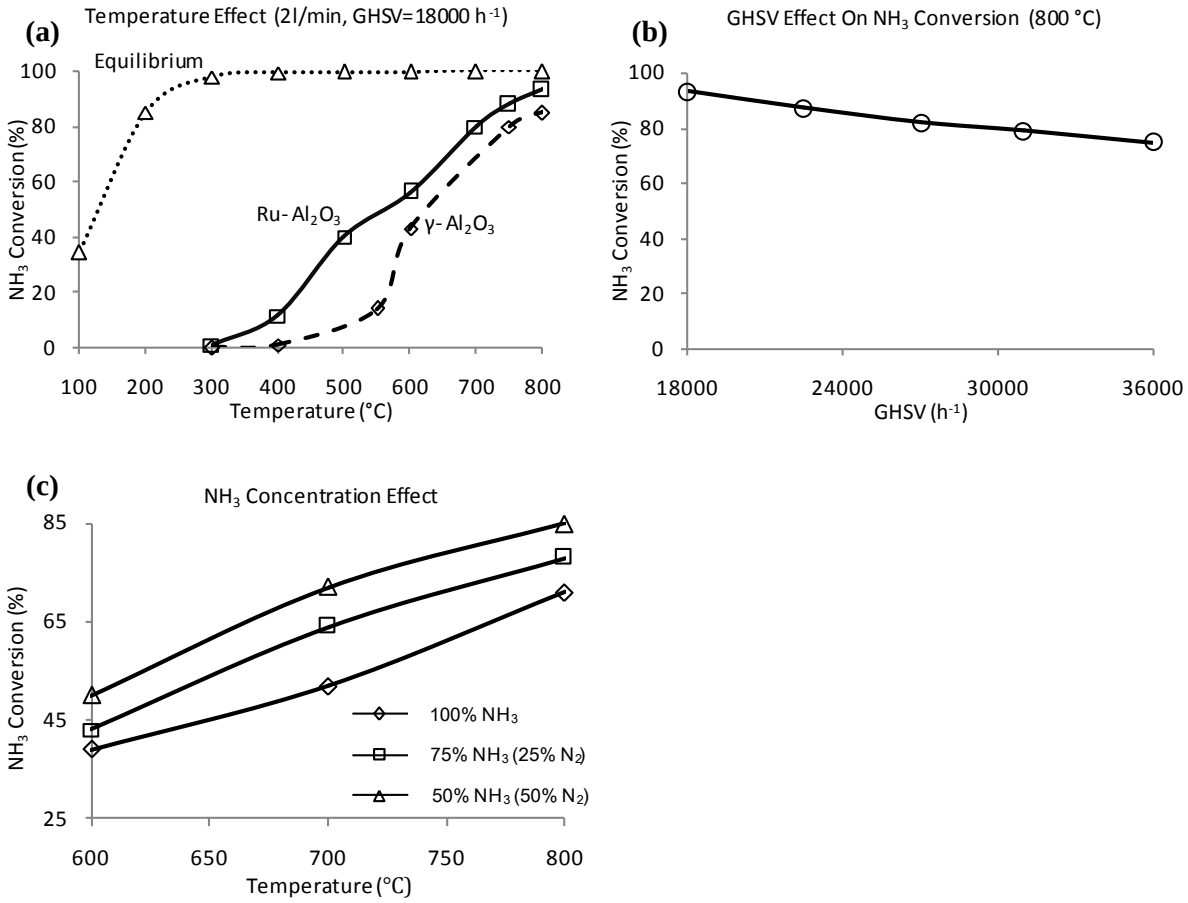


**Figure 4.2:** $NH_3$ decomposition over Ru – $Al_2O_3$ catalyst: (a) 2 l/min (GHSV = 18000 $h^{-1}$) of pure ammonia decomposed at different temperatures, (b) 2 – 4 l/min of pure ammonia decomposition at different GHSV, and (c) ammonia conversion at different $NH_3$ concentrations in the $NH_3$ – $N_2$ mixtures and temperatures.

***Temperature effect***: Fig. 4.2 (a) depicts the decomposition of pure $NH_3$ at different reactor inlet temperatures. In addition to experimental results, an equilibrium calculation for $NH_3$ decomposition was made using a STANJAN equilibrium model (v 3.91, Stanford University) at the same temperatures as those of the experimental studies. As predicted by the equilibrium simulation, increased temperature leads to increased $NH_3$ conversion due to enhanced

decomposition kinetics and rate (Gay and Ehsani 2003). 100% conversion without catalytic promotion is calculated for temperatures as low as 300 ℃. However, when the non-catalytic decomposition was experimentally performed over the plain $\gamma$-$Al_2O_3$ pellet support, no significant $NH_3$ conversion was observed until the reactor inlet temperature reached 500 ℃. The same discrepancy was observed in literature (Yin, Zhang et al. 2004) and (Ishimatsu, Saika et al. 2004), which implies the equilibrium of non – catalytic $NH_3$ decomposition was hard to achieve at lower reaction temperatures. Hence, catalytic assistance must be adopted for easier activation: in the presence of ruthenium catalyst, the $NH_3$ decomposition light off temperature was reduced to 300 ℃ in the current study, and NH3 conversion was higher, than with only alumina, across the whole temperature range.

From the results presented, it is clear that to achieve $NH_3$ decomposition in the relatively low temperature range applicable to diesel exhaust i.e. 150 – 400 ℃, the decomposition needs to be accompanied by an exothermic reaction. Therefore, adding an oxygen containing flow (air or exhaust) into the reactor is needed to promote the desired autothermal reaction, i.e. Eq. (4.3). This results in a variation in GHSV (increased total flow), and in diluted $NH_3$ feed ($NH_3$ mixed with oxygen containing flow). Thus prior to the $NH_3$ – ATR and $NH_3$ exhaust gas reforming, both GHSV and $NH_3$ inlet concentration were varied separately to study their impacts on the catalyst activity.

***GHSV effect***: As shown by Fig. 4.2 (b), when the catalyst inlet temperature was fixed at 800 ℃, increasing GHSV decreased the ammonia conversion from around 95% at 18000 $h^{-1}$ to 75% at 36000 $h^{-1}$. This is due to reduced residence time of the $NH_3$ over the catalyst at the region where

the endothermic reaction is active (i.e. will be described in the following sections) resulting in lowered decomposition efficiencies (Chein, Chen et al. 2010).

***$NH_3$ Concentration effect***: Fig. 4.2 (c) illustrates the ammonia conversion as a function of temperature and ammonia concentration in the feed gas. Instead of using pure $NH_3$, nitrogen was co - fed into the reactant stream. The total inlet flow was kept constant at 4 l/min, resulting in a GHSV of 36000 $h^{-1}$. It is shown that as the inlet ammonia concentration reduced, the $NH_3$ conversion increased for a fixed temperature. In earlier studies, hydrogen was found to be inhibitive to $NH_3$ decomposition. This is because the $NH_3$ decomposition is limited by a chemical equilibrium between the forward and reverse reactions. A high $H_2$ partial pressure and a low reaction temperature will contribute to a retarded forward rate of the $NH_3$ decomposition (Löffler and Schmidt 1976, Tsai, Vajo et al. 1985, Bradford, Fanning et al. 1997, Zheng, Zhang et al. 2007, Prasad, Karim et al. 2009). This explains the shift of $NH_3$ conversion to higher temperatures as the ammonia concentration in the feed gas increased. When the $NH_3$ concentration is higher in a constant reactant flow, the amount of $H_2$ produced is higher and thus the inhibition is more pronounced (Plana, Armenise et al. 2010). The other product of the reaction, $N_2$, is seen to have negligible influence on the forward rate (Zheng, Zhang et al. 2007, Prasad, Karim et al. 2009, Plana, Armenise et al. 2010). In the current study, nitrogen behaved mainly as an inert gas, which diluted the inlet $NH_3$ to lower concentrations. In this case, reactions with lower inlet $NH_3$ concentrations show similar conversions at lower temperatures as those with high concentrations of $NH_3$.

## 4.3 Combined $NH_3$ oxidation and decomposition: $NH_3$ – ATR and $NH_3$ exhaust gas reforming

### 4.3.1 Temperature profiles

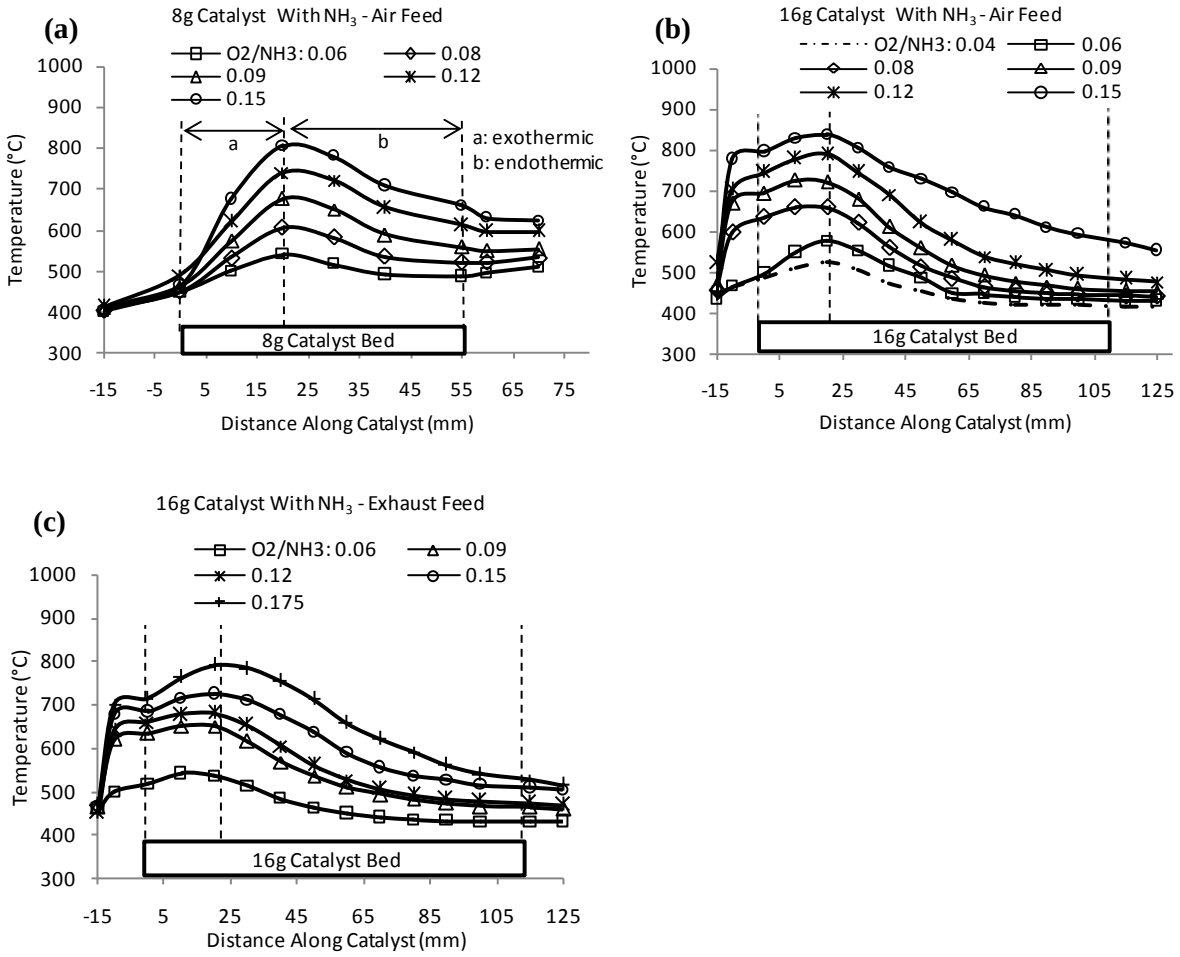


**Figure 4.3:** Temperature profiles: (a) and (b) temperature profiles of $NH_3$ - ATR over 8g and 16g catalyst beds (c) temperature profiles of $NH_3$ exhaust gas reforming over 16g catalyst bed.

In Fig. 4.3 (a) – (c), the thermal behaviour of the combined reaction (Eq. (4.3)) at different $O_2/NH_3$ ratios was reflected by the temperature profile along the catalyst bed. For both $NH_3$ – ATR and $NH_3$ exhaust gas reforming, the reactor temperature increased abruptly near the catalyst

inlet and declined thereafter. The temperature rise at catalyst inlet was due to $NH_3$ oxidation (Eq. (4.1)); the decrease was associated with the endothermic ammonia decomposition (Eq. (4.2)) and the reactor heat losses (Tsolakis, Megaritis et al. 2005). Such observation is in agreement with previous researches (Löffler and Schmidt 1976, Tsolakis and Golunski 2006), where mechanisms of exothermic and endothermic were combined and performed.

In general, by varying the $O_2/NH_3$ ratio from 0.04 to 0.175 in both $NH_3$ – ATR and exhaust gas reforming, the temperature increase along the catalyst bed was enhanced, meaning increased oxygen input promoted the exothermic reaction. In addition to that, the higher the $O_2/NH_3$ ratio, the larger the temperature drop in the endothermic area, indicating improved $NH_3$ decomposition along the catalyst bed (this will be confirmed by increased hydrogen formation shown in the next section).

For $NH_3$ – ATR (Fig. 4.3 (a) and (b)), similar temperature increases were observed over the 8 g and 16 g catalyst beds. However, compared to the 8 g catalyst bed, the temperature decrease was found to be more pronounced at the 16 g catalyst at each tested $O_2/NH_3$ ratio. This is caused by the greatly increased residence time over the 16 g catalyst strengthening the $NH_3$ decomposition through a better use of the available enthalpy (Chein, Chen et al. 2010).

When $NH_3$ – exhaust mixtures were introduced into the 16 g catalyst, the rise in temperature profiles (Fig. 4.3 (c)) were slightly weakened at each $O_2/NH_3$ condition compared to those for the tests with air. As the engine exhaust contains only 10 – 15% oxygen by volume, the flow of the exhaust required to maintain the same $O_2/NH_3$ ratio was increased from that of the air,

and so was the GHSV (Table. 4.2). The main diesel exhaust gas components (e.g. $CO_2$ and $H_2O$) are known as heat absorbers due to their relatively large specific heat capacities (Ladommatos, Adelhalim et al. 2000). Therefore, the temperature decrease in the reactor could be associated with the heat absorption of those species.

### 4.3.2 $NH_3$ conversion and $H_2$ production.

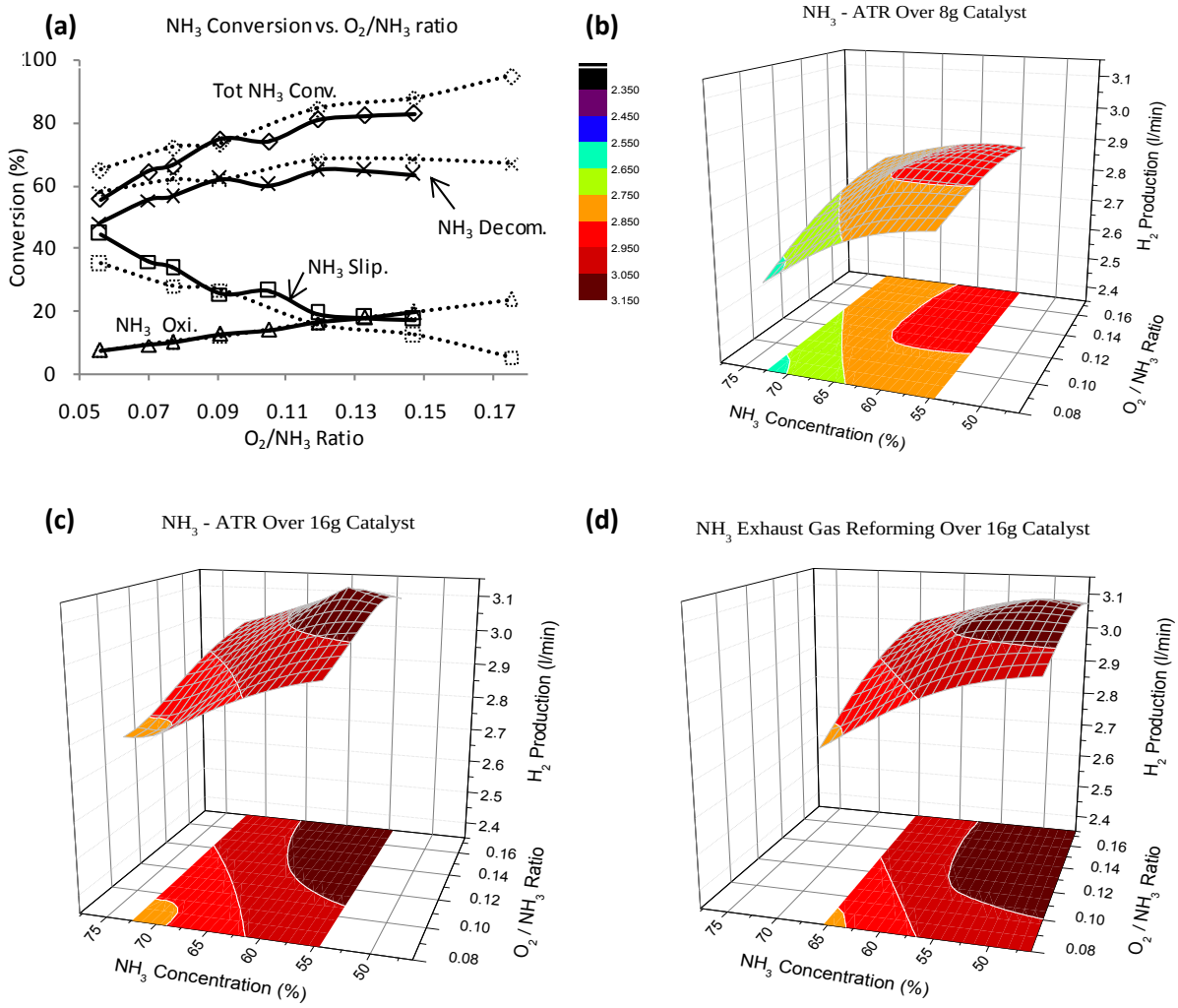


**Figure 4.4:** (a) $NH_3$ conversion in $NH_3$ – ATR at different $O_2/NH_3$ ratios over 8g and 16g catalysts; dotted line: 16g catalyst, solid line: 8g catalyst. (b) – (d): $H_2$ production as a function of

$NH_3$ concentration and $O_2/NH_3$ ratio; (b) $NH_3$ – ATR over 8g catalyst, (c) $NH_3$ –ATR over 16g catalyst and (d) $NH_3$ exhaust gas reforming over 16g catalyst.

The $NH_3$ conversion at different $O_2/NH_3$ ratio is depicted in Fig. 4.4 (a) for $NH_3$ – ATR over the 8 g and 16 g catalysts. The amounts (in percentage) of $NH_3$ decomposed and oxidised are shown separately. The overall $NH_3$ conversion is presented as the sum of oxidised and decomposed $NH_3$ excluding any $NH_3$ slippage. As being consistent to the reaction's thermal behaviour indicated in Fig. 4.3 (a) and (b), the increased $O_2/NH_3$ ratio enhanced simultaneously the $NH_3$ oxidation and decomposition. Nevertheless, increasing $O_2/NH_3$ ratio to 0.175 did not further promote the $NH_3$ decomposition. However, it suppressed the $NH_3$ slippage through oxidation: the amount of $NH_3$ consumed in oxidation reached the maximum. It is also worth noticing that the $O_2$ content in each individual run was used completely, and no NO, $NO_2$ or $N_2O$ formation was detected.

In addition to the $NH_3$ conversion, Fig. 4.4 (b) – (d) plot the produced $H_2$ as a function of $O_2/NH_3$ ratio and the $NH_3$ inlet concentration (at each $O_2/NH_3$ ratio, see Table 4.2) for both of the $NH_3$ – ATR and $NH_3$ exhaust gas reforming. With more $NH_3$ decomposed at higher $O_2/NH_3$ ratios, higher $H_2$ production was achieved.

Furthermore, the $NH_3$ inlet concentration at every $O_2/NH_3$ ratio is identical for $NH_3$ – ATR over the 8 g and 16 g catalyst beds (the same projected area in Fig. 4.4 (b) and (c)). Therefore, the improved $H_2$ production at the 16 g bed confirmed the more favorable reaction conditions provided by the longer catalyst, and is in agreement with the temperature profiles discussed earlier.

Compared to the $NH_3$ – ATR at the 16 g catalyst, the $NH_3$ exhaust gas reforming over the same catalyst (Fig. 4.4 (d)) was performed at lower inlet $NH_3$ concentration at each tested $O_2/NH_3$ ratio (due to the increased overall inlet flow, Table 4.2). Although the reactor temperature was reduced during the $NH_3$ exhaust gas reforming (Fig. 4.3 (c)), at the same $O_2/NH_3$ ratio, hydrogen production is found to be approximately equivalent to that of the $NH_3$ – ATR. This observation can be explained by the $NH_3$ concentration effect shown in Fig. 4.2 (c): less concentrated $NH_3$ in the exhaust allows ammonia decomposition to perform similarly to that of the $NH_3$ – ATR, but at lower temperatures.

**4.4 Reforming efficiencies.**

The process efficiency $\eta$ was defined as the lower combustion enthalpy rate (kJ/sec) of the product stream divided by the lower combustion enthalpy rate (kJ/sec) of the reactant stream. Here, the product stream can be either defined as the produced $H_2$ alone or $H_2$ combined with any unconverted $NH_3$ (both can be considered as fuel alternative to the engine). Thus two efficiencies, namely hydrogen efficiency and reforming process efficiency can be adopted to evaluate the reforming performance. These are defined by Eq. (4.4) and (4.5) below:

$$\eta_{H_2}(\%) = \frac{LCV_{H_2} \times \dot{m}_{H_2}}{LCV_{NH_3} \times \dot{m}_{NH_3}} \times 100\% \qquad (4.4)$$

$$\eta_{ref}(\%) = \frac{(LCV_{H_2} \times \dot{m}_{H_2}) + (LCV_{NH_3} \times \dot{m}_{NH_3})}{LCV_{NH_3} \times \dot{m}_{NH_3}} \times 100\% \qquad (4.5)$$

Where $LCV_{H2}$ and $LCV_{NH3}$ are the lower calorific values of the produced $H_2$ and the gas feed $NH_3$, whereas $\dot{m}_{NH3}$ and $\dot{m}_{H2}$ are the mass flow rates of $NH_3$ and $H_2$ respectively.

The hydrogen efficiency (Eq. (4.4)) and reforming process efficiency (Eq. (4.5)) of the $NH_3$ exhaust gas reforming are shown in Fig. 4.5. Although the hydrogen efficiency was improved at high $O_2/NH_3$ ratios i.e. higher $H_2$ production, the reforming process efficiency decreased due to larger $NH_3$ consumption in exothermic oxidation. Thus a trade – off is shown between these efficiencies. Based on the fact that the produced reformate could be provided with higher energy content (due to heat recovery) than its original form i.e. $NH_3$ also assuming the combustion efficiencies of $NH_3$ and $H_2$ are the same as the diesel's, then it seems that applying the carbon – free reformate (as fuel/energy carrier) to an engine under a lower $O_2/NH_3$ ratio (e.g. 0.06) would be more beneficial in terms of diesel fuel replacement and engine $CO_2$ emission.

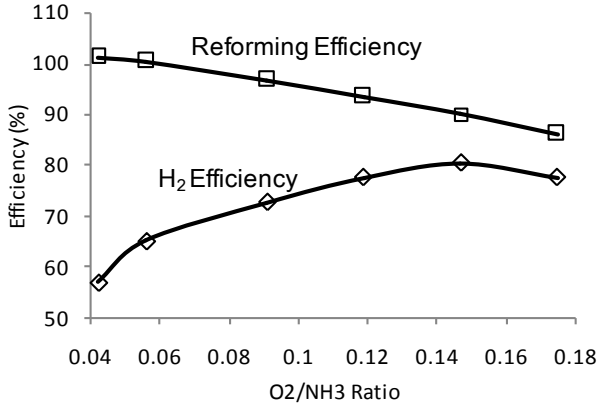


**Figure 4.5:** $NH_3$ exhaust gas reforming Process efficiencies

## 4.5 Summary

From the study presented here, the feasibility of ammonia exhaust gas reforming as a strategy for hydrogen production used in transportation was shown. The $O_2/NH_3$ ratio and $NH_3$ concentration were the key factors that dominated both of the hydrogen production and the reforming process efficiencies. By applying an $O_2/NH_3$ ratio ranging from 0.04 to 0.175, 2.5 to 3.2 l/min of gaseous $H_2$ production was achieved using a fixed $NH_3$ feed flow of 3 l/min.

However, A trade – off was shown between the $H_2$ production and the reforming efficiency when higher $H_2$ purity (i.e. low unconverted $NH_3$ with high $H_2$ efficiency) was pursued. Nevertheless, to maximise the reformate's energy (i.e. higher LHV value) content available for engine combustion, those produced at lower $O_2/NH_3$ ratios (i.e. less $H_2$ and more unconverted $NH_3$) seemed to be more advantageous in energy carrying, so is expected to replace more diesel fuel in the combustion process. However, this is only based on an assumption that the reformate's combustion could be as efficient as that of diesel. Hence an actual combustion process is suggested to verify the reformate's effectiveness as a fuel alternative.

In addition to the engine combustions, potential application of the $NH_3$ reformate can also be suggested over the exhaust gas aftertreatment devices, at which "$H_2$ effect" is observed on promoting the devices performances, e.g. NO to $NO_2$ conversion over DOC or NOx reduction over a SCR. However, the application can be highly subject to the reformate's hydrogen purity and limited by the nature of the application. The DOC for instance could oxidise the $NH_3$ if any being brought by the reformate to form NOx, Therefore, reforming process with high $H_2$

efficiency would be needed for this specific application. Nevertheless, for the NOx abatement over a SCR catalyst, e.g. $Ag/Al_2O_3$, the application would be potentially favoured by both of the presences of $H_2$ and $NH_3$.

# CHAPTER 5: COMBUSION OF $NH_3$ REFORMATE IN DIESEL OPERATION; THE IMPACTS ON ENGINE PERFORMANCE AND EMISSIONS

## 5.1 Introduction

In this chapter, the $NH_3$ reformate produced by the reformer or simulated by means of bottled gas was sent back to the engine for partial diesel replacements. To start with, an engine study was carried out using small amounts of reformate produced under different reforming efficiencies (demonstrated in Chapter 4). The $NH_3$ flow of 3 l/min used previously in chapter 4 for $NH_3$ exhaust gas reforming was kept the same for the current study, while several $O_2/NH_3$ conditions were selected representing different combinations of $H_2 - NH_3$ compositions and the reforming efficiencies. Table 5.1 lists the engine intake volumetric flow rates of hydrogen and ammonia. The same experimental setup used in chapter 4 (Fig. 4.1) was adopted but with the reactor outlet being connected back to the engine intake, so the produced reformate was able to be redirected and premixed into the intake air charge. The identical engine condition i.e. 4 Bar IMEP at 1500 rpm was also adopted for consistency.

**Table 5.1:** Reformate flow rates under different reactor conditions and their compositions in the engine intake

| $O_2/NH_3$ | $\eta_{ref}$ (%) | $\eta_{H2}$ (%) | $H_2$ (l/min) | $NH_3$ (l/min) | Total (l/min) |
|---|---|---|---|---|---|
| 0.06 | 102 | 67 | 2.6 | 1.05 | 3.65 |
| 0.12 | 95 | 78 | 2.9 | 0.47 | 3.37 |
| 0.15 | 91 | 80 | 3.2 | 0.29 | 3.49 |
| 0.175 | 88 | 77 | 3.0 | 0.28 | 3.28 |

Following the above study, the reformate was simulated by means of bottled hydrogen and $NH_3$, and the same induction strategy used for the produced reformate was employed here too i.e. in a form of port fuel injection, see Figure 5.1. For the purpose of this engine combustion study, only $H_2$ and $NH_3$ were considered as the effective (combustible) reforming products. The obtained volumetric $H_2$ to reformate ($H_2$ + $NH_3$) ratio in the previous chapter was ranging from 0.5 to 0.9 with roughly an increase of 0.1 from one reforming condition to another. Hence to simulate the reformate gas, the same $H_2$/reformate ratio obtained in the previous study was applied here. The $H_2$ flows were chosen at 10.0, 15.0 and 20.0 l/min with the $NH_3$ flows selected accordingly to meet those actual $H_2$/reformate ratios. Pure forms of $H_2$ and $NH_3$ were also adopted for comparison purpose. All the $H_2$ – $NH_3$ combinations are listed in Table 5.2. The properties of the gaseous additions were given in Table 5.3 (Reiter and Kong 2008).

**Table 5.2:** The $H_2$ and $NH_3$ additions used

| **$H_2$ (l /min)** | **20.0** | | | | **15.0** | | | | **10.0** | | | | **0.0** | | | |
|---|---|---|---|---|---|---|---|---|---|---|---|---|---|---|---|---|
| **$NH_3$ (l/min)** | 0.0 | 3.0 | 7.5 | 14.0 | 0.0 | 3.0 | 7.5 | 14.0 | 0.0 | 1.0 | 7.5 | 14.0 | 1.0 | 3.0 | 7.5 | 14.0 |
| **$H_2$/Ref. Ratio** | 1.0 | 0.87 | 0.73 | 0.59 | 1.0 | 0.83 | 0.67 | 0.52 | 1.0 | 0.91 | 0.57 | 0.42 | 0 | 0 | 0 | 0 |

**Table 5.3:** Key properties of the gaseous additions

| **Fuel** | **Formula** | **Latent heat (kJ/kg)** | **Lower heating value (MJ/kg)** | **Stoichiometric Air/Fuel ratio by weight** | **Energy content (MJ/kg – stoichiometric mixture)** | **Auto – ignition temperature (℃)** |
|---|---|---|---|---|---|---|
| Ammonia | $NH_3$ | 1371.2 | 18.8 | 6.1 | 2.6 | 651 |
| Hydrogen | $H_2$ | 58.12 | 120.0 | 34.3 | 3.4 | 571 |

For all the above studies, the primary diesel was used to start and warm up the engine. Then, the produced or simulated reformate was sent into the air intake. The amount of liquid fuel injection was modified accordingly after the gaseous additions to keep the engine running at the same load condition. At least 20 minutes was allowed in each run for stabilising the engine and recording all the measurements.

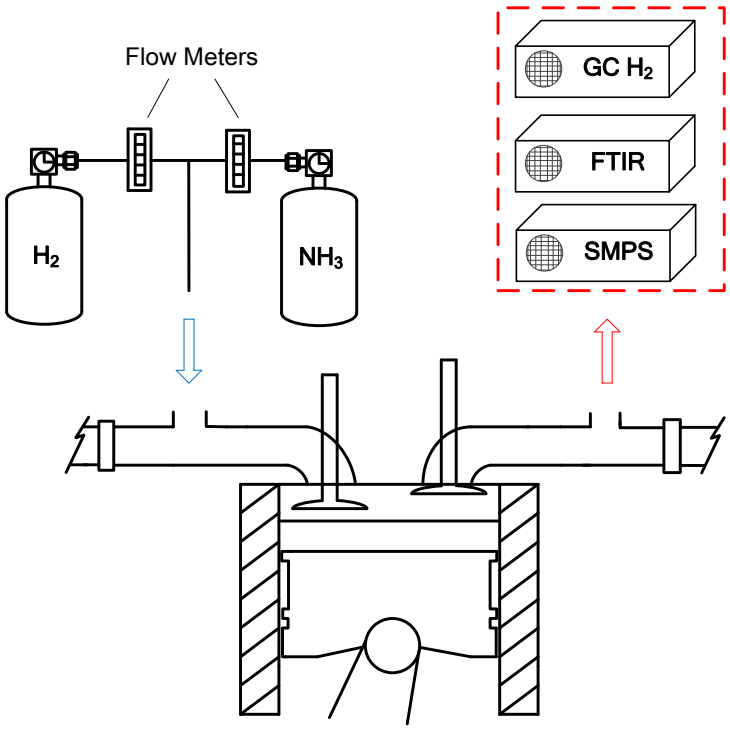


**Figure 5.1:** Experimental setup for simulated reformate addition

## 5.2 The impact of small amount of reformate on engine combustion and emission

The combustion characteristics with the addition of produced reformate are expressed by in-cylinder pressure and rate of heat release (ROHR) in Fig. 5.2. Compared to the standard diesel operation, introducing small amount of reformate did not change the combustion pattern

significantly. This implies no modification in the engine strategy is needed to optimise the combustion.

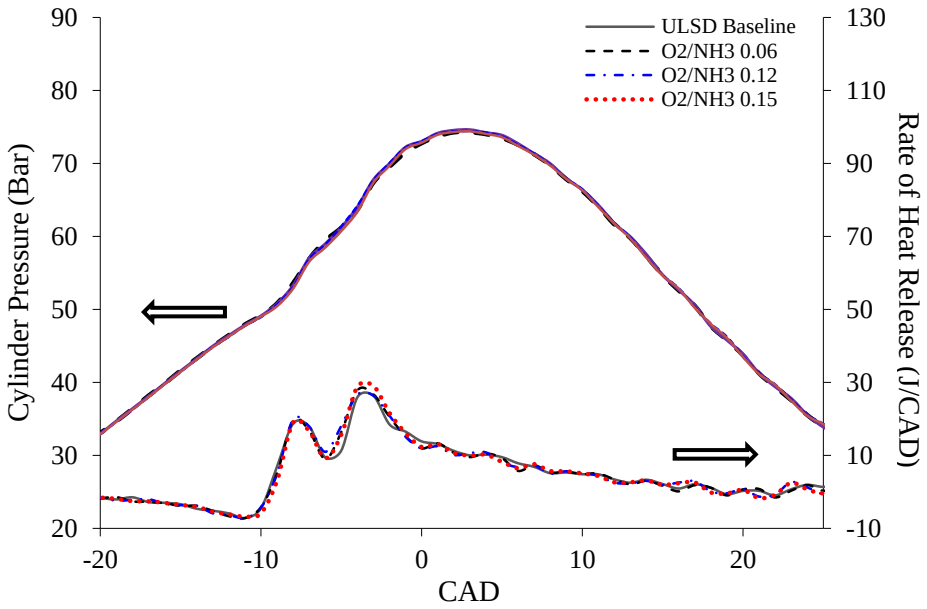


**Figure 5.2:** Engine in-cylinder pressure and rate of heat release at different reformate (produced) additions.

However, the reformate addition caused a reduction in engine brake thermal efficiency (Fig. 5.3 (a)), but as the $H_2$ concentration was increased the efficiency reduction decreased. Nevertheless, Fig. 5.3 (b) shows the use of reformate did result in a 4 – 5% reduction in injected diesel fuel (to maintain the engine speed and load). These observations indicate the reformate $H_2$ worked as the primary substituent to the diesel fuel, while the $NH_3$ combustion was comparatively less efficient, as a result of its high auto – ignition resistance i.e. 651 ℃ (more will be explained later at higher $NH_3$ induction).

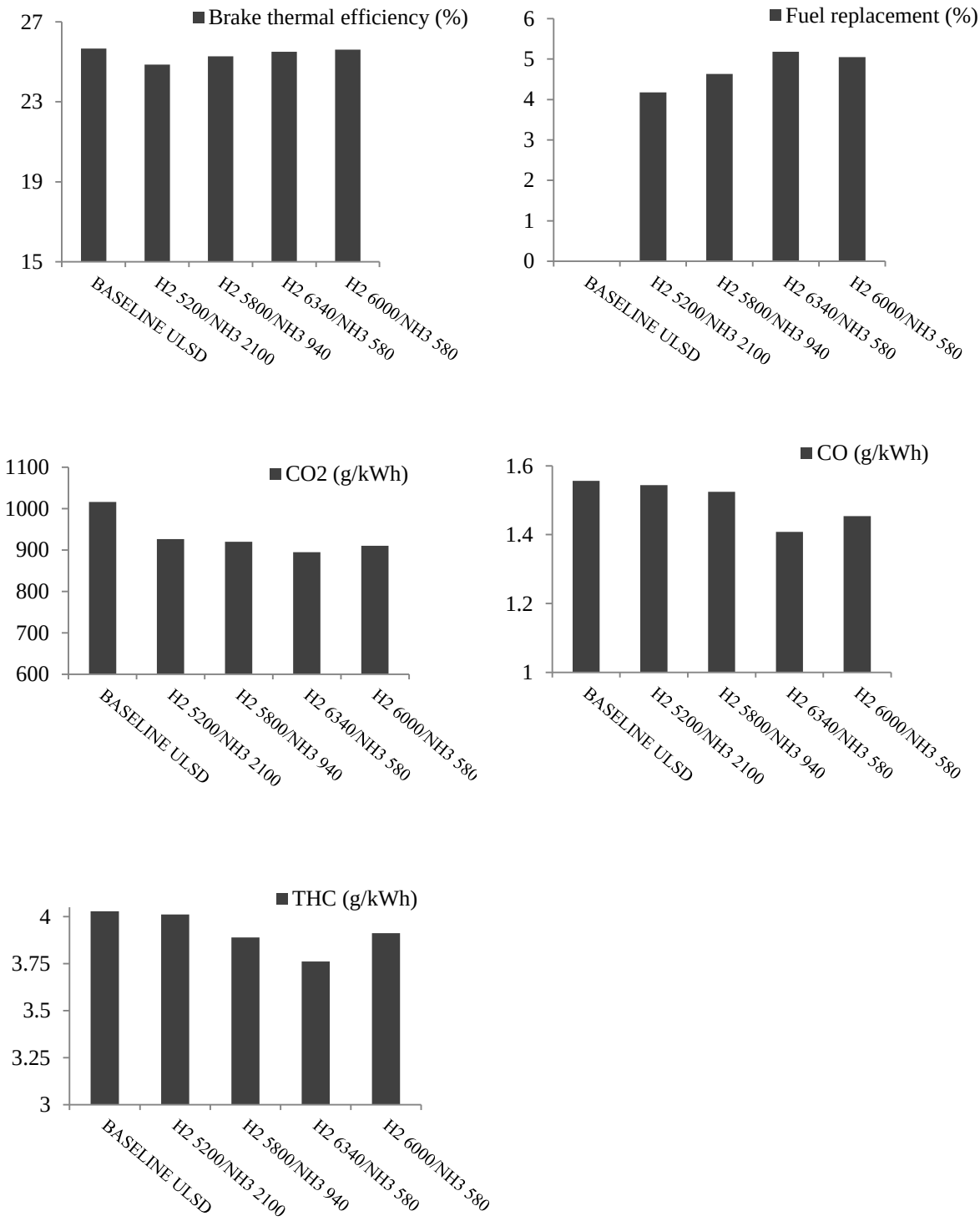


**Figure.5.3:** Engine performance and emissions under different $NH_3$ reformate (produced) additions: (a) engine brake thermal efficiency, (b) diesel fuel replacement, (c) $CO_2$ emissions, (d) total hydrocarbon emission, (e) CO emissions.

As for the engine emissions, replacing the primary diesel by non – carbon based reformate was able to reduce the engine – out carbon emissions. These are reflected by the decreased $CO_2$, CO and THC shown in Fig. 5.3 (c) – (e). However, with increased $NH_3$ involved in the combustion, the $NH_3$ concentration in the exhaust significantly increased, which ranged from 90 ppm to almost 700 ppm. Apart from its poor combustion, the ammonia emission can also be related to $NH_3$ being trapped in the combustion chamber crevices and when flame quenching on the chamber walls, i.e. the same mechanisms that are responsible for unburned hydrocarbons in Internal Combustion (IC) engines (Reiter and Kong 2011).

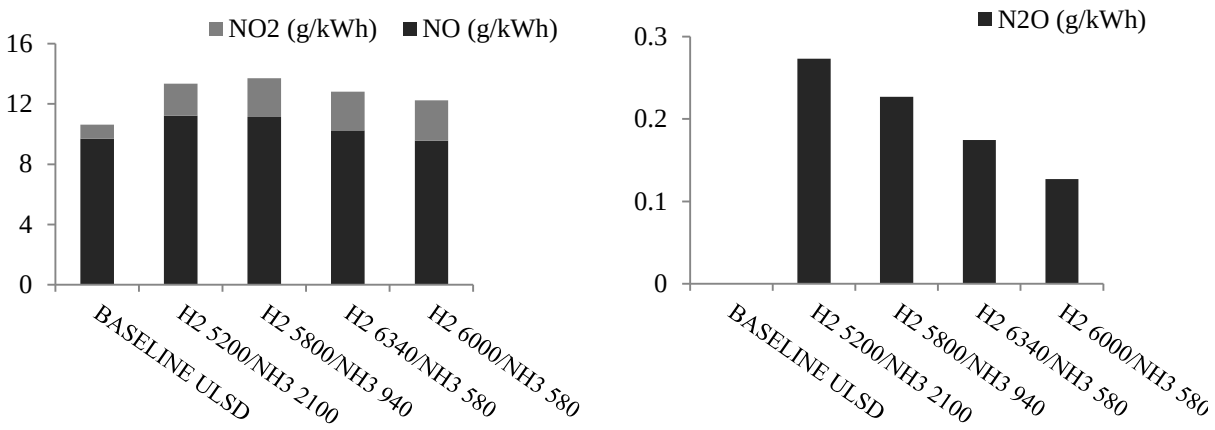


**Figure 5.4:** Engine NOx emissions under produced reformate additions: (a) $NO_2$ and NO emissions, (b) $N_2O$ emission.

Fig. 5.4 (a) and (b) show the reformate addition increase the NOx emission, which is found in relation to the increased $NH_3$ at the engine intake. As $NH_3$ is nitrogen bounded, its

oxidation in the combustion process allowed the formation of nitrogen oxides. Therefore, it reveals that the reformer out $NH_3$ level needs to be controlled to maintain the NOx emission.

As well as the heightened overall NOx emission, the $NO_2$/NO ratio is substantially increased compared to the pure diesel operation. Based on the literatures (Varde and Frame 1983, Lilik, Zhang et al. 2010), this is thought to be caused by the well – known $H_2$ effect. At low temperatures, peroxy radicals ($HO_2$ and $RO_2$) formed during combustion are crucial in promoting NO conversion into $NO_2$. At relatively cooler in-cylinder temperatures associated with low/medium engine load conditions, a small portion of $H_2$ – remains uncombusted (Liu, Li et al. 2011), which can be then mixed with NO – rich combustion products and converted into $HO_2$, which then reinforces the conversion of NO to $NO_2$ (Varde and Frame 1983):

$$HO_2+NO = NO_2 + OH \quad (5.1)$$

$$RO_2 +NO = RO + NO_2 \quad (5.2)$$

The increased $NO_2$ fraction in the engine exhaust is potentially beneficial as it can be utilised in catalytic aftertreatment systems for NOx and PM removal (Gill, Chatha et al. 2011)

Conversely to the energetic benefits postulated earlier with the use of low oxygen to ammonia ratio in the reformer (Fig. 4.5, Chapter 4), the observed engine combustion and emission with small amount of reformate suggest a use of high purity reformate hydrogen (reformer operated at high $O_2/NH_3$ ratio), as it is able to replace effectively the carbon fuels, minimise the emitted $NH_3$ without affecting the engine performance. Although this will incur a reduction in the reforming process efficiency through higher $NH_3$ oxidation, the amount of $NH_3$ oxidised at the

optimised $O_2/NH_3$ condition (0.15 in the current study, representing the reforming process that consumed the highest quantity of $NH_3$ in the oxidative portion) is calculated, using Eq. (5.3), to present only 1.3% of the total diesel fuel input at the studied engine condition, which indicates a reasonably small fuel penalty.

$$\text{Fuel penalty} = \frac{\dot{m}_{NH_3}(\text{oxidised}) \times \text{LHV}_{NH_3}}{\dot{m}_{\text{ULSD}}(\text{input}) \times \text{LHV}_{\text{ULSD}}} \times 100\% \qquad (5.3)$$

Where $\dot{m}$ and LHV are the flow rate and heating value of ULSD and ammonia respectively.

However, to continue using the studied catalyst it is necessary to improve the reactor geometry to reduce the heat loss and strengthen the average reactor temperature. The loss of heat generated both during and following the reaction can be used to improve the overall process efficiency. Recently, Kim et al (Kim, Um et al. 2012) provided a detailed study of a microreforming system, where a Micro – Combustor (for $NH_3$ combustion) and a Micro – Reactor (for $NH_3$ decomposition) are integrated in cylindrical/annular design for $H_2$ production. The system's configuration is shown to be effective in heat – recirculation: extracting heat from exhaust (reacted) gas for preheating fresh reactive mixtures. Hence a similar design can be adopted in the current reformer for better thermal management, leading to improved heat insulation and energy recovery. This would potentially increase the overall process efficiency and further suppress the fuel penalty.

## 5.3 Effects on engine combustion and emission using reformate simulated at larger amounts

### 5.3.1 Engine combustions under large amount of reformate additions

The diesel fuel replaced on an energy basis at various $H_2$ and $NH_3$ additions was in the range of approximately 10% to 60% and was dependant on the engine load as indicated in Fig. 5.5.

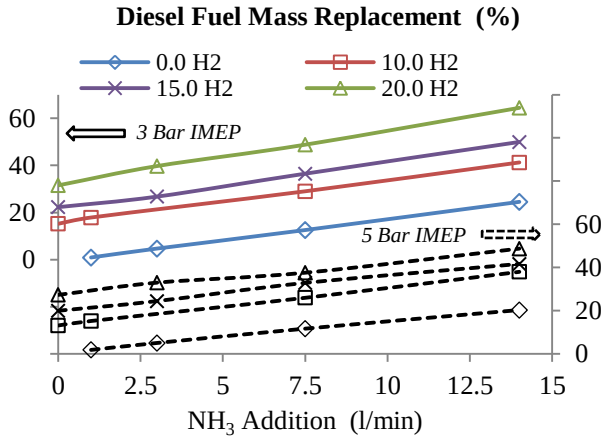


**Figure 5.5:** Diesel fuel replacement by different $H_2$ and $NH_3$ additions

Further substitution of diesel fuel by $H_2$ and $NH_3$ in this study was limited by combustion instability. The engine combustion stability as indicated by the coefficient of variance (COV) of the IMEP (Fig. 5.6), which was deteriorated as the concentration of $H_2$ and/or $NH_3$ concentration was increased. This was thought to be a result of the inconsistency of the $H_2$ and $NH_3$ combustion from one cycle to another, which had due to inconsistency of the mixture homogeneity, reduced intake oxygen concentration and poor auto-ignition properties of the gaseous fuels. Generally, the COVs recorded at 3 Bar IMEP were higher than those of 5 Bar due to the enlarged energy dependence from the gaseous fuelling (higher diesel fuel replacement) and much lower combustion and in-cylinder bulk temperatures (hindered $H_2$ and $NH_3$ oxidation).

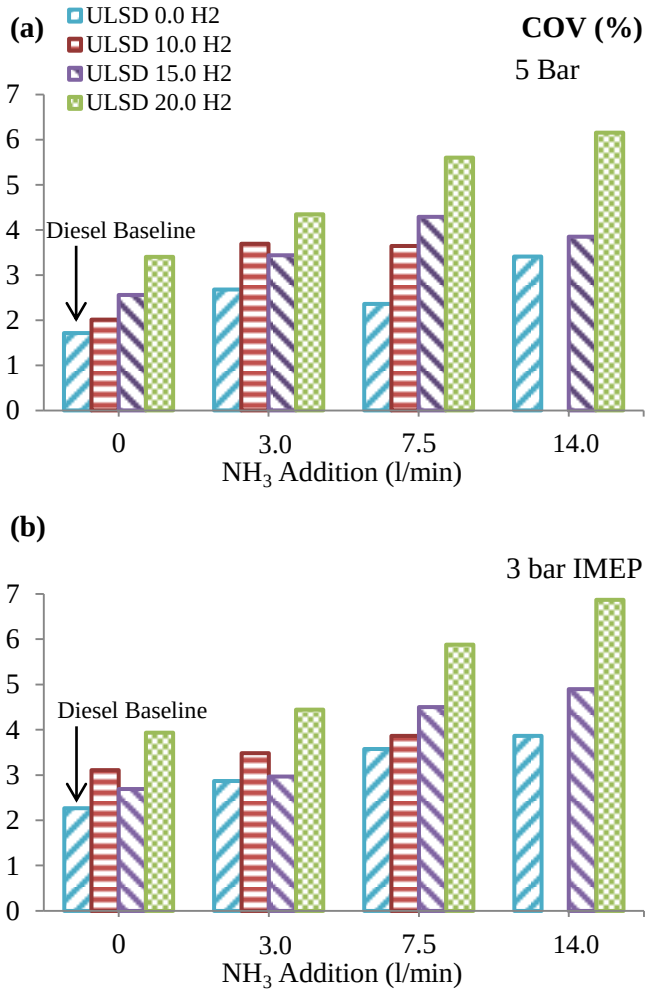


**Figure 5.6:** Coefficient of variation of IMEP under the $H_2$ and $NH_3$ additions at engine load condition of (a) 5 bar IMEP and (b) 3 bar IMEP

The in – cylinder pressure and rate of heat release (ROHR) acquired with different gaseous additions are plotted in Fig. 5.7 (a) and (b). Co – fuelling diesel and ammonia contributed to retarded ignitions in both engine conditions. As in the case of COV, it is believed that this is caused by (i) poor auto-ignition properties of $NH_3$ such as high auto-ignition temperature (651 ℃) and high octane rating i.e. 120 of $NH_3$ vs. 87 – 93 of gasoline (Ryu, Zacharakis-Jutz et al. 2014), (ii) lower oxygen availability which has been replaced by the gaseous fuels (similar to dilution effect in the case of exhaust gas recirculation), (iii) lower flame velocity than in the case of the

diesel fuel. This was especially apparent in the case of 3 bar IMEP, where the lower in – cylinder temperature obstructed the ignition (Gross and Kong 2013). In contrast, fuelling the engine with the diesel – hydrogen (at 15 l/min) mixture did not result in any obvious ignition delay, despite the higher auto-ignition temperature (571℃ vs. 254 ℃) and lower cetane number of hydrogen compare to diesel. It has to be noticed that the minimum energy required for igniting the hydrogen/air stoichiometric mixture (0.02 MJ/kg) is actually much lower compared to many of the hydrocarbon/air mixtures', e.g. 0.24 and 0.28 MJ/kg respectively for the fuel/air mixtures of gasoline and methane (Heywood 1988, White, Steeper et al. 2006).

As reflected by the ROHR in the premixed phase (Fig. 5.7), combustion of the diesel – NH3 mixture in the premixed phase was comparatively intensified, which resulted in sharpened heat releases in both of the engine conditions compared to diesel. It is suggested that this could be due to the NH3 combusted in the premixed phase and probably because of increased proportion of diesel fuel burnt in the premixed combustion (because of the longer available time to mix air, NH3 and the liquid diesel). Provided with a higher flame velocity (Saravanan, Nagarajan et al. 2008, Liew, Li et al. 2010), $H_2$ was suggested to intensify the burning rate in the premixed phase, which can be shown by the overall increased ROHR observed in the premixed combustion (compared to the diesel and $NH_3$ combustions).

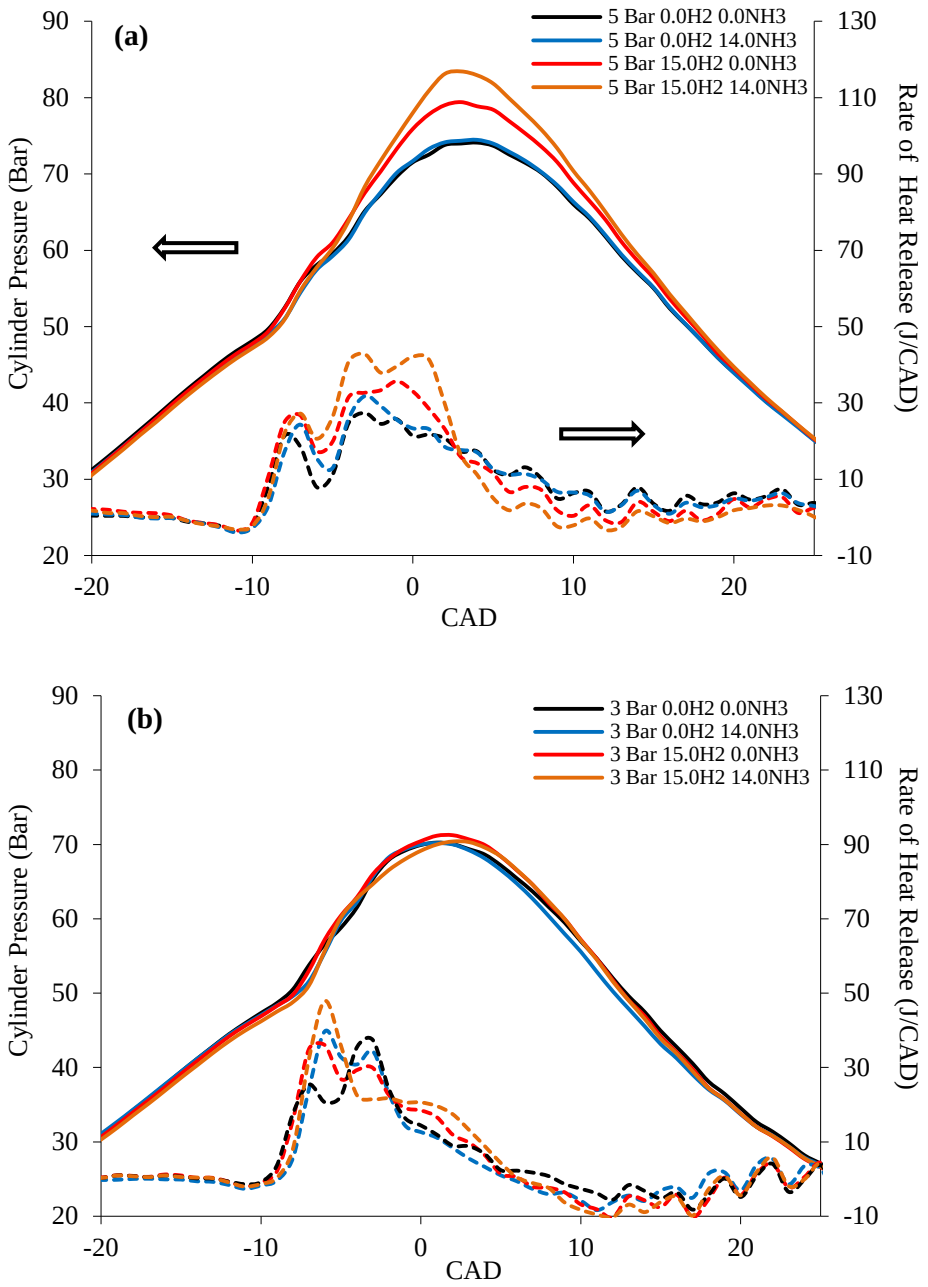


**Figure 5.7**: In – cylinder pressure and ROHR of the combustions with different additions of $H_2$ and $NH_3$: (a) at 5 Bar IMEP and (b) at 3 Bar IMEP

The combustion duration and the ROHR in the diffusion phase for $NH_3$ - diesel at both engine loads and $H_2$ - diesel at low load were similar to the combustion duration and ROHR of diesel combustion. However, in the case of 5 bar IMEP with $H_2$ addition, the higher in – cylinder pressure and temperature with respect to conventional diesel combustion (Abu-Jrai, Tsolakis et al.

2007, Saravanan, Nagarajan et al. 2008) through an increased peak measurement of ROHR as well as the reduction in the quantity of liquid fuel burnt in diffusion combustion (it has been replaced by $H_2$) was seen to shorten the overall combustion duration.

After the $H_2$ (15 l/min) and $NH_3$ (14 l/min) additions being combined, the prolonged ignition delay caused by the $NH_3$ addition was shown to be shortened for both engine conditions. In addition, a more pronounced premixed combustion phase was achieved with the $H_2$ – $NH_3$ mixture than in the other cases. The hydrogen intensified premixed combustion and/or the rapid $H_2$ burning velocity was believed to thermally favor the ignition of ammonia reducing the ignition delay and enables increased proportions of $NH_3$ and diesel burnt in premixed combustion phase. Supported by combustion studies of $NH_3$ – $H_2$ – air mixture by Li et al and Kwon et al, the burning velocity of ammonia can be improved with hydrogen co – fuelling (Kwon and Faeth 2001, Li, Huang et al. 2014) as increased $H_2$ presenting in the ammonia flame (Kwon and Faeth 2001), or some of the $NH_3$ could even thermally decompose to form $H_2$ during the oxidation. Shown in Fig. 4a, the high temperature (highest cylinder pressure) at 5 Bar IMEP promoted quite significantly this $H_2$ – assisted combustion, reflected by a largely enhanced rate of increase and peak measurement of ROHR and an overall shortened combustion duration.

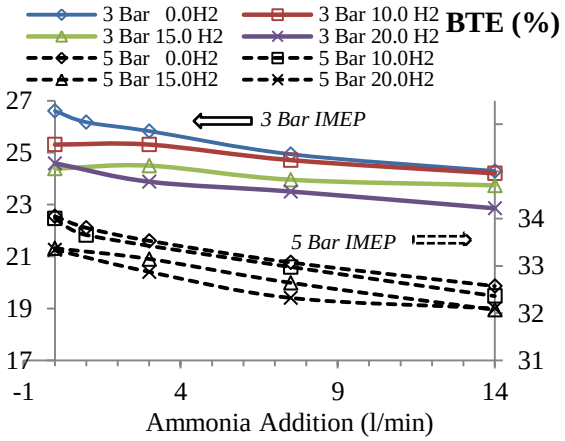


**Figure 5.8:** Engine brake thermal efficiencies and different combined additions of $H_2$ and $NH_3$

The brake thermal efficiencies (BTE) of the engine at different $H_2$ – $NH_3$ additions were compared and are shown in Fig. 5.8.

In each load condition, replacing the primary diesel with gaseous fuels decreased the engine brake thermal efficiency mainly due to incomplete combustion of $H_2$ and $NH_3$ (combustion efficiency). Overall, the thermal efficiencies at 3 Bar IMEP were comparatively lower than those at 5 bar IMEP as a result of the poorer $H_2$ and $NH_3$ utilisation as explained earlier. In addition, some researches have reported that the engine efficiency can be also reduced with $H_2$ in diesel combustion through the increased heat loss in the combustion chamber (Shudo, Nabetani et al. 2001). This is due to hydrogen's high flame velocity and smaller quenching distance leading to eased convection and heat mixing within the burning gas and the heat transfer to the cylinder wall (Shudo 2007)

The measured concentrations of unburned $H_2$ and $NH_3$ in the engine exhaust also support the argument that this is the reason for the reduction in engine brake thermal efficiency (Fig. 5.9 (a) and (b)). Although the same volumetric flow of $H_2$ was delivered for both of the engine conditions,

the $H_2$ detected in the engine exhaust at 3 bar IMEP was much higher than that in the 5 Bar IMEP operation (Fig. 5.9 (a)), which coincides with the lower brake thermal efficiency presented in Fig. 5.8.

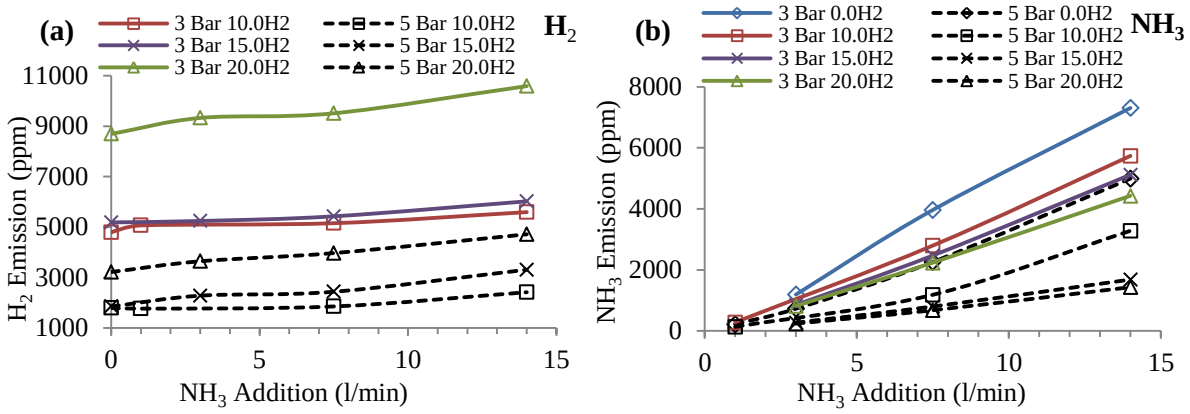


**Figure 5.9:** Unburned $H_2$ and $NH_3$ with different combined additions of $H_2$ and $NH_3$: (a) $H_2$ and (b) $NH_3$

The un-combusted $NH_3$ detected in the exhaust (Fig. 5.9 (b)) was reduced considerably with the increased $H_2$ addition for both engine operations, which proves that $H_2$ promoted the $NH_3$ combustion. This positive hydrogen effect on $NH_3$ combustion was reduced at 3 Bar IMEP as the lower in-cylinder pressures and temperatures also reduced the hydrogen oxidation rates, thus the increased $NH_3$ and $H_2$ concentration detected in the exhaust. In Fig. 5.9 (a), except the case where the highest hydrogen (i.e. 20 l/min) and/or ammonia (i.e. 14 l/min) were applied, the hydrogen measured in the engine exhaust was generally kept at similar concentration independently of the $NH_3$ and $H_2$ additions. In this condition, as 20 to 34 l/min of $H_2$ or combined $H_2$ – $NH_3$ mixture, the same amounts of air were replaced (i.e. 5 to 7 %) at the engine intake, which restricted the in – cylinder oxygen concentration.

### 5.3.2 Engine emissions under high amount of reformate addition

#### a) NOx and $N_2O$ emission

NOx emissions including NO, $NO_2$ and $N_2O$ are shown in Fig. 5.10 (a) – (c) accordingly.

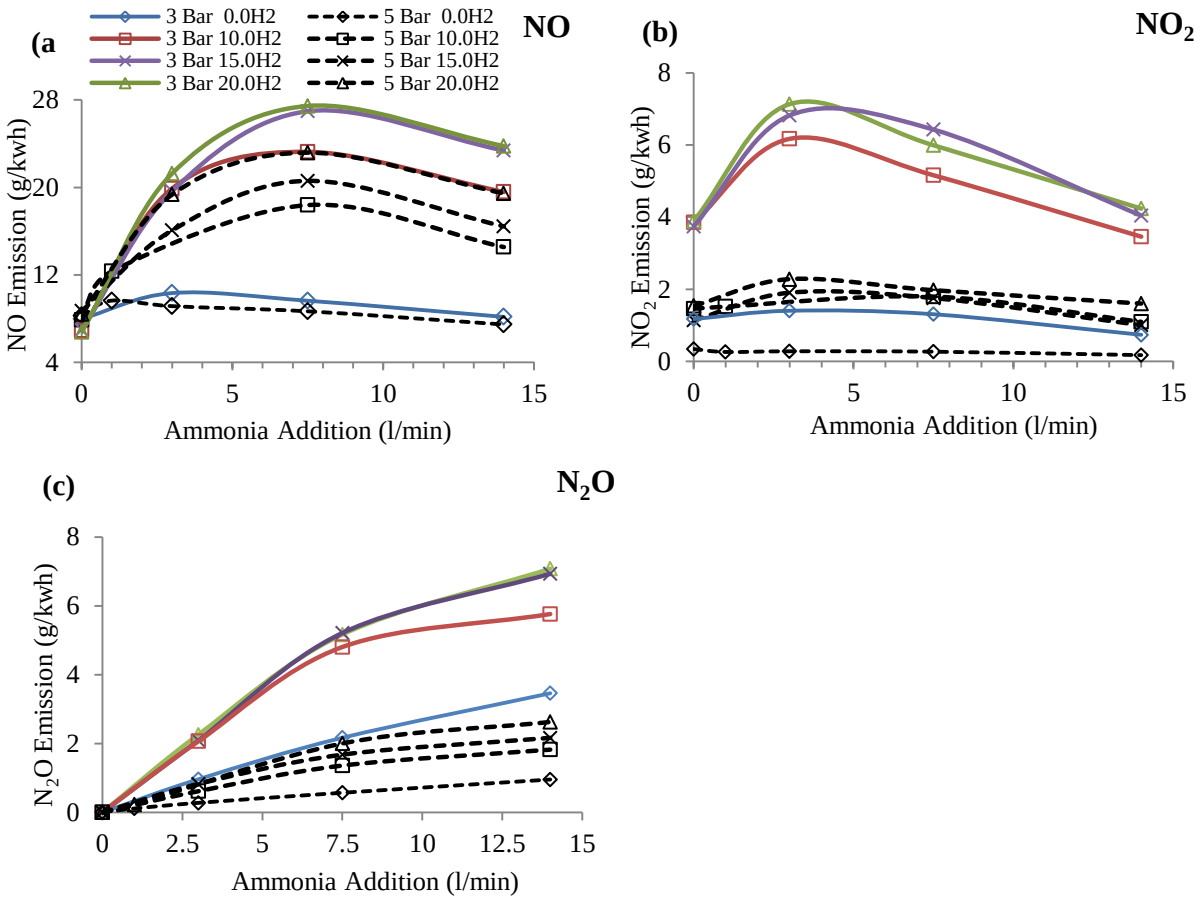


**Figure 5.10:** NOx emissions obtained at different combined $H_2$ and $NH_3$ additions: (a) NO, (b) $NO_2$ and (c) $N_2O$

Without hydrogen, the NOx emission is shown to increase under small amount of $NH_3$ addition (up to 3 l/min). As $NH_3$ is nitrogen bounded, its in-cylinder oxidation will inevitably lead to the formation of NOx species. However, when larger quantities of ammonia were added (Fig. 5.10 (a)), the effects of (i) low combustion flame temperature of $NH_3$ (Gross and Kong 2013) (ii) delayed ignition shifting the combustion more into the expansion stroke (iii) lower oxygen

availability were dominant in suppressing NOx production from $NH_3$ combustion. Shown in the same plot, when the highest $NH_3$ flow (14 l/min) was used, the NOx emission became even slightly lower than that of diesel baseline. This observation was in agreement with a diesel – ammonia dual fuel combustion test conducted by Reiter et al (Reiter and Kong 2011) where NOx reduction was obtained when $NH_3$ was substituting the total fuel energy by around 20 %.

It is reported that the induction of hydrogen in compression ignition engines could increase NO emissions especially at high engine load operation due to the fast hydrogen combustion (see combustion plots). It is also reported that the introduction of hydrogen increases the levels of hydroperoxyl ($HO_2$) radical, as shown experimentally by (Bika, Franklin et al. 2008) and numerically by (Lilik, Zhang et al. 2010) leading to increased $NO_2$ emissions. This effect is also shown in Fig. 5.10 in the case of diesel – $H_2$ combustion. The increase in NOx emissions is more noticeable when $H_2$ is inducted in the presence of $NH_3$. This result is in accordance with the combustion characteristics shown in the earlier section (i.e. increased premixed combustion), which gives further evidence to the hydrogen promoted $NH_3$ combustion and thus the increased NO and $NO_2$ emissions. The hydrogen's promotional effect on NO formation was shown to be maximised at 7.5 l/min of $NH_3$ co – fuelling. Then it started to decrease, parallel to the NO reduction found in $NH_3$ – diesel combustion, indicating the retraction in oxygen availability. The $NO_2$ emissions under $H_2$ – $NH_3$ – diesel fuelling followed a similar pattern to NO, but the incorporation of $NH_3$ reduced $NO_2$ emissions at lower flow rates than in the case of NO. The $N_2O$ emissions in both engine loads were increased with increased $H_2$ and $NH_3$ additions.

According to the results displayed above, the primary drawback of the combined $H_2$ and $NH_3$ addition was the NOx formation. Recent study (Doronkin, Fogel et al. 2012, Tamm, Fogel et al. 2013) on diesel aftertreatment systems has shown that a silver based SCR system ($Ag/Al_2O_3$) is quite effective in low temperature NOx reduction through a utilisation of the unburned $NH_3$ and $H_2$. More than 95% of NOx can effectively be removed at low exhaust gas temperatures (e.g. 200 ℃).

**b) Gaseous carbonaceous emission**

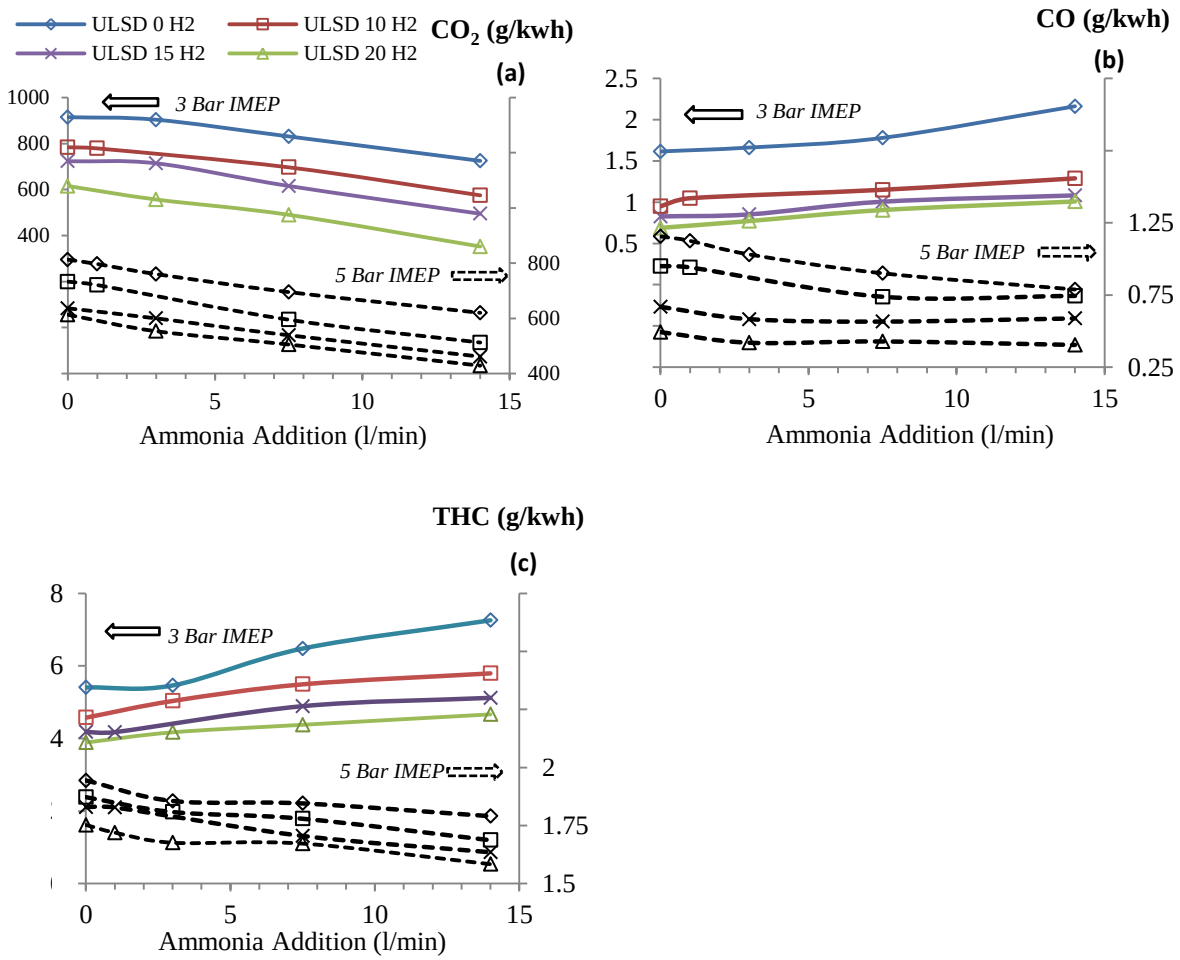


**Figure 5.11:** Carbonaceous emissions with different combined $H_2$ and $NH_3$ additions: (a) $CO_2$, (b) CO and (c) THC.

The engine's gaseous emissions including $CO_2$, CO and THC are presented in Fig. 5.11 (a) – (c) accordingly. The absence of carbon element from the gaseous substances reduces engine out $CO_2$, CO and THC emissions. The $CO_2$ reductions trends are in agreement with the fuel replacements on the mass basis (Fig. 5.5). However, different trends in CO and THC emissions were observed between the low and high engine conditions. At 5 Bar IMEP, the CO and THC emissions both declined when hydrogen and ammonia were inducted. However at 3 Bar IMEP, although both of the CO and THC could be reduced from the diesel baseline with the overall increased gaseous additions ($H_2$ and $NH_3$ together), their emissions were negatively affected by the incorporation of $NH_3$. As compared to the higher load operation, combustion at 3 Bar IMEP was not providing with a high in – cylinder temperature to compensate the lower temperature combustion of ammonia and the oxygen dilution effect when a high level of $H_2$ and $NH_3$ were employed. Also, with the increased ignition delay, the overall combustion phase at 3 Bar IMEP was shifted more into the expansion stroke and thus subject to late combustion. Hence the oxidation of the carbon – containing species in the presence of high levels of $NH_3$ tends to be more incomplete than in the high engine load condition. In general, with the increased addition of $H_2$ and the subsequently improved $NH_3$ and diesel combustions, reductions in CO and THC emissions were still observed at the low load operation.

**c) PM emissions**

The particle size distribution and mass concentrations with various $H_2$ and $NH_3$ additions are shown in Fig. 5.12. The total PM emission on mass basis is shown in Fig. 5.13. The particle mass distribution was obtained from the particle number distribution through a size – dependent agglomerate density function as described by Lapuerta et al (Lapuerta, Armas et al. 2003).

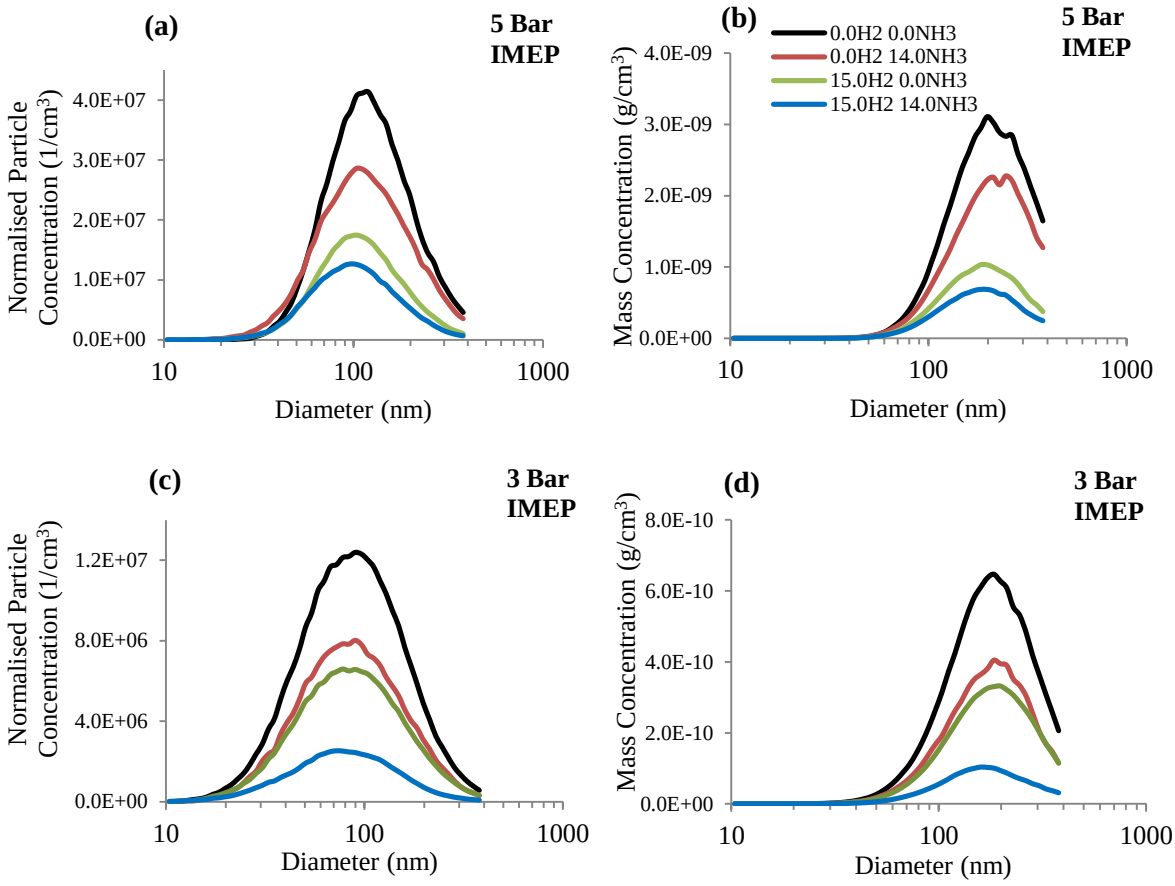


**Figure 5.12:** Particulate size distributions for the selected combinations of $H_2$-$NH_3$-diesel combustion (a) number concentration at 5bar IMEP, (b) mass concentration at 5bar IMEP, (c) number concentration at 3bar IMEP, (d) mass concentration at 3bar IMEP.

The PM emissions at 5 Bar IMEP are higher than at 3 Bar IMEP (Fig. 5.12 and 5.13). This is due to the higher quantity of fuel which is injected and burnt in diffusion combustion (where soot is produced) and the lower air/fuel ratio at high engine load operation (Tsolakis 2006).

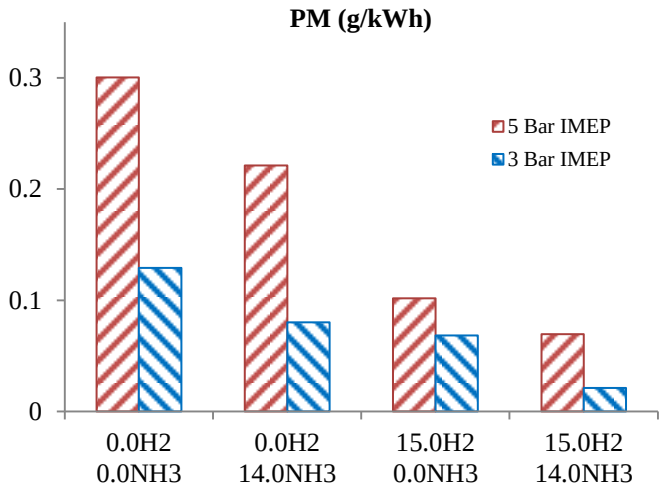


**Figure 5.13:** PM emissions at selected combined $H_2$ and $NH_3$ additions

Shown in Fig. 5.12 (a) and (b), the addition of hydrogen and/or NH3 resulted in a reduction in the particulate matter concentration for all the particulate sizes. The reasons to justify the decrease in particulate matter by the gaseous fuels are (i) the liquid fuel replacement and (ii) the decrease of fuel burnt in diffusion combustion which both in turn reduces the number of locally fuel rich zones in the combustion chamber (where soot precursors and particulates formation are initiated) inhibiting soot formation. Furthermore, it has been reported that hydrogen promoted the formation of OH radical (Saxena and Williams 2006) which is efficient in soot and precursor oxidation (Pandey, Pundir et al. 2007).

Comparing between the gaseous fuels, the PM reduction by $NH_3$ addition is shown to be less efficient than that of the $H_2$ for both engine conditions. Provided the $NH_3$ at 14 l/min was in fact

carrying more energy (11. 43 MJ/hr) in terms of combustion than the energy carried by the 15 l/min of $H_2$ (9.72 MJ/hr), its less effective combustion was therefore implied as the main reason for replacing less amount of diesel and thus impaired the carbon reduction. In addition, as shown previously by Fig. 5.7 (a) and (b), the hydrogen promoted premixed combustion was stronger than that of $NH_3$. Therefore, when $H_2$ and $NH_3$ are added together, not only the highest amount of diesel is replaced, but also the highest proportion of premixed combustion is obtained, achieving the highest PM removal.

**5.4 Summaries:**

In the above study, the potential of $H_2$ and $NH_3$ being used as partial fuel substitution to decarbonise a diesel engine was presented.

Overall, $NH_3$ in its reformed form i.e. $H_2 – NH_3$ mixture is suggested to be a more viable fuel substitution in diesel combustion.

$NH_3$ by itself was demonstrated to have a less effective combustion within the diesel operation, especially in low load condition, where the $NH_3$'s auto – ignition barrier became increasingly difficult to be overcome. This suggested a thermally intensified in - cylinder condition could be quite beneficial to the ignition and combustion of $NH_3$. This was supported by the later observed increased engine NOx after the induction of $H_2$, especially at low $NH_3$ concentrations.

On the other hand, increasing the $NH_3$ fueling (to 20 wt % of diesel replacement) was shown to restrict the systems NOx formation due the $NH_3$'s lower flame temperature and burning rate

and/or the in – cylinder oxygen dilution resulting from the $NH_3$'s induction at the air intake. Hydrogen is expected to increase NOx, but thanks to the combination of hydrogen and ammonia, the low temperature combustion of increased $NH_3$ addition and the even more enlarged "EGR effects" after the co – fuelling of $H_2$ compensated this $H_2$ effect, reducing some of the heightened engine NOx.

Depending on the engine conditions and the additions of the reformate components, different amount of unconverted $H_2$ and $NH_3$ could be observed in the exhaust. This demonstrated a great potential of incorporating the reformate combustion with an exhaust aftertreatment that consumes the NOx, $H_2$ and $NH_3$ all at one reaction i.e. $NH_3$ – SCR over $Ag/Al_2O_3$

# CHAPTER 6: IMPROVED $H_2$ – $NH_3$ REFORMATE COMBUSTION FOR EFFECTIVE DIESEL ENGINE DECARBONISATION THROUGH USE OF DGE AS AN IGNITION ENHANCER

## 6.1 Introduction

In chapter 5, the CI combustion of $NH_3$ reformate was revealed as not easy as that of diesel, especially for the $NH_3$ content, whose high auto – ignition resistance was shown to barricade its ignition and combustion.

In the existing literatures, difficult combustions in compression – ignition engine were also reported for hydrocarbons like LPG and CNG, whose auto – ignition resistances are considerably high (featured with high octane or low cetane ratings) compared to that of the diesel. Therefore, to overcome the lack of ignitability, combustion improvers with higher CN numbers were co – fed with these fuels for ignition purpose (Alam, Goto et al. 2001). Successful combustion improvement was observed in a study of LPG fueled diesel engine using diethyl ether (DEE, CN >125) (Miller Jothi, Nagarajan et al. 2008), where engine efficiency was reported to increase while HC and particulate emissions were both decreased. In addition to that, co – fueling CNG and DEE to diesel engine also yielded similar enhancement. Most recently, Ryu et al. (Ryu, Zacharakis-Jutz et al. 2014) investigated a compression – ignition combustion of ammonia and dimethyl ether (DME, CN = 60), where several appropriate strategies and fuel/gas mixtures were shown for the use of ammonia in direct – injection compression – ignition engines. Apart from that, DME is also

referred as a cetaner blended with different fuels/fuel mixtures for the purpose of particulate emission control (Smith, Ott et al. 2008).

Apart from the ignition improvers stated above, diethyl glycol diethyl ether (DGE) is discovered as another potential ignition enhancer based on its very high cetane (CN = 140) number and its high content of fuel – born oxygen. Because of its featured high ignitability, DGE combustion in diesel engine possessed shortened ignition delay and was demonstrated to burn sufficiently in low – temperature combustion regime under charge – gas dilution and cooling (Ito, Ueda et al. 2003). All these characteristics led to improved NOx/soot trade – off from DGE combustion. Also as being similar to DEE, its presence (as fuel or fuel blend) in CI type of combustion is thought to be capable of lending combustion assistance to those less ignitable fuel alternatives, such as $H_2$ and $NH_3$.

In the current study, $H_2$ and $NH_3$ in pure or combined in a form of $NH_3$ reformate (the same as before) were sent to the engine for partial diesel substitution. The combustion characteristics and emission performances of both of the gaseous additions were investigated with standard diesel. This built up a baseline reference for any further comparison. Following that, DGE at different amount was mixed into diesel, which allowed the prepared fuel blends to have increased CN ratings and oxygen contents. The fuel blends were later studied with the same gas mixtures in combustion. Hence, with the changes in cetane number, oxygen content and ignition property of the primary liquid fuel, the combustion characteristics and emission performances of the gaseous additions could be assessed and compared, to show improved ignition and combustion, if there was any.

The engine, data acquisition and emission analysis systems adopted previously in chapter 5 were equally applied in the current study (Fig 5.1). The gaseous substitution of $H_2$ and $NH_3$ were also followed for the reformate composition simulated in the previous chapter, see Table 5.1.

In the current study, the ULSD was used as the primary liquid fuel for baseline operation. DGE was mixed volumetrically into the diesel to obtain the desired blends. Two blends with volumetric concentrations of 20 and 40 % of DGE (DGE20 and DGE40 accordingly) were selected. This allowed a comparison between 3 different CN ratings and fuel – borne oxygen contents. The fuel properties are listed in Table 6.1 for each tested fuel/fuel blend.

**Table 6.1:** Fuel properties of the tested liquid fuel/blend

| | **ULSD** | **DGE** | **DGE20** | **DGE40** |
|---|---|---|---|---|
| **Chemical Formula** | $C_{14}H_{26.18}$ | $C_8H_{18}O_3$ | $C_{12.52}H_{24.16}O_{0.74}$ | $C_{11.20}H_{22.36}O_{1.40}$ |
| **Molar Mass (kg/kmol)** | 194.18 | 162 | 186.24 | 179.16 |
| **Density at 15 ℃ (kg/m$^3$)*** | 827.1 | 908 | 843.3 | 859.46 |
| **LHV (MJ/kg)**** | 42.99 | 31.4 | 40.49 | 38.10 |
| **Cetane Number**** | **53.9** | **140** | **72.46** | **103.70** |
| **C (wt %)** | 86.52 | 59.2 | 80.67 | 75.02 |
| **H (wt %)** | 13.48 | 11.1 | 12.97 | 12.48 |
| **O (wt %)** | 0 | 29.7 | 6.36 | 12.50 |

* Estimated based on volumetric fraction

** Estimated based on mass fraction

The experimental runs were carried out in three separate sets for diesel and two DGE blends i.e. DGE20 and DGE40. All tests were performed under steady – state conditions at a controlled engine speed of 1500 rpm and a constant engine load of 5 bar IMEP throughout. In all test sets, the liquid fuel was used to start and warm up the engine. Then, different flows of $NH_3$ and $H_2$ or both combined were sent into the air intake. The amount of liquid fuel injection was modified

accordingly after the gaseous additions to keep the engine running at the same load. At least 20 minutes was allowed in each run for stabilising the engine and recording all the measurements.

## 6.2 Liquid fuel replacement

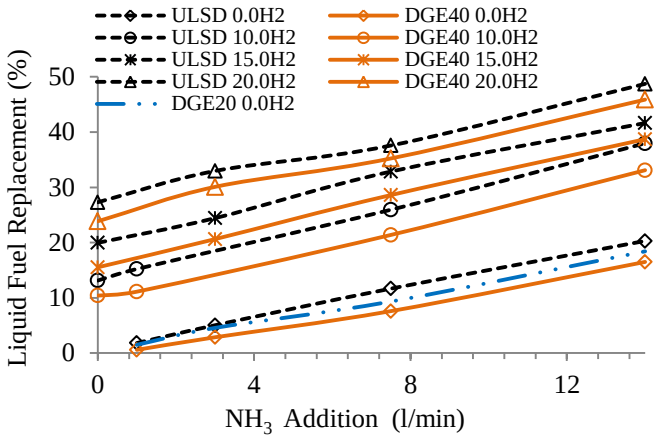


**Figure 6.1**: Liquid fuel replacement by different $H_2$ and $NH_3$ additions

Compared to the pure diesel baseline, increased DGE content in the liquid fuels reduced the amount of liquid fuel being replaced at each $H_2$ and $NH_3$ level (Fig. 6.1). This was due to the lower LHV (i.e. higher fuel – borne oxygen content, Table 6.1) of DGE than that of diesel that increased its amount to keep the engine load constant.

## 6.3 Combustion characteristics

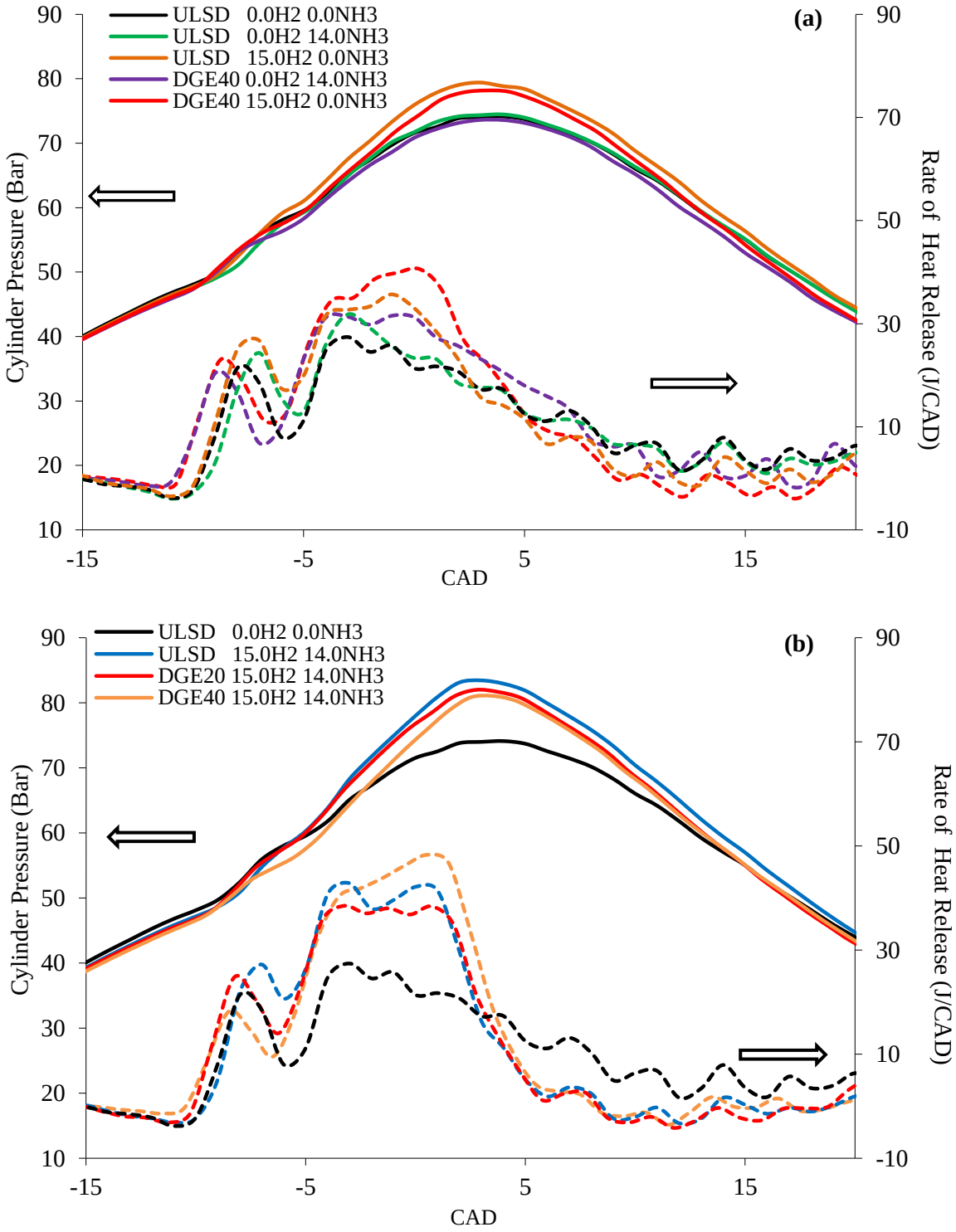


**Figure 6.2**: In – cylinder pressure and ROHR of the combustions of diesel and DGE blends with (a) separate additions of $NH_3$ and $H_2$ and (b) simultaneous addition of $NH_3$ and $H_2$, the flow rates for $NH_3$ and $H_2$ are 14 and 15 l/min respectively.

The in – cylinder pressure and rate of heat release (ROHR) of diesel and DGE blends with different gaseous additions are plotted in Fig. 6.2 (a) and (b). As presented in Fig. 6.2 (a), while the addition of $NH_3$ (14 l/min) prolonged the ignition delay in diesel combustion, the DGE's high CN rating, see Table 1 advanced the start of combustion of the $NH_3$ (Ryu, Zacharakis-Jutz et al. 2014). It is considered, as the $NH_3$/air pre – mixture being carried into the ignition fuel (DGE + diesel) spray periphery, the ignition of the pilot fuel initiated flame propagation within the combustible mixture (Karabektas, Ergen et al. 2014), enhancing the ammonia oxidation. The fuel – borne oxygen of the DGE was also believed to compensate the decreased intake air with the $NH_3$ addition, increasing the local oxygen/fuel ratio and thus facilitating the oxidation of the gas/fuel mixture. In addition, the DGE's lower compressibility than diesel (usually inverse to density, see Table 6.1), could result in advanced fuel injection and ignition that in turn benefited also the $NH_3$ ignition.

As described earlier in Chapter 5, due to hydrogen's low minimum ignition energy requirement, the $H_2$'s high auto - ignition temperature and poor cetane rating did not retard the start of its combustion with and without the presence of ammonia (Fig. 6.2). In terms of the ROHR in the premixed combustion, the previous chapter showed both of the diesel – $H_2$ and diesel – $NH_3$ mixtures intensified the premixed phase and resulted in sharpened heat releases compared to diesel. However these were shown to be both reduced after the use of DGE. This was due to the DGE's much higher latent heat of evaporation (360 kJ/kg) compared to that of diesel (240 - 270 kJ/kg) (Kusano, Wads et al. 1971). As the DGE content increased, the fuel mixture

requires higher energy adsorption for evaporation and therefore suppressed the rate of heat release at the same time.

Shown also in the previous chapter, co – feeding $H_2$ and $NH_3$ into the diesel combustion cancelled the $NH_3$'s retardation of the mixture's ignition, which was due to hydrogen's promotional effect on the $NH_3$ combustion. The presence of DGE in the combined $H_2$ – $NH_3$ combustion was again shown to reduce the intensity of the premixed combustion and enhance the total combustion duration with respect to the diesel – $H_2$ – $NH_3$ combustion. The higher DGE concentration (i.e. DGE40) even shifted the peak ROHR more to the expansion stroke, which reduced therefore the peak cylinder pressure, indicating the decreased combustion temperature. The total combustion duration (combining the premixed and diffusion phases) and the ROHR in the diffusion phase were shown to increase for both of the gases when applied with the DGE blend. These were based on their diminished premixed phases, which indicate increased heat was released in the subsequent diffusion phase compared to the combustion with diesel, and the overall increased heat release duration of DGE than that of diesel in a broader range of in – cylinder conditions, enhances $H_2$ and $NH_3$ combustion.

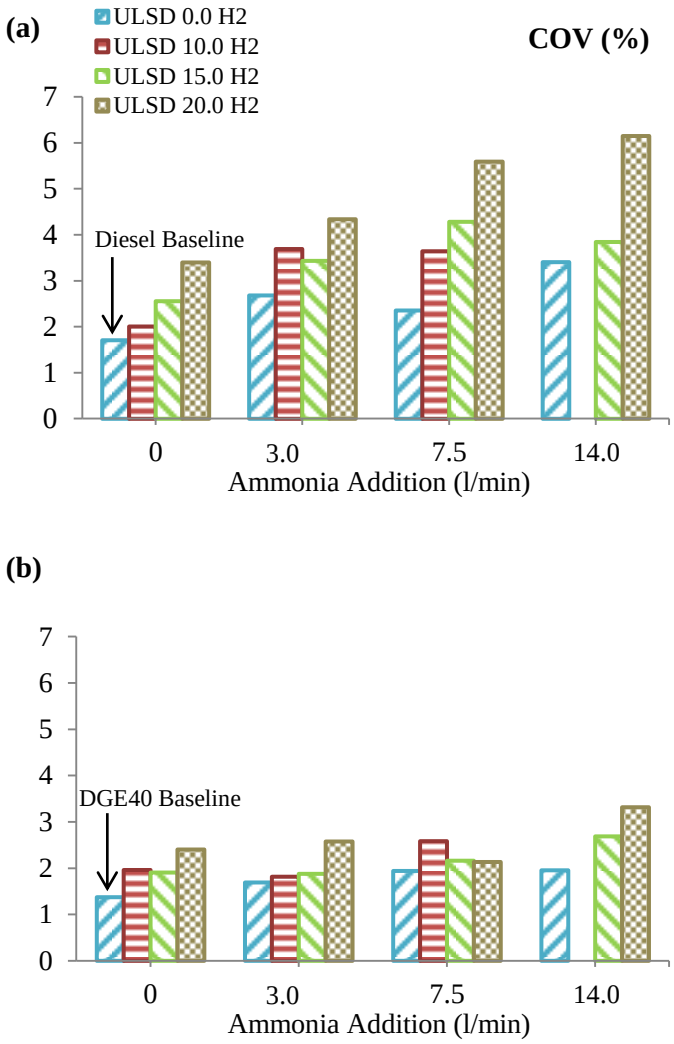


**Figure 6.3:** coefficient of variation of IMEP obtained from the combustions with different combinations $H_2$ and $NH_3$; (a) diesel and (b) DGE20.

Shown in Fig. 6.3, the use of DGE improves the engine stability by its combustion characteristics described earlier i.e. a) reducing the cylinder pressure and hence the volatile in – cylinder condition through its low temperature combustion and b) improving the combustions of $H_2$ and $NH_3$ via its higher ignitability (Goto, Lee et al. 1999) and overall increased combustion duration.

## 6.4 Unburned gaseous additions and brake thermal efficiency

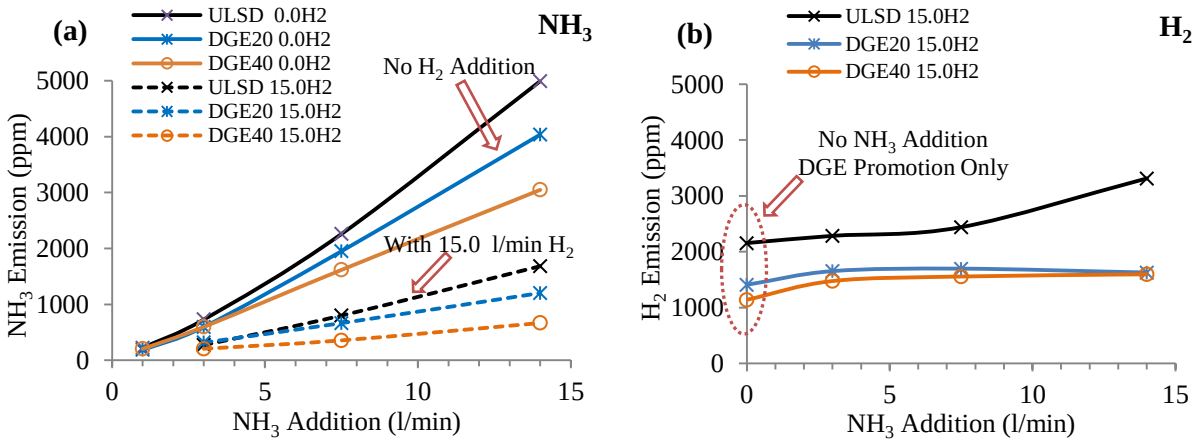


**Figure 6.4:** Unburned gaseous additions (exhaust emissions) of (a) $NH_3$ and (b) $H_2$ at different fuelling conditions

The volumetric $NH_3$ and $H_2$ emissions under different fuelling conditions are plotted in Fig. 6.4 (a) and (b) respectively. Similar to the results observed in the previous chapter, Ammonia's concentration in the engine exhaust was reduced significantly with $H_2$ addition. The presence of DGE decreased further the emissions of $NH_3$ and $H_2$ for all the studied cases (diesel- $NH_3$, diesel-$H_2$ and diesel – $H_2$ – $NH_3$ combustion). It is believed that the ignition properties of DGE and the changes in the combustion patterns (see Fig. 6.2) enhanced the ammonia and $H_2$ oxidation. Apart from that, the increased fuel replacement at high gaseous additions (Fig. 6.1) not only reduced the intake air but also decreased largely the diesel spray (due to the fuel replacement), which together restricted the source of ignition for the gaseous additions. Therefore, the DGE's superior ignitability and the increased fuel – borne oxygen brought by DGE were inferred to assist the mixture's ignition and combustion and counteracting the intake air shortage and the consequently reduced local oxygen availability. As a result, the addition of DGE was shown (Fig.

6.5) to increase the BTE due to the improved $H_2$ and $NH_3$ utilisation as can be proved by the reduced emissions of $H_2$ and $NH_3$.

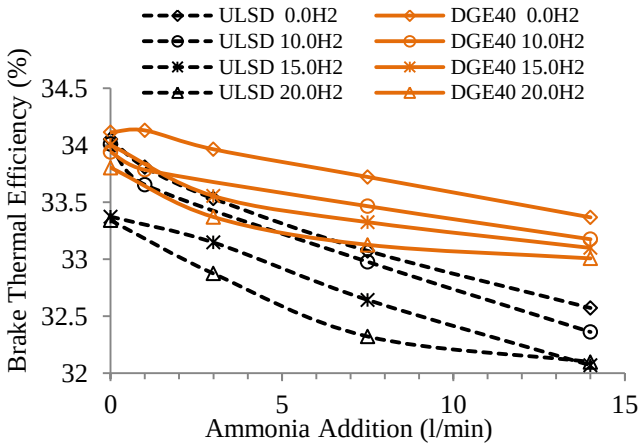


**Figure 6.5:** Engine brake thermal efficiency for the different fuelling.

From the results presented above, it is suggested the high reduction in $NH_3$ could be contributed by a pattern of sequenced improvement, where the DGE could enhance first the individual combustions of $H_2$ and $NH_3$, and more importantly, the improved $H_2$ combustion and its fast flame speed and propagation subsequently favoured the $NH_3$'s combustion, resulting in an overall improved combustion. This sequenced pattern is displayed in Fig. 6.6.

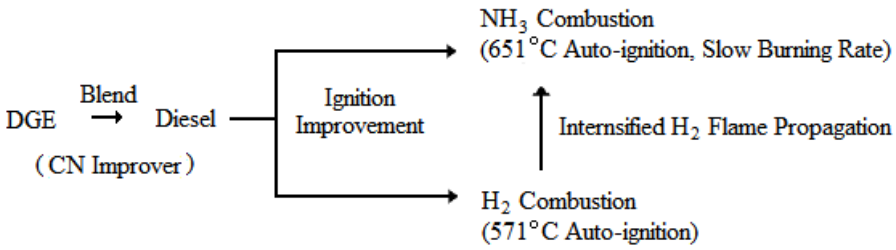


**Figure 6.6:** Proposed combustion pattern enhanced $NH_3$ and $H_2$ combustion with DGE

## 6.5 Gaseous emissions

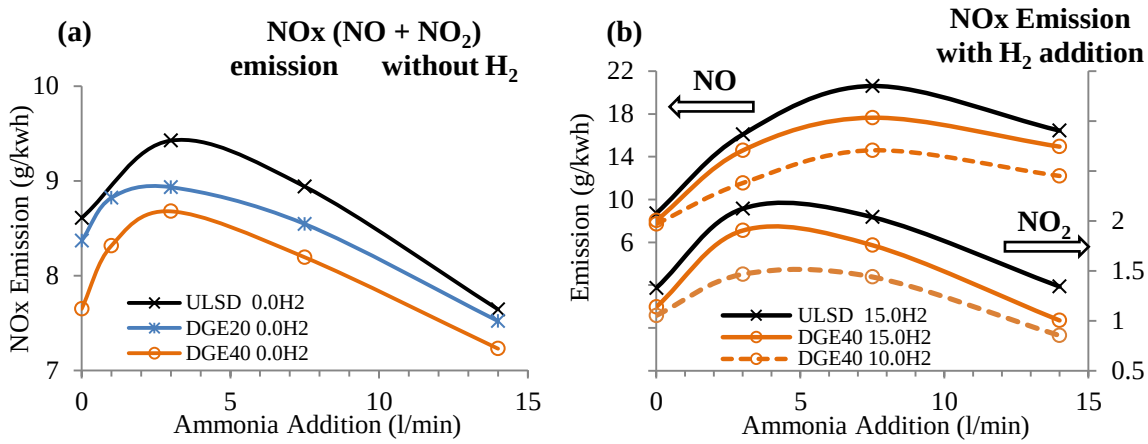


**Figure 6.7**: (a) NOx (NO + $NO_2$) emission of diesel and DGE blends with $NH_3$ addition; (b) NOx (NO + $NO_2$) emission of diesel and DGE blends with $NH_3$ and $H_2$ additions

The NOx emissions (NO + $NO_2$) of the diesel and DGE blends are plotted in Fig. 6.7 (a) against different $NH_3$ additions when $H_2$ was excluded from the combustion. After $H_2$ being co – fed with $NH_3$, the NOx emissions are expressed specifically by the NO and $NO_2$ emissions and shown in Fig. 6.7 (b).

As in agreement to the results presented in chapter 5, the NOx emission in Fig. 6.7 (a) ($H_2$ in absence) is shown to increase with comparatively lower amount of $NH_3$ (up to 3 l/min) but reduced later with increased ammonia addition (i.e. 14 l/min). On the other hand, the improved $NH_3$ combustion with hydrogen inevitably strengthened the NO and $NO_2$ emission from that of the diesel baseline and is shown to be proportional to the hydrogen level (Fig. 6.7(b)). Although DGE was demonstrated to improve the $NH_3$'s combustion, further decrease in NOx was observed due to the increased DGE presence (with and without the hydrogen addition). As indicated earlier in the combustion profile (Fig. 6.2), the addition of DGE reduced the cylinder pressure (i.e.

combustion temperature), especially in the premixed combustion phase where the NOx formation was the most significant. As a result, more NOx formation was suppressed even the hydrogen promotion effect on $NH_3$ combustion.

Some $N_2O$ formation (i.e. up to 2.2 g/kWh, results not shown) was also detected with the combined fuelling of $H_2$, $NH_3$ and diesel. Around 10 - 15 % of the $N_2O$ was reduced after the DGE blends being applied.

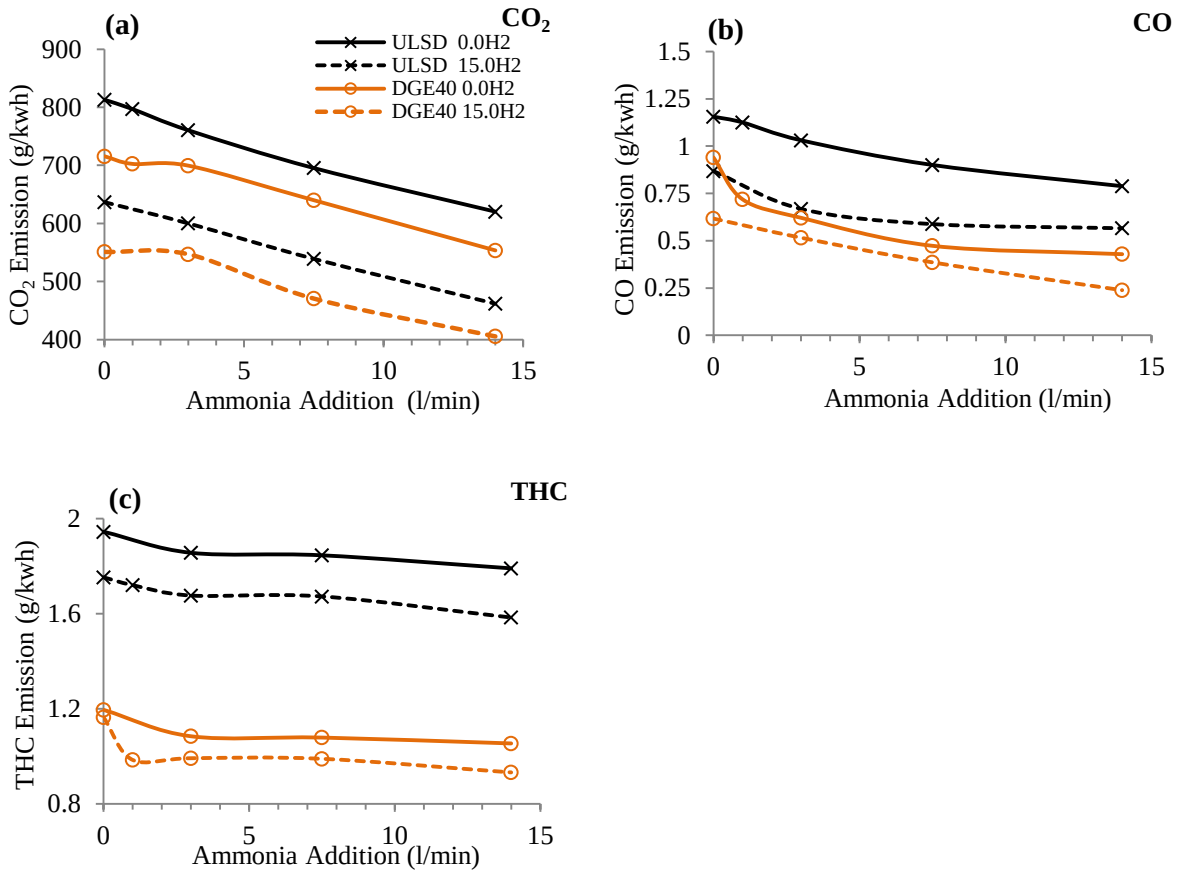


**Figure 6.8:** Engine carbonaceous emissions under different fuelling; (a) $CO_2$, (b) CO and (c) unburned total hydrocarbons (THC).

The carbonaceous emissions including $CO_2$, CO and THC are shown in Fig. 6.8 (a) – (c) respectively. Due to the increased oxygen content in the DGE blend (decreased molecular carbon ratio), $CO_2$ was able to be reduced compared to diesel combustion even without the carbon free gaseous additions. Then, with the enlarged carbon removal due to the replacement of diesel and/or DGE by $H_2$ and $NH_3$ addition, led to the $CO_2$ emission gradual drop reaching to about 50 % of its initial concentration. Similar trends were also observed for the CO and unburned hydrocarbons. In addition in the case of DGE fuelling the locally enriched fuel – borne oxygen enhanced the complete fuel combustion and suppressed the formation of CO and THC (Miyamoto, Ogawa et al. 2000). Furthermore the advanced start of combustion and overall prolonged combustion duration with the DGE blends (Fig. 3b), increased the time for the oxidation of CO and THC.

## 6.6 Particulate matter emissions

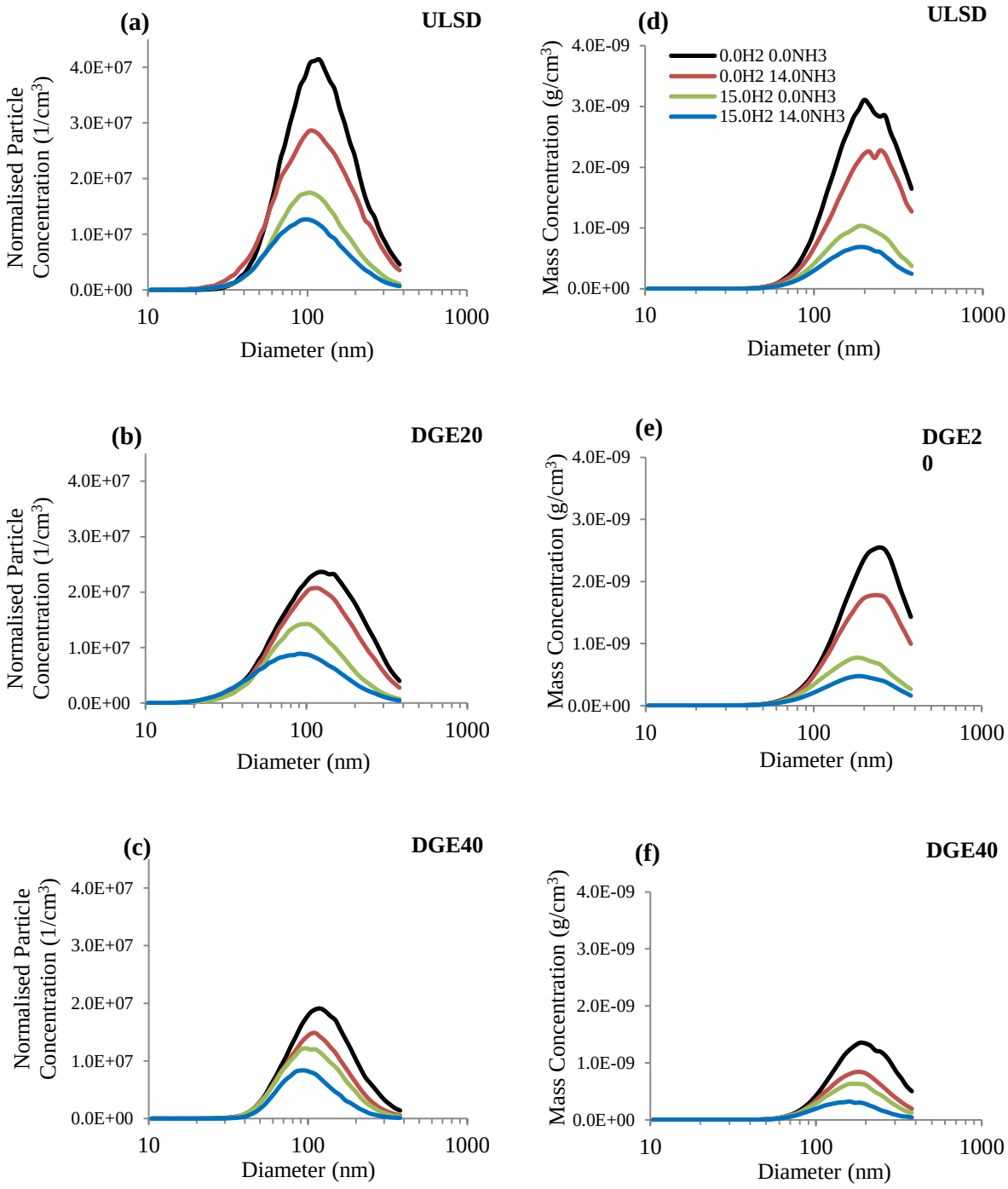


**Figure 6.9**: (a) – (c) PM mass concentrations of standard diesel and DGE blend with different $H_2$ and $NH_3$ additions: (a) diesel, (b) DGE20 and (c) DGE40. (d) – (f) PM number distributions

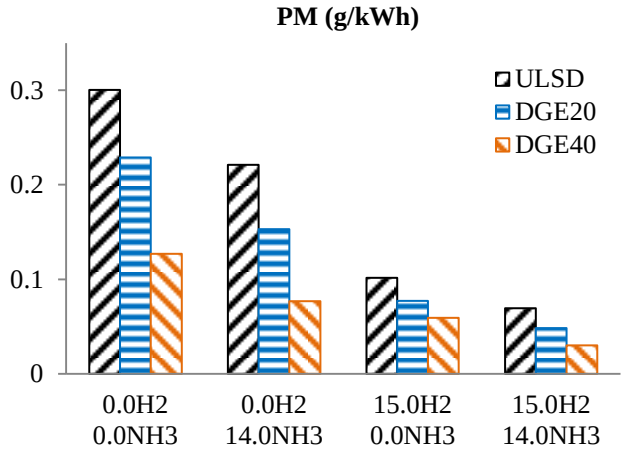


**Figure 6.10:** PM emissions of standard diesel and DGE blends with different $H_2$ and $NH_3$ additions

The particulate size distribution and mass concentrations at different levels of DGE, $H_2$ and $NH_3$ are shown in Fig. 6.9 (a) – (c) and (b) – (f) respectively. The total PM emissions are expressed in g/kWh and are shown in Fig. 6.10. The particle mass distribution was obtained from the particle number distribution through a size dependent agglomerate density function as described by Lapuerta et al (Lapuerta, Armas et al. 2003).

Combustions of the DGE blend show reductions in PM emission with and without gaseous additions. The primary reason was again the strengthened oxygenation of the DGE blend. This would allow enhanced combustion to take place even in the fuel rich area, which helped to oxidise the PMs that were already formed or improve the oxidation particle and particle precursors (McCormick, Ross et al. 1997, Nord and Haupt 2005, Lapuerta, Armas et al. 2008). In addition to that, the prolonged combustion duration (Fig. 6.2) at increased DGE level also provided longer time for the PM oxidation. Another reason for this PM reduction was based on the fact that DGE is in the form of ether (Westbrook, Pitz et al. 2006, Smith, Ott et al. 2008). Due to its atomic

structure of being one oxygen atom bonded to two carbon atoms, the DGE structure was reported to effectively inhibit soot formation, which counts for a large portion in total PM.

After adding hydrogen and ammonia, the mass and number of PM were reduced for both diesel and DGE blends due to the large replacement of carbon element: it is known that PM can be produced from the rich zone diesel combustion, the chance of PM formation was reduced by the additions of carbon – free substitutions. The individual performance of $H_2$ and $NH_3$ are shown to improve at increased DGE level. This is supported by the reduced $H_2$ and $NH_3$ emission shown earlier, meaning enhanced carbon replacement were achieved by better $H_2$ and $NH_3$ combustions. It is seen that $H_2$ alone performed better in PM reduction than that of $NH_3$. This is in accordance with the more pronounced premixed phase in $H_2$ combustion. The PM emission went down when simultaneous additions of $NH_3$ and $H_2$ were adopted and decreased further with use of DGE. The particulate matter size distributions were decreased emission on number concentration as well as mass basis across the size spectrum (Fig. 6.9), and hence decreased the total mass emission as shown in Fig. 6.10. These trends further support the above proposed DGE combustion enhancement (Fig .6.6), which in turn improved also the PM reduction.

## 6.7 Summaries

In the above research, performance of DGE as an oxygenated additive and ignition improver was assessed in a diesel engine with combustions of reformed $NH_3$ (simulated) for partial hydrocarbon fuel substitution and engine decarbonisation.

Due to the DGE' better ignition properties, both of the $H_2$ and $NH_3$'s ignitions and combustions were shown to be facilitated. The improved $H_2$ and $NH_3$ combustion tended to promote the engine's NOx formation. However, DGE was shown to suppress this NOx formation through its featured low temperature combustion. This suggests the currently observed trade – off between the carbon and NOx emissions could be potentially diminished by the increased presence of DGE.

On the other hand, the DGE's high oxygenation in combustion would also mean enhanced local oxygen/fuel ratio for improved fuel oxidation. Hence, increased DGE level could also imply its strengthened effect on counteracting the shortage of in – cylinder oxygen due to the air replacement (i.e. gaseous additions of $NH_3$ reformate or even EGR) at the engine intake.

# CHAPTER 7: $H_2$ – $NH_3$ REFORMATE ASSISTED LEAN NOx ABATEMENT OVER SILVER/ALUMINA CATALYST

## 7.1 Introduction

In chapter 5 and 6, the combustion of $NH_3$ reformate was shown to reduce significantly the diesel engine's carbonaceous emissions. However, the natures of the combustion were on the other hand demonstrated to increase the engine NOx and result in some emission of the unburned reformate gases i.e. $H_2$ and $NH_3$.

Nevertheless, the existence of $H_2$ and $NH_3$ in the engine exhaust is potentially good for some catalytic aftreatment, such as the silver loaded SCR system. Recent literatures showed successful NOx reduction over $Ag/Al_2O_3$ catalyst using a mechanism of $NH_3$ – SCR under promotion of $H_2$ (Richter, Fricke et al. 2004). The reaction was demonstrated to take place at low temperature with reduced catalyst light – off temperature (Doronkin, Khan et al. 2012, Fogel, Doronkin et al. 2012, Tamm, Fogel et al. 2013).

Existing literature on $H_2$ assisted $NH_3$ – SCR over $Ag/Al_2O_3$ were carried out using simulated engine exhaust gas (Houel, Millington et al. 2007, Kondratenko, Bentrup et al. 2008, Theinnoi, Sitshebo et al. 2008), and most importantly, all these studies assumed that the required $H_2$ could be available on – board the vehicle. In this work, the studies of NOx reduction were performed by incorporating the $NH_3$ exhaust gas reformer.

In addition, due to the existence of unburned hydrocarbon in the diesel exhaust, possible reaction of HC – SCR could happen parallel to the $NH_3$ – SCR mechanism. This allows a simultaneous study of these two reactions and provides an understanding of how these two reactions might influence each other and how they might affect the overall engine NOx reduction when different levels of $NH_3$ and hydrocarbon, i.e. different $NH_3$:NOx and $C_1$:NOx ratios, are used.

Therefore, the $NH_3 - H_2$ gas mixture produced or simulated was sent directly into the diesel exhaust (i.e. source of HC and NOx emissions, indicated in Fig. 7.1) for a downstream $Ag/Al_2O_3$ catalyst. The use of $H_2$ (8000 ppm in the exhaust throughout) was solely determined by the reformer's production at selected operation conditions, which were based on the previous study's (Chapter 4). The hydrogen's ratio against other main reactants ($NH_3$, THC and NOx) was excluded as well, as it is not one of the primary concern in current reach.

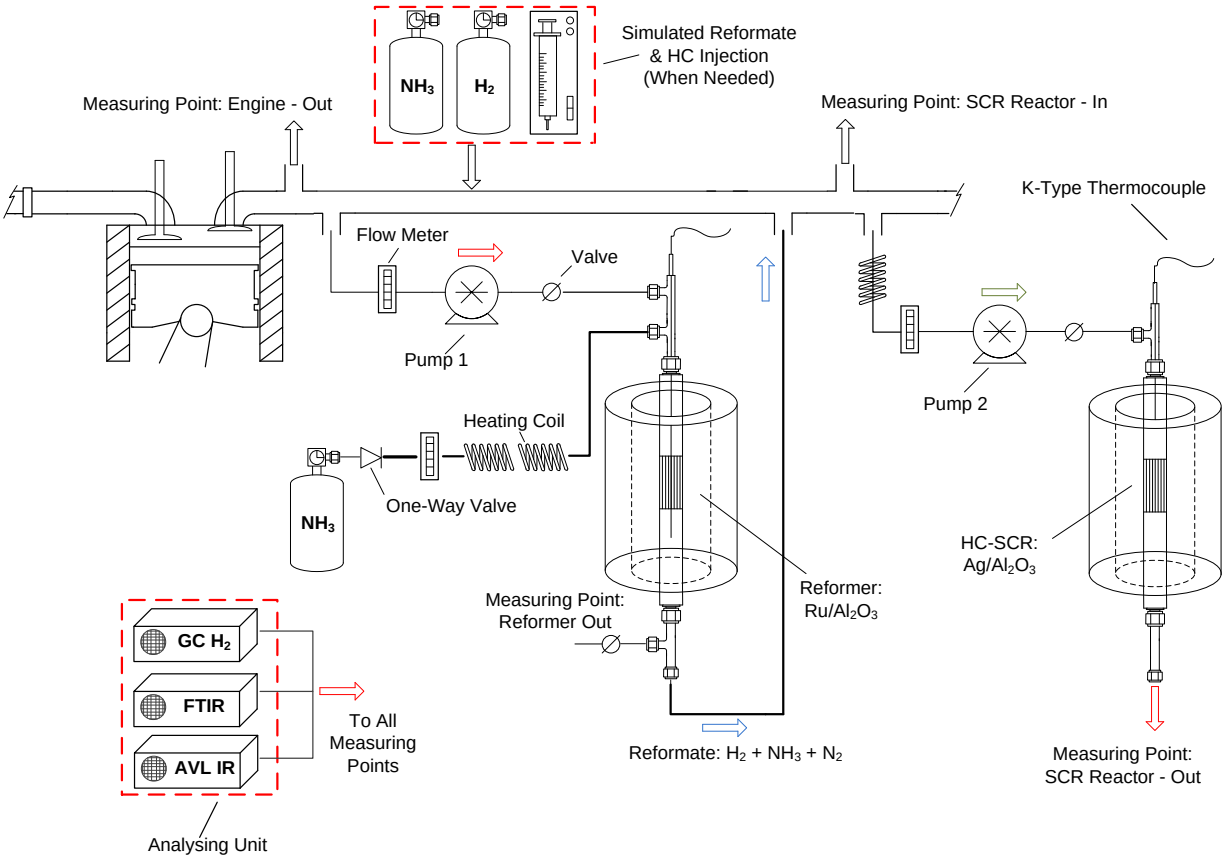


**Figure 7.1:** Equipment configuration for combined $NH_3$ reformer and $Ag/Al_2O_3$ SCR system

In the end, the catalyst activity was also studied in exhaust with reduced NOx concentration. This was in order to investigate the catalyst's performance at low load engine operation or with increased exhaust gas recirculation ratio (EGR).

In the current study, the engine was operated at 4 bar IMEP and 1500 rpm engine speed. The engine operation was kept constant throughout the study, giving fixed major exhaust components such as NOx, THC and etc. The corresponding engine emissions are shown in Table 7.1.

**Table 7.1:** Average engine exhaust composition at 4 bar IMEP engine load and 1500 rpm

| $CO_2$ (%) | CO (ppm) | THC (ppm) | NO (ppm) | $NO_2$ (ppm) | $N_2O$ (ppm) | NOx (ppm) | $H_2O$ (%) | $O_2$ (%) |
|---|---|---|---|---|---|---|---|---|
| 5.1 | 110 | 430 | 690 | 40 | 0 | 730 | 5.1 | 14.9 |

For the exhaust gas reformer, the engine exhaust was extracted at a flow rate of 3 l/min. In addition, a 3 l/min $NH_3$ stream was supplied from a gas cylinder and mixed with the extracted exhaust at an $O_2/NH_3$ ratio of 0.15. This resulted in a reformate production of around 3 l/min of gaseous $H_2$ and 0.3 l/min of unconverted $NH_3$ (approximately 8000 ppm and 720 ppm respectively when used in the engine main exhaust).

As for test procedure, the SCR catalyst's activity using different reformates was assessed first within a temperature ramp ranging from 140 – 550 ℃ and gas – hourly – space – velocity (GHSV) of 35000 $h^{-1}$. A test matrix was designed to assess a range of reformate additions as shown in Table A7.1 (Appendix) below in order to study the combined HC –SCR and $NH_3$ – SCR. Following that, the $NH_3$ level was reduced stepwise to study its effect over the THC conversion (performance of HC – SCR) and to get further evidence for the combined SCR. After the temperature ramps, reactions performed at various $C_1$:NOx and $NH_3$:NOx ratios were studied by means of external HC injection and $NH_3$ addition. For investigating any effect of low NOx concentration on the combined system, the engine was operated with EGR in the end. The produced exhaust with changed gas components was fed into the catalyst along with the simulated reformates. All the tests are summarised and shown in Table A7.1.

### 7.2 $H_2$ assisted $NH_3$ – HC – SCR

Comparing Fig. 7.2 (a) and (b) suggests the use of $H_2$ initiated the HC – SCR reaction of $NO_X$ at much lower temperature (<200 ℃). This has previously been explained as $H_2$ is essential in the reductive activation of molecular oxygen ($O_2$ contents in the exhaust) into reactive oxygen species,

which is then involved in oxidative activation of hydrocarbon in the exhaust (Shimizu, Shibata et al. 2006). In the absence of hydrogen (Fig.7.2 (a)), significant hydrocarbon conversion could only be detected at temperatures higher than 380 ℃, as a result of its rapid oxidation instead of being used in NOx reduction.

Nearly no NOx conversion was also observed when $NH_3$ was fed into the main exhaust without $H_2$ and at a $NH_3$:NOx ratio of 1:1 (Fig. 7.2 (c)). The injected $NH_3$ started to convert at around 350 – 380 ℃ due to its oxidation over the catalyst active site. This contributed to NOx production and in turn affected negatively NOx conversion.

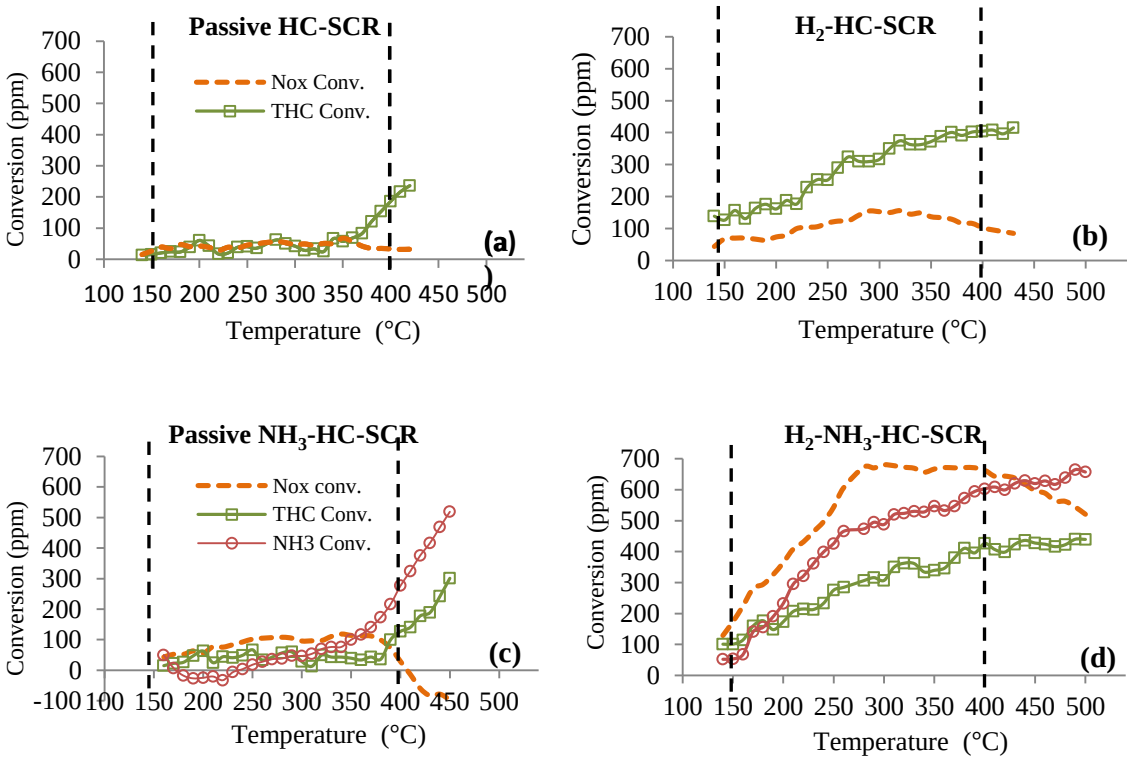


**Figure 7.2:** Conversion of NOx (730 ppm exhaust NOx fixed at catalyst inlet), $NH_3$ and THC (constant engine exhaust THC produced at 430 ppm) in the SCR process: (a) with engine exhaust only; (b) with engine exhaust and 8000ppm $H_2$; (c) with engine exhaust and 720ppm simulated

$NH_3$ reformate, $NH_3$:NOx =1; (d) engine exhaust and produced reformate $NH_3$ (720 ppm) and $H_2$ (8000 ppm).

Furthermore, Fig. 7.2 (a) and (c) show the exhaust hydrocarbons remained inactive regardless of the $NH_3$ addition. After the reformer system was connected to the engine exhaust ($H_2$ assisted $NH_3$ – HC – SCR, Fig. 7.2 (d)), the low temperature (< 250 ℃) NOx reduction activity of the catalyst was remarkably improved. A stable approximately 90 % NOx reduction was achieved between the temperatures range of 260 to 400 ℃. The improvement in NOx conversion, especially in the temperatures range of 150 to 260 ℃, was proportional to $NH_3$ conversion over the catalyst, indicating strong $NH_3$ – SCR activity. However, in Fig 7.2 (d), the $NH_3$ conversion did not keep up with the reduced NOx on a 1:1 stoichiometry as shown in Eq. (2.16), Chapter 2. Therefore, this "additional" reduction of NOx is a result of the $H_2$ assisted HC – SCR, using the exhaust hydrocarbons.

A recent study (Shimizu, Tsuzuki et al. 2006) proposed that the role of $H_2$ in HC – SCR is the formation of Ag clusters ($Ag_n^{\delta+}$) on $Ag/Al_2O_3$ via $H_2$ reduction of $Ag^+$ ions. It was proposed that the formed Ag clusters work with $H^+$ ions in reducing $O_2$ to yield superoxide $O_2^-$, which is known as the key intermediate for the activation of radical reactions involving both hydrocarbon and NO species that finally leads to $N_2$ production (Shibata, Shimizu et al. 2003, Yeom, Li et al. 2006). A similar reaction scheme was proposed for $H_2$ assisted $NH_3$ – SCR over $Ag/Al_2O_3$, where the formation of Ag clusters and $O_2^-$ equally existed and initiated intermediates reaction derived from $NH_3$ and NO to produce gaseous nitrogen (Shimizu and Satsuma 2007). Based on these findings and the experimental observations, it is reasonable that, under the diesel exhaust environment ($O_2$

and unburned THC present in diesel engine exhausts), $H_2$ over $Ag/Al_2O_3$ is able to provide the same necessary chemical conditions for both the HC – SCR and $NH_3$ – SCR, allowing their activation over the same catalyst. The addition of $NH_3$ neither interacted with the exhaust hydrocarbon in the absence of $H_2$, nor changed significantly the THC conversion in the presence of $H_2$ (Fig. 7.2 (b) and (d)). Thus it is suggested that in this system the $H_2$ assisted HC – SCR and $NH_3$ – SCR proceed independently, with the overall deNOx performance being a result of their combined performances.

### 7.3 Influence of $NH_3$:NOx ratio on the SCR reactions

In order to further study the coexistence of HC and $NH_3$ - SCR, the $NH_3$ reformate was simulated at lower concentrations (decreased $NH_3$:NOx ratio) and the system's $H_2$ concentration was fixed at 8000 ppm (either from the bottle gas simulation or the reformer production).

Fig. 7.3 (a) shows the NOx and $NH_3$ conversions, whereas Fig. 7.3 (b) shows the conversions of the exhaust hydrocarbons at each $NH_3$ level. By decreasing the $NH_3$:NOx ratio, the NOx conversion was decreased (Fig. 7.3 (a)). However, despite the variation in ammonia concentration, the amount of utilised THC in NOx reduction (for additional NOx reduction) at different $NH_3$ level was similar to each other (Fig. 7.3 (b)). Therefore, these observations indicate that the performance of the HC – SCR was unchanged and the decline in the overall NOx reduction was primarily due to the decreased $NH_3$ level, i.e. the reaction was primarily determined by the $NH_3$ – SCR activity at the selected $NH_3$ level.

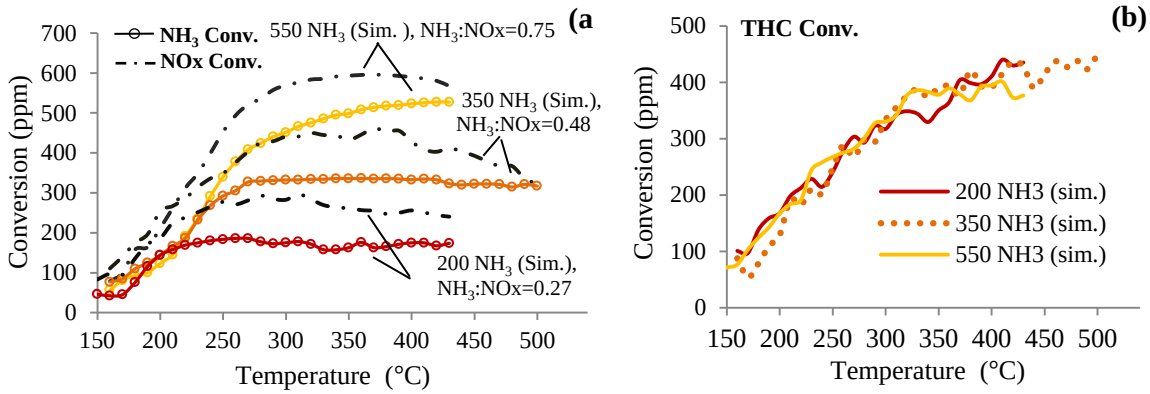


**Figure 7.3:** (a) NOx (730 ppm exhaust NOx fixed at catalyst inlet, and constant engine exhaust HC produced at 430 ppm) and $NH_3$ conversions at different levels of simulated $NH_3$reformate ($NH_3$/NOx ratios); (b) THC conversions at different levels of simulated $NH_3$ reformate.

During the above runs, increased amount of $NO_2$ was recorded downstream the catalyst at different $NH_3$ concentrations, Fig. 7.4 (a). Comparing this $NO_2$ production to the $NH_3$ and THC conversion without $H_2$ addition (Fig. 7.2), it was found that the oxidative activation of NO started at much lower temperature (~ 150 ℃) than that of the $NH_3$ and THC (~ 350 – 380 ℃). In addition, this NO activation also matched the light – off of the $H_2$ assisted $NH_3$ – HC – SCR at all $NH_3$ levels (Fig. 2d and Fig. 3a). Therefore, the $H_2$ promotion of the NO oxidation is shown as an important step in the overall SCR mechanism. This is especially important for the promotion of $NH_3$ – SCR, which can be therefore assumed to partially behave according to the Fast– SCR route using the promoted $NO_2$ (Eq. (2.19), Chapter 2) (Doronkin, Fogel et al. 2012).

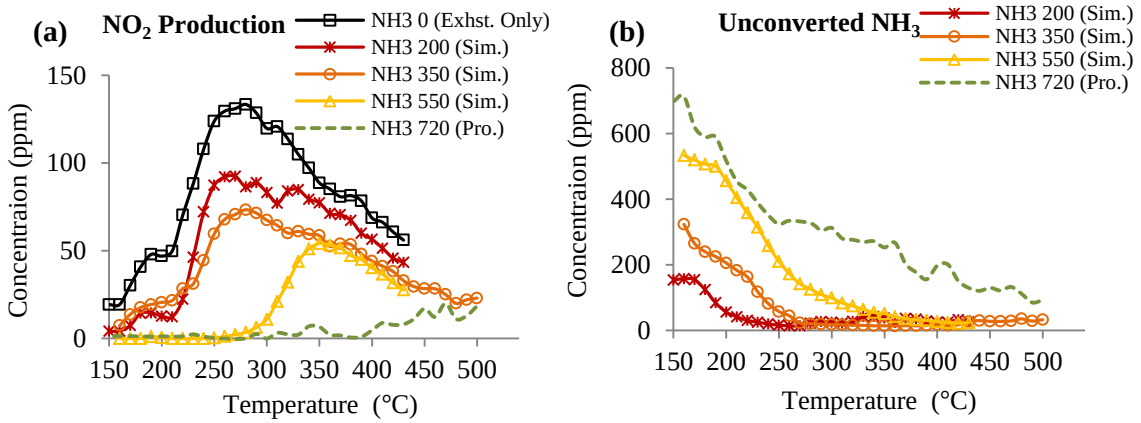


**Figure 7.4:** Effect of different levels of $NH_3$ reformate (both simulated and produced, where 8000 ppm of $H_2$ reformate was fixed) on the SCR process, a) $NO_2$ production and b) concentration of the unconverted $NH_3$ at each $NH_3$ feed level.

Fig. 7.4 (b) shows the system's $NH_3$ concentrations during the SCR reactions at each $NH_3$ addition and at different temperatures. Comparison between Fig. 7.4 (a) and (b) suggests that the sharp $NO_2$ increase was in response to the depletion of $NH_3$ at each level of addition. Also, when less $NH_3$ was added into the system (e.g. 200 ppm $NH_3$ vs. 350 ppm $NH_3$), not only the amount of $NO_2$ was increased, but also the temperature at which the $NO_2$ started to appear was lowered as well. The highest $NO_2$ production was detected with no $NH_3$ addition (i.e. only engine exhaust, Fig. 7.4 (a)). Hence it suggests, with the primary reactant $NH_3$ being gradually reduced, less of the formed $NO_2$ was involved in the main SCR reaction. The improved $NH_3$ conversion at lower temperatures when the $NH_3$ addition to the SCR catalyst was reduced (Fig. 7.4 (b)) could be associated with the formation of surface nitrate species, whose adsorption over the catalyst can reduce the active sites (Richter, Fricke et al. 2004, Shimizu, Shibata et al. 2006, Hellman and Grönbeck 2009, Chansai, Burch et al. 2012). Although, providing $NH_3$ at around the 1:1

stoichiometry is shown to give high NOx reduction, the unconverted $NH_3$ was detected at unwanted levels. Recent studies found that $NH_3$ can itself retard the removal of these surface nitrates via NO oxidation (see Eq. (7.1)) (Grossale, Nova et al. 2008, Grossale, Nova et al. 2009). This blocking effect becomes more detrimental at low reaction temperatures, especially for the Fast SCR reaction. In the current study, the hydrogen availability was suggested as an enhancer in accelerating the removal of these surface nitrates. In addition, with the $NH_3$ concentration being gradually decreased, the low temperature catalyst blockage seems to be alleviated, as a result of the surface nitrates being released through dissociation of the ammonia – nitrate complex (Grossale, Nova et al. 2009).

$$HNO_3 + NO \leftrightarrow NO_2 + HONO \qquad (7.1)$$

In addition, carbonaceous deposits (referred as coking) can develop over the catalyst surface under diesel exhaust conditions. This is equally effective in deactivating the catalyst at lower temperatures. Previous studies (Chong, Tsolakis et al. 2010, Gill, Chatha et al. 2011) showed that $NO_2$ is an active low temperature oxidation agent, which enables the reduction of C – containing species at the catalyst surface through strong oxidation. Thus the increased $NO_2$ availability at decreased $NH_3$ concentration may also serve to clean the $Ag/Al_2O_3$, making it more active with respect to SCR at lower temperatures.

## 7.4 Influence of the $C_1$:NOx ratio on the SCR reactions

The use of a $NH_3$:NOx ratio lower than the stoichiometric amount limited $NH_3$ slip, but decreased the overall NOx reduction with respect to that obtained using an excess of ammonia. To counteract this decrease in NOx conversion the injection of external hydrocarbons is proposed. Houel et al. (Houel, Millington et al. 2007) reported previously that a $C_1$:NOx ratio ranging from 2 to 3 was shown to be the required one for the $Ag/Al_2O_3$ catalyst optimum activity. In the current study, using only the exhaust THC ($C_1$:NOx = ～ 0.58) would therefore limit the HC – SCR activity.

In order to assess the effect of HC – SCR on the overall NOx reduction, at both steady state and transient conditions, experiments were performed at 300 ℃ using different levels of hydrocarbon and ammonia.

As shown in Fig. 7.5 (a), the steady state NOx conversion improved when ULSD was externally injected, increasing the system's THC level from 430 to 1600 ppm ($C_1$:NOx = ～ 0.58 – 2.2). This shows that the enhanced HC – SCR benefited the overall NOx reduction independently of the $NH_3$ levels. It also seems that, increasing both the THC and $NH_3$ concentrations the total NOx conversion can also be improved.

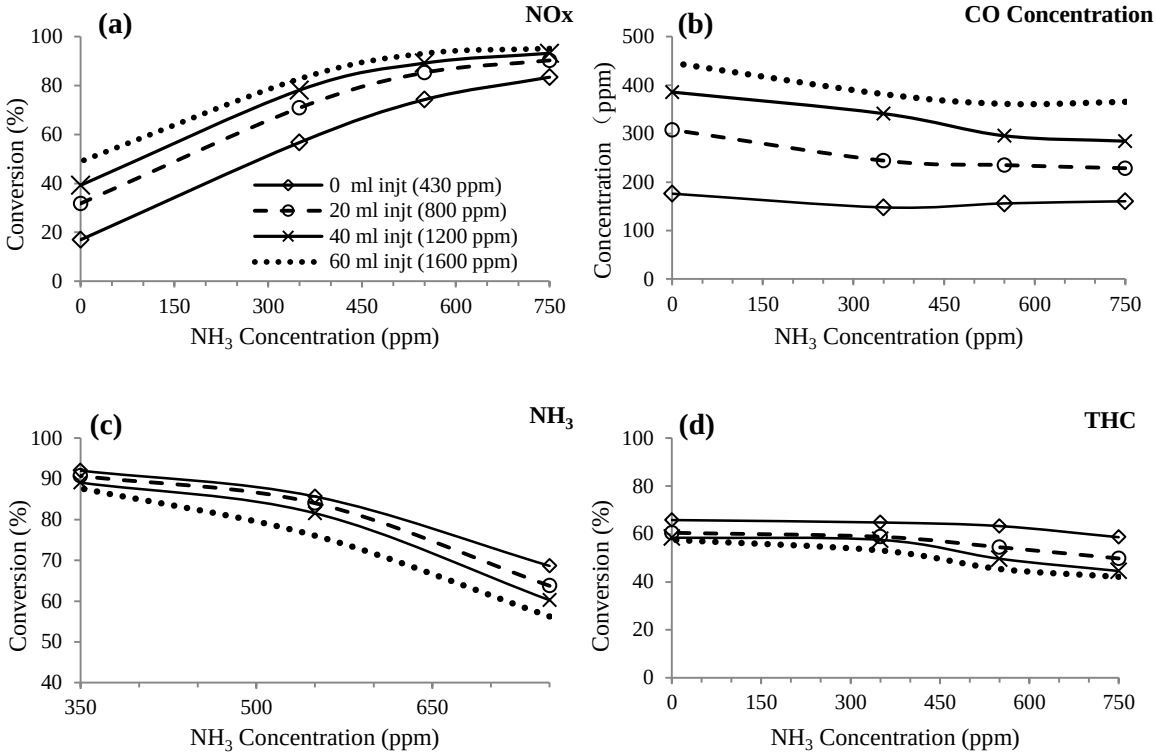


**Figure 7.5:** $NH_3$ and THC concentration effects on: (a) NOx conversion, (b) CO production, (c) $NH_3$ conversion and (d) THC conversions.

This is more pronounced at lower ammonia concentrations as can be seen in Fig. 7.6 (a), where while the SCR reaction was stabilised with 350 ppm of $NH_3$ addition ($NH_3$:NOx = 0.48), improvements in NOx reduction can be achieved through an externally injected 1200 ppm of ULSD ($C_1$:NOx = 1.6).

This was supported by the increase in carbon monoxide production (Fig. 7.6 (b)) in the SCR right after each fuel injection. With the presence of $H_2$, the promotion in the oxidative reaction of hydrocarbon becomes significant. Part of the externally injected hydrocarbon was activated to yield hydrocarbon radicals (Chansai, Burch et al. 2011), whose presence reinforced the HC – SCR

activity. With the THC availability stepped up in the exhaust mixture, not only the HC – SCR activity but also the level of CO (Fig. 7.5 (b)) were increased at a given $NH_3$ concentration.

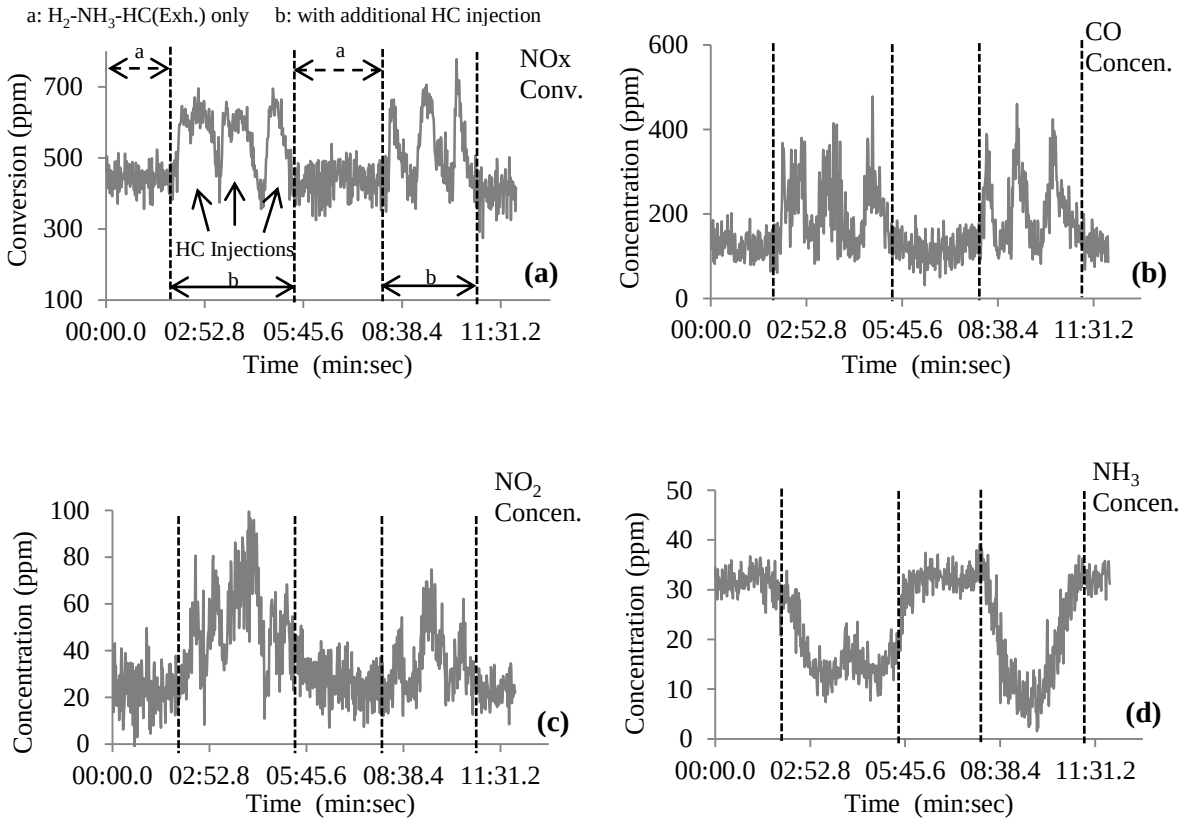


**Figure 7.6:** NOx reduction and exhaust components during the start – stop hydrocarbon transient injection: (a) NO reduction, (b) CO concentration, (c) $NO_2$ concentration and (d) $NH_3$ concentration.

It was also noticed in the transient study (Fig. 7.6 (c)), after each hydrocarbon injection that the enrichment in CO seemed to promote $NO_2$ production. This was attributed to a three – step, self – propagating mechanism that involves CO and NO oxidations by hydroxides and hydroperoxy radicals (see Eq. 7.2 – 7.5) (Feitelberg and Correa 2000, Tayyeb Javed, Irfan et al. 2007).

$$CO + OH^- \rightarrow CO_2 + H^+ \quad (7.2)$$

$$NO + HO_2 \rightarrow NO_2 + OH^- \quad (7.3)$$

$$H^+ + O_2 + M \rightarrow HO_2 + M \text{ (M: any third body)} \quad (7.4)$$

$$\text{Eq. 7.2 + Eq. 7.3 + Eq. 7.4: } CO + NO + O_2 \rightarrow CO_2 + NO_2 \quad (7.5)$$

The produced CO subsequently favoured the $NO_2$ production, which was found to enhance the $NH_3$ conversion in Fig. 7.6 (d). The observed reaction profile matches the Fast – SCR described earlier in Eq. (2.16), Chapter 2, indicating this further promotion is essentially a result of the sudden increase in THC. Hence the sequenced reactions, shown from Fig. 6a to 6d, could further the overall NOx reduction. In addition to that, the results also suggest that, by applying different $NH_3$:NOx and $C_1$:NOx ratios, it is possible to have the combined SCR operating successfully and achieve the highest NOx removal.

However, despite the enhanced NOx reduction (80 % - 90 %), the simultaneous increases in THC and $NH_3$, e.g. $NH_3$ at 750 ppm and THC at 1600 ppm, retarded each of their conversions (Fig. 7.5 (c) and (d)). The excessive addition of both reductants leads to unnecessary reactant slippage in the SCR catalyst. Therefore, examining on Fig. 7.5 (c), it is suggested to use 350 ppm of $NH_3$ ($NH_3$:NOx = 0.48), as a high $NH_3$ conversion could be kept regardless of the THC level. Similarly, Fig. 7.5 (d) advocates a hydrocarbon addition at 1200 ppm ($C_1$:NOx = 1.64) or less, as its conversion did not differ significantly from that of the exhaust hydrocarbon. Therefore, with respect to $H_2$ – HC – SCR, the addition of $NH_3$ reformate helps to reduce the fuel penalty

associated with i) high levels of HC injection over the SCR and ii) the hydrogen production if HC is considered as source of $H_2$.

### 7.5 Influence of NOx concentration in the SCR reactions

In this section, the work was expanded to study the combined HC – $NH_3$ –SCR with a reduced level of engine out NOx emissions, similar to engine operation at low load or with increased EGR concentrations. To achieve low NOx concentration in the exhaust, 20% EGR was incorporated, while the engine was kept at the same speed – load conditions as before. As EGR was mainly reduced the engine – out NOx, the $C_1$ – NOx ratio was increased from 0.6 to 1.2. Some key exhaust gas components after the EGR addition are shown in Table. 4. Following that, 8000 ppm of $H_2$ and 200 ppm of $NH_3$ were introduced into the main exhaust, giving a $NH_3$:NOx ratio of 0.5, close to the optimised value reported in section 7.3.3. The catalyst temperature was kept as low as 200 ℃ throughout the test. The whole experiment was again carried out in a transient study based on real time, where NOx reduction, CO conversion and THC conversion are shown in Fig. 7.7 (a) – (c), respectively.

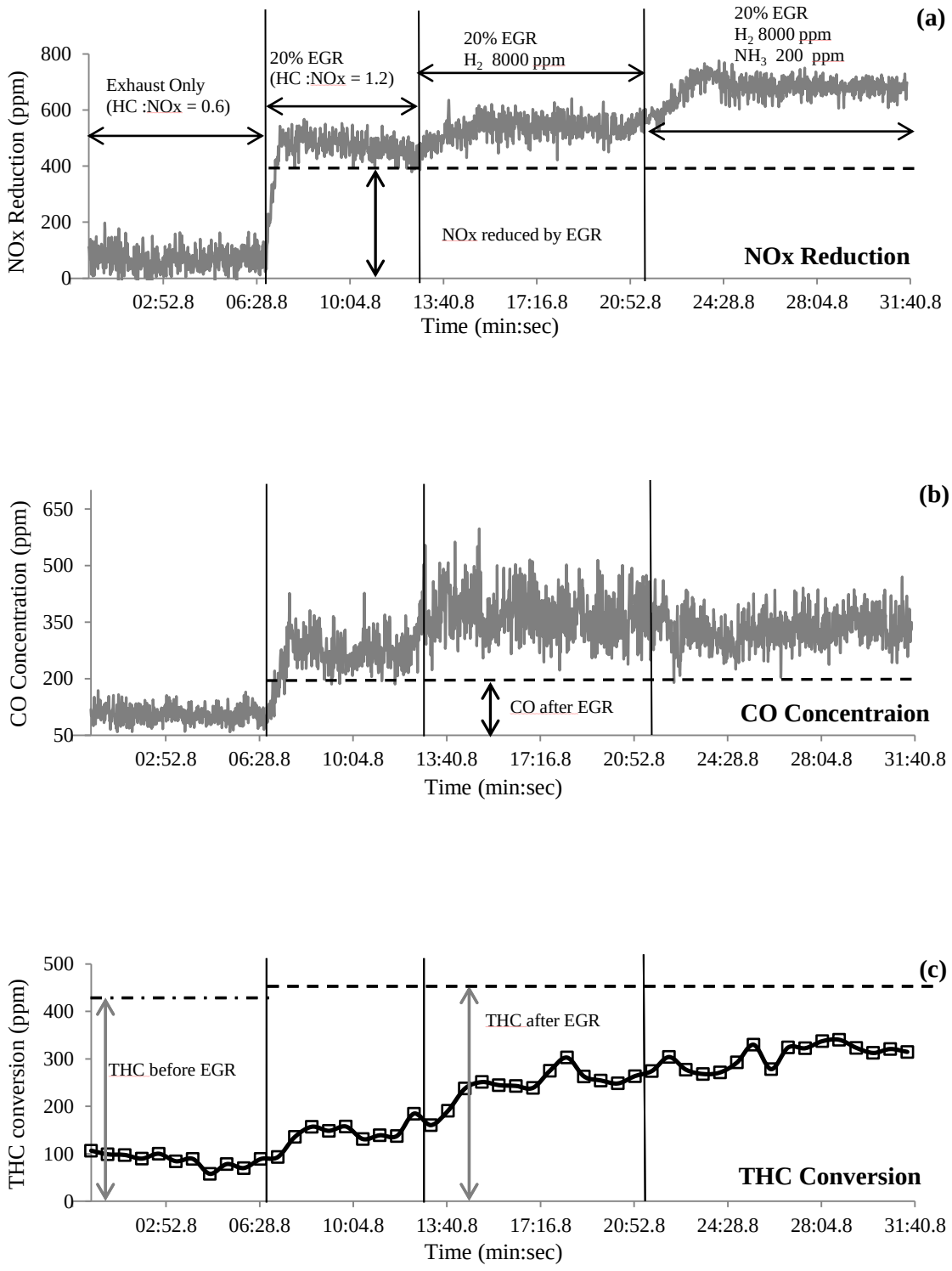


**Figure 7.7:** Transient (a) NOx conversion (engine exhaust NOx fixed at 730 ppm), (b) CO detection and (c) converted THC during passive HC – SCR, with use of 20 % EGR (increased $C_1$:NOx ratio), with use of EGR and simulated $H_2$ reformate (fixed at 8000 ppm) and the use of EGR and simulated $NH_3$ (200 ppm) – $H_2$ (8000 ppm) reformate.

As reflected by Fig. 7.7 (a), without EGR the catalyst provided with the untreated exhaust (high NOx) demonstrated the lowest activity. The incorporation of EGR resulted in a large engine – out NOx reduction (indicated by the dotted line). Hence, even without external injection, the hydrocarbon availability against NOx was improved and thus enhanced catalyst performance was observed. However, the activity decayed slowly because of C – containing species' deposition over the active site. With the addition of hydrogen, the NOx conversion was recovered and improved. Meanwhile, due to the "$H_2$ effect", increases in both of the CO concentration (Fig. 7.7 (b)) and the system's hydrocarbon conversion (Fig. 7.7 (c)) were detected.

As expected, the combined reaction took place when the simulated $NH_3$ reformate was introduced, boosting the overall NOx conversion to around 90%. Although the catalyst temperature was further reduced to 200 ℃, the sharply reduced NOx concentration with the incorporation of EGR, allowed the use of less $NH_3$ (200 ppm), which in turn promoted the ammonia conversion as shown earlier in section 7.3.2. A slight decrease in CO concentration was also observed after the $NH_3$ addition revealing the occurrence of the 'chain reaction' shown in section 7.3.3 (where the CO was consumed to contribute to the NOx improvement). Therefore, the reduced NOx after EGR favoured both the HC – SCR and $NH_3$– SCR (via improved $C_1$:NOx and $NH_3$:NOx ratios), contributing together to the overall NOx reduction.

As both of the $C_1$:NOx and $NH_3$:NOx ratios were shown as appropriate after the NOx reduction by EGR, the THC and $NH_3$ emissions were both low downstream the catalyst i.e. about 160 ppm THC (approximately 70 % reduction from the engine out) and only 15 – 20 ppm unconverted $NH_3$ (ammonia slip). This shows the reformer – SCR system is adaptable to various

engine operations, satisfying emission controls in both high and mid – low conditions (where engine – out NOx is comparatively lower).

## 7.6 Summaries

A prototype system combining a $NH_3$ reformer and a silver – based SCR system has demonstrated a feasible way of vehicle on – board $H_2$ production and its promotion effect on a silver based SCR system. By using different $NH_3$ – $H_2$ reformate mixture and incorporating external hydrocarbon injections, the results demonstrated:

- $H_2$ was the essential reaction promoter. Its presence under diesel exhaust conditions was shown as a prerequisite for the simultaneous activation of HC – SCR and $NH_3$ – SCR over $Ag/Al_2O_3$catalyst.
- The $NH_3$:NOx and $C_1$:NOx ratios were suggested as crucial factors that not only determined the performance of the combined SCR, but also affected the interrelationship between the $NH_3$ – SCR and HC – SCR reactions.

With the study being further extended with the incorporation of EGR, i.e. low exhaust NOx, the reformer – SCR system was shown to be adaptable to various engine conditions, where both the high performance of SCR and low slippage of reactants, i.e. $NH_3$ and exhaust hydrocarbons, could be efficiently maintained.

Hence, from the study presented above, it is suggested to combine both of the combustion and the SCR reaction that are powered by the $NH_3$ reformate. With careful calibration on the

engine and catalyst conditions, simultaneous reductions in carbon (from the engine combustion) and NOx emissions (over the SCR catalyst) would be expected.

## 7.7 Appendix

**Table A7.1:** Test matrix using different reformate

| | ***Major gas components at catalyst inlet*** | Inlet $NH_3$ (ppm) | Exhaust HC (ppm) | Exhaust NOx (ppm) | $NH_3$:NOx | $C_1$:NOx | Inlet $H_2$ (ppm) |
|---|---|---|---|---|---|---|---|
| **Conditions for temperature ramp** | Exhaust only (Passive HC – SCR) | 0 | ~430 (Ex.) | ~730 (Ex.) | 0 | 0.6 | 0 |
| | Exhaust +$H_2$($H_2$ assisted HC – SCR) | 0 | | | 0 | | 8000 (Sim.) |
| | Exhaust +$NH_3$($NH_3$ – HC – SCR) | 720 (Sim.) | | | 1.0 | | 0 |
| | Exhaust + Reformate ($H_2$ – $NH_3$ – HC –SCR) | 720 (Pro.) | | | 1.0 | | 8000 (Pro.) |
| | Exhaust+$NH_3$+ $H_2$($H_2$ – $NH_3$ – HC –SCR) | 550 (Sim.) | ~430 (Ex.) | ~730 (Ex.) | 0.75 | 0.6 | 8000 (Sim.) |
| | | 350 (Sim.) | | | 0.48 | | |
| | | 200 (Sim.) | | | 0.27 | | |
| | Exhaust +$NH_3$+ $H_2$with constant HC injection | 0 – 750 (sim.) | 430 to 1600 (Ex. + Const. Injt.) | ~730 (Ex.) | 0.3 – 1.0 | 0.6 – 2.2 | 8000 (Sim.) |
| | Exhaust +$NH_3$+ $H_2$with transient HC injection | 350 (Sim.) | 1230 (Ex. + Tran. Injt.) | ~730 (Ex.) | 0.48 | 1.6 | 8000 (Sim.) |

Ex.: component in engine exhaust

Pro.: reformer produced reformate

Sim.: reformate component simulated by bottled gas

Const. Injt.: constant HC injection

Tran. Injt.: transient HC injection

# CHAPTER 8: INCREASED $NO_2$ CONCENTRATION IN THE DIESEL ENGINE EXHAUST FOR IMPROVED $H_2$ – $NH_3$ – SCR ACTIVITY OVER $Ag/Al_2O_3$ CATALYST

## 8.1 Introduction

In the previous chapter, it was shown that the $H_2$ assisted $NH_3$ – SCR over $Ag/Al_2O_3$ might react partially in the form of Fast – SCR; the NO to $NO_2$ oxidation was revealed to be an essential step that activates the overall SCR reaction. The fast mechanism has the great potential to make effective low temperature (< 250 ℃) NOx removal, which is quite ideal for lean burn diesel engines.

The current study is largely motivated by the above possible mechanism, where the effect of $NO_2$ on the low temperature SCR activity is aimed to be investigated with the use of lean burned engine exhaust. A diesel oxidation catalyst (DOC) made from $Pt/Al_2O_3$ was adopted. This was because of the $Pt/Al_2O_3$'s well- known function in HCs and CO removal and, most importantly, its effective enhancement in NO to $NO_2$ conversion (Schott, Steigert et al. 2012). Therefore, if both $H_2$ and $NH_3$ can be injected after the DOC to simulate the unburned reformate, the treated exhaust will then contain similar components as those produced by the reformate combustion. Apart from that, it is widely known that $H_2$ can also improve the $Pt/Al_2O_3$'s performance in NO oxidation at low exhaust temperature (engine running at low load condition) (Herreros, Gill et al.

2014). Thus, with different levels of $H_2$ promotion on the DOC, the exhaust $NO_2$/NO ratio is allowed to be adjusted. Therefore, with the proposed setup, it is possible to investigate the $H_2$ effects on each of the DOC and SCR catalysts. Then, with the acquired information, a comparative study can be made between the individual and the combined catalyst systems to 1) study the importance of $NO_2$ in the $H_2$ promoted $NH_3$ – SCR over $Ag/Al_2O_3$ under real exhaust condition and 2) discover how $H_2$ can overall promote the total NOx reduction

The test rig is illustrated in Fig. 8.1. The $Ag/Al_2O_3$ monolith was loaded in a tubular reactor, which was connected through a temperature controlled heating line to the engine exhaust pipe downstream the engine outlet. The flow rate of the exhaust gas directed towards the SCR was controlled using a flow meter to keep a constant catalyst gas hourly space velocity (GHSV), and the reactor temperature is controlled by means of furnace. A K – type thermocouple was placed before SCR to record its inlet temperature. Before the SCR catalyst, the DOC could be loaded into the exhaust manifold when needed. Temperature measurements were made both before (engine – out) and after the DOC. $H_2$ was injected before and after the DOC while $NH_3$ was introduced only after the DOC (upstream the silver catalyst) for the purpose of $NH_3$ – SCR.

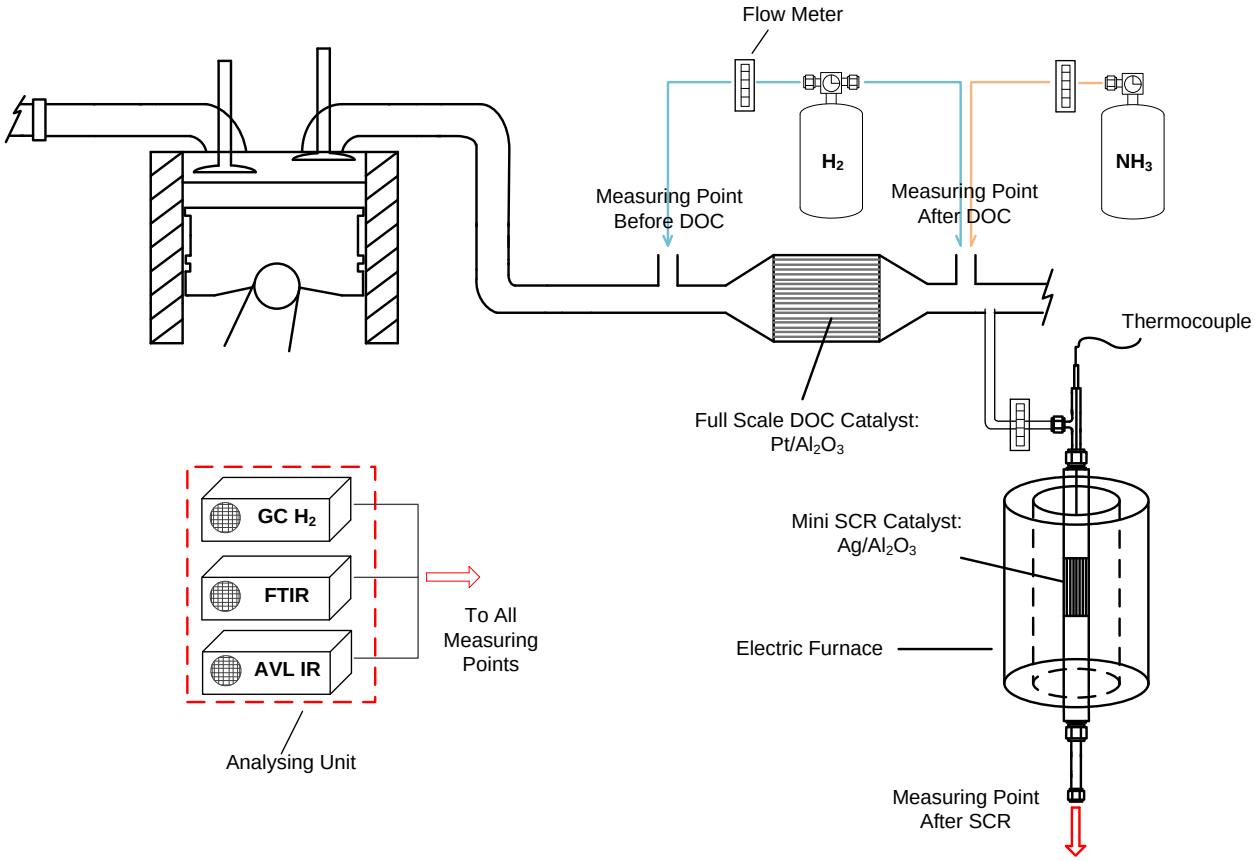


**Figure 8.1:** Experimental setup for combined reformer and SCR rector in diesel exhaust loop

The engine was operated at various load conditions producing exhaust gas with range of emission NOx, THC, CO and etc. concentrations. All the emissions are shown in Table A8.1, section 8.7 Appendix.

In terms of the test procedures, the study was carried out using different $H_2$ additions onto the DOC and SCR catalysts. Each of the catalysts was investigated in isolation. Their individual performances in changing the exhaust gas components were assessed at various engine loads. Due to the existence of the engine produced $NO_2$ (Table A8.1, 8.7 Appendix), the NO to $NO_2$ conversion and the overall $NO_2$/NO ratio at the DOC outlet were calculated separately by Eq. 8.1 and 8.2.

$$\text{NO to } NO_2 \text{ Conversion} = \frac{NO_{2\ After\ DOC} - NO_{2\ Before\ DOC}}{NO_{\ Before\ DOC}} \times 100\ \% \qquad (8.1)$$

$$NO_2/NO \text{ Ratio} = \frac{NO_{2\ After\ DOC}}{NO_{\ After\ DOC}} \qquad (8.2)$$

Then the DOC and SCR catalysts were put together (DOC in the front) in the engine exhaust in a combined form. Different levels of $H_2$ were introduced to study their performance in producing $NO_2$ or promoting the $NH_3$ - SCR through the enhanced $NO_2$ production. Since the DOC wasn't placed inside a furnace but directly into the exhaust manifold, its temperature was dependant on the engine exhaust temperature at each load. Therefore $H_2$ might not be needed when DOC could be fully activated by the exhaust temperature. On the other hand, the temperature of the SCR catalyst was controlled by means of furnace for both transient (for the individual study) and steady – state experiments (for combined system). In transient condition, the reactor temperature ramped at 10 ℃ per every 2 minutes, giving a reaction region from 150 to 500 ℃, whereas the temperature in the steady – state condition was selected and kept constant for at least 20 minutes. Some of the temperatures in the steady – state conditions are chosen to match the exhaust temperatures. Depending on the specific engine load, $NH_3$ was delivered at equal molar ratio to the engine NOx ($NH_3$:NOx = 1.0) for all SCR reactions, unless stated otherwise. The total use of $H_2$, either on the individual catalyst or in the combined system, did not exceed 8000 ppm. The engine speed at 1500 rpm resulted in a GHSV of approximately 35000 $h^{-1}$ over the DOC catalyst. This value was kept throughout the study. The same GHSV was also applied to the $Ag/Al_2O_3$ catalyst. For convenience, all the test conditions are summarised in Table A8.2, section 8.7 Appendix.

## 8.2 NO to $NO_2$ conversion through $H_2$ addition over DOC ($Pt/Al_2O_3$)

The effects of $H_2$ on the $Pt/Al_2O_3$ catalyst outlet temperature, exhaust hydrocarbon (HC) and NO to $NO_2$ conversion are shown in Fig. 8.2. In addition, the calculated NO to $NO_2$ conversion based on the reaction's equilibrium (STANJAN v2.09) is also presented. Expressed by Fig. 8.2 (a), increasing the hydrogen, raised linearly the catalyst outlet temperature; the overall increment (from the inlet/exhaust temperature) and the rate of increase were similar at every $H_2$ level for all the engine load conditions. The exhaust gas analysis downstream the catalyst indicated that all the $H_2$ was consumed.

The $H_2$ effect on $NO_2$ promotion was shown to be the most effective at low engine exhaust temperatures i.e. 175 ℃. As the NO oxidation is suggested to be equilibrium limited, hydrogen promotion at higher exhaust temperature became less efficient. The experimentally observed $NO_2$ concentration started to decrease after the catalyst temperature reached 300 ℃ and above, indicating the reaction's thermodynamic limits, Fig. 8.2 (c).

In the literature (Katare, Patterson et al. 2007, Boubnov, Dahl et al. 2012, Hauff, Tuttlies et al. 2012), it has been extensively shown that $NO_2$ participates in the reactions involving C-containing species oxidation at low temperatures. The above observed exothermic effect of $H_2$ was seemed to be the main reason behind these improvements. Nevertheless, Fig. 8.2 (a) shows at 2 Bar IMEP (low engine load), a $H_2$ addition of 6000 ppm increased the DOC outlet temperature from 180 ℃ to 230 ℃. As indicated in the same figure, this temperature is identical to the temperature reached under 3 Bar IMEP (middle load operation) without $H_2$ addition (fed with engine exhaust only). However, in Fig. 8.2 (b) a difference of nearly 20 % in HC conversion was

found between these two conditions, reflects a combination of hydrogen's effects rather than just a result of the improved catalyst local temperature.

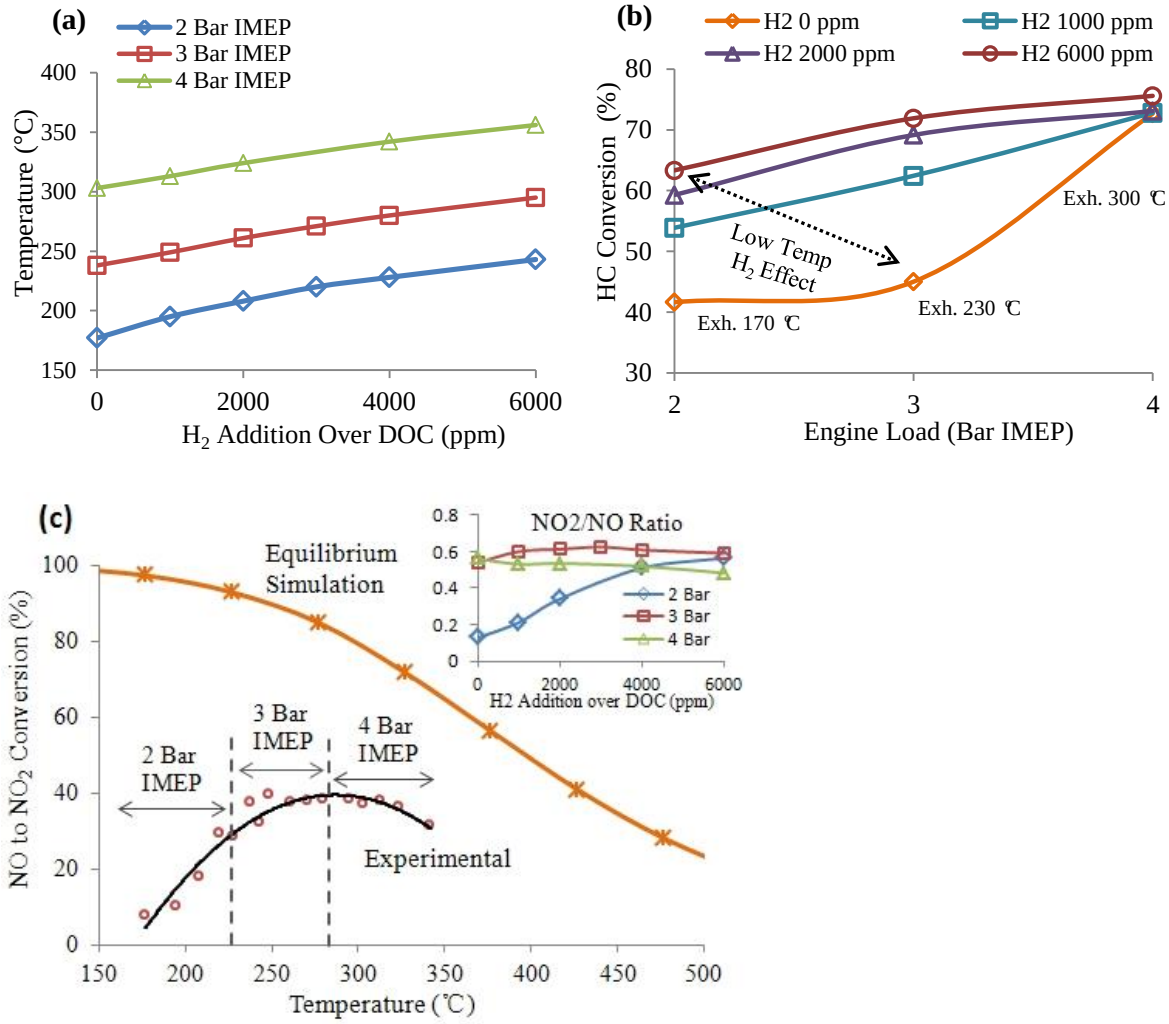


**Figure 8.2:** Effect of hydrogen addition over the DOC on (a) outlet temperature; (b) HC conversion and (c) NO to $NO_2$ conversion and the changes to the overall $NO_2$/NO ratio at the DOC outlet

Therefore, the reduction of CO and hydrocarbons not only (i) facilitated the NO in reaching the active site (Lefort, Herreros et al. 2014), but also (ii) resulted in less $NO_2$ being consumed in the oxidative conversions. In addition, it is also reported that the presence of hydrogen (iii) can increase the formation of some hydrogen – containing oxidation species (e.g. OH and $HO_2$ radicals) (Hori, Koshiishi et al. 2002) that further promote the low temperature HCs oxidation and NO to $NO_2$ conversion.

## 8.3 NO to $NO_2$ conversion through $H_2$ addition over $Ag/Al_2O_3$ for $NH_3$ – SCR reaction

Hydrogen addition onto $Ag/Al_2O_3$ with engine exhaust that contains 730 ppm of $NO_x$ (4 Bar IMEP) with no $NH_3$ addition in the transient study also enhanced the NO to $NO_2$ conversion (Fig 8.3(a)). Some of the results shown in the previous chapter (Fig 7.2 and 7.4) were plotted here as well for convenience and comparison purposes.

The $H_2$ promotion oxidative activation did not exclusively enhance the NO conversion. At the same time, increased CO concentration was detected at the SCR outlet, which was a product of (unburned) hydrocarbon oxidation at increased $H_2$ level (Fig. 8.3(b)).

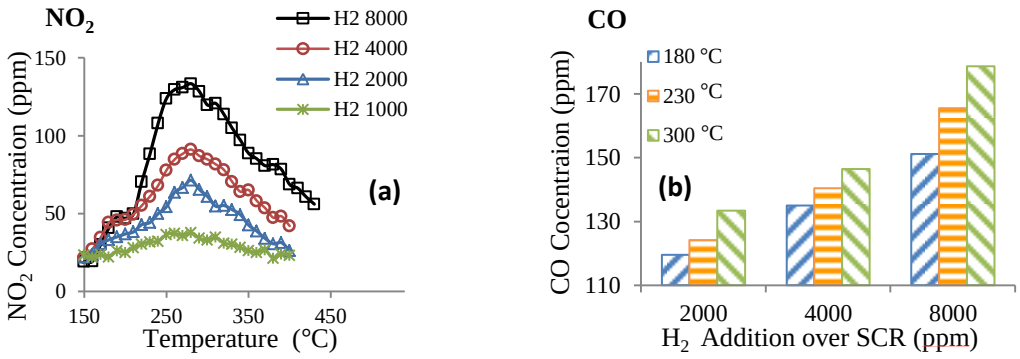


**Figure 8.3:** Concentration after the SCR catalyst under various $H_2$ additions without $NH_3$ (a) $NO_2$ and (b) CO.

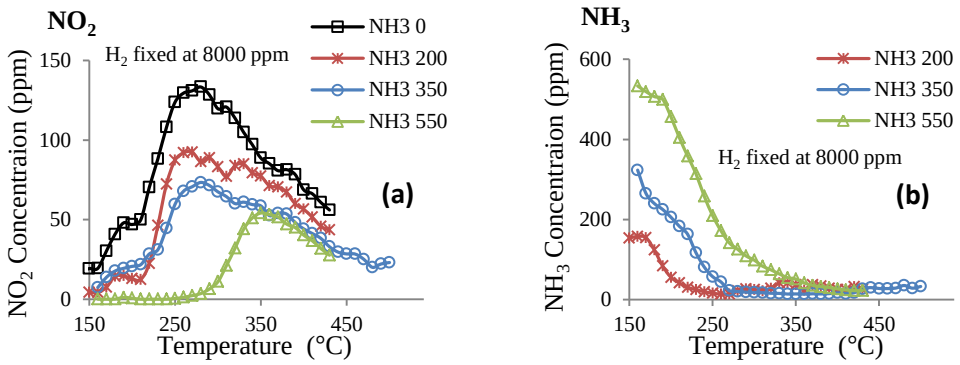


**Figure 8.4:** Concentration after the SCR under various NH3 additions with a fixed H2 addition (a) $NO_2$ and (b) $NH_3$.

However, since the reaction is thermodynamically limited (Fig. 8.2 (c)), the $NO_2$ production was found to peak at around the same temperatures as those detected over the DOC. This outcome was in agreement with a recent micro – kinetic modelling over $Ag/Al_2O_3$ catalyst (Azis, Härelind et al. 2013), where the $H_2$'s promotional mechanism was found to improve the NO oxidation mainly at low reaction temperature. The "$H_2$ effect" here was primarily attributed to a decomposition of self - inhibiting surface nitrate species, which were formed due to the presence of NO and $NO_2$ (as precursors of the nitrate species) and strongly adsorbed onto the catalyst's active site to hinder the rest of the reactions. As can be inferred from Fig. 8.3(a), this blocking effect was not sufficiently removed at low catalyst temperature (< 180 ℃) until a $H_2$ addition of 2000 ppm was applied, i.e. $H_2$ of 1000 ppm could not promote apparently the NO oxidation across the whole temperature range.

As described earlier in Chapter 7, once $NH_3$ was co – fed into the engine exhaust with $H_2$ (fixed at 8000 ppm, Fig. 8.4 (a)), the $NO_2$ was shown to slide down, indicating the produced $NO_2$ being immediately consumed in the reactions that are involving NO, $NO_2$ and $NH_3$. In addition, Fig 8.4 (a) also suggests the demand of the produced $NO_2$ became the largest at high $NH_3$ addition

i.e. 550 ppm and at low temperature region below 200 ℃. Compared to the $NH_3$ conversions at lower $NH_3$ additions (Fig. 8.4 (b)), the lack of $NO_2$ within this temperature region might restrict the SCR activity when the $NH_3$:$NO_x$ ratio was getting more close to the equal molar ratio. Therefore, increased $NO_2$ concentration would be inferred as beneficial to the $NO_x$ conversion under this temperature condition.

In addition to the above experiments, the transient condition was also applied to the combined system (DOC+SCR) with the same exhaust (without $NH_3$) and 8000 ppm of $H_2$ over the SCR catalyst, to investigate whether there was any exhaust component (i.e. unburned HC) except $NH_3$ could contribute largely to the NOx conversion within the studied temperature. The results showed negligible NOx conversion across the temperature ramp (Fig. A1, 8.7 Appendix).

## 8.4 SCR activity at low reaction temperature (< 200 ℃) with increased $NO_2$ concentration

For the combined system at 3 Bar IMEP operation (230 ℃, exhaust temperature), a $NO_2$/NO ratio of ~ 0.5 could be constantly maintained at the DOC outlet, therefore no $H_2$ promotion was needed over the DOC (as shown in Fig. 8.2 (c)).

Shown in Fig. 8.5(a) is the SCR's NOx conversion at 3bar IMEP and at the lowest temperature (150 ˚C). Increasing the SCR's inlet $NO_2$ concentration in the steady – state condition improved the overall NOx conversion. As shown by Fig. 8.5(b), the use of the $NO_2$ was improved over the SCR catalyst at increased hydrogen level but noticeable amounts of unconverted $NO_2$ were still recorded after the catalyst. Assuming the only reaction occurring at the SCR catalyst

was following the reaction stoichiometry involving both of the NO and $NO_2$ i.e. Fast – SCR, Eq. 2.17, the theoretical NOx conversion can be therefore estimated using the amount of $NO_2$ and NO available at the SCR catalyst's inlet: the engine – out NOx (listed in Table A8.1) and the $NO_2$/NO ratio after the DOC (Fig. 8.2 (c)). When the stoichiometric prediction was made for the Fast – SCR process (Fig. 8.5(c)), it was found that the reacted NO and $NO_2$ did not follow the stoichiometry expressed by Eq. 2.17. The total NOx conversion was contributed primarily by the reduction of $NO_2$, whereas the reduction in NO was shown to be much lower.

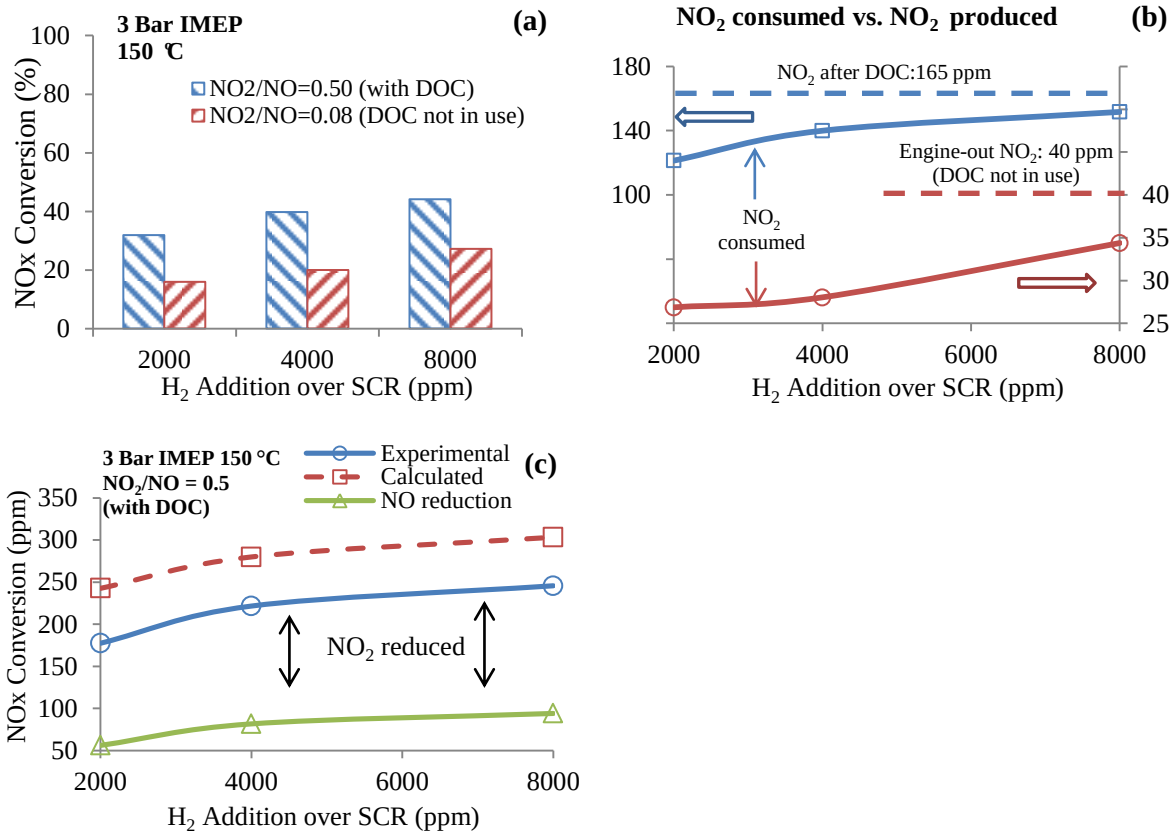


**Figure 8.5**: Emissions at 3 Bar IMEP, (a) NOx conversions with and without the increased $NO_2$ concentration (b) $NO_2$ detected downstream the SCR vs. the $NO_2$ being available at the SCR inlet, and (c) the experimentally observed NO and total NOx reduction vs. the calculated (based on Fast – SCR stoichiometry) NOx reduction.

In a recent study, Ciardelli et al showed ammonium nitrate ($NH_4NO_3$) was an essential intermediate in the Fast – SCR mechanism (Ciardelli, Nova et al. 2007). The formation of $NH_4NO_3$ is mainly due to the presence of $NO_2$ (Eq. 8.1), and it is decomposed with NO at favourable temperatures to release nitrogen and water (Eq. 8.2) (Koebel, Elsener et al. 2000). The summation of these two reactions returns exactly the Fast – SCR stoichiometry (Ciardelli, Nova et al. 2007). However, when temperature is below 170 ℃, the formed $NH_4NO_3$ will rapidly deposit on the catalyst. Hence the unexpected surface coverage and the $NO_2$ occupancy in $NH_4NO_3$ formation were both competing with the Fast – SCR mechanism, resulting in a deviation in NO and $NO_2$ conversions as such observed in Fig 5c.

$$2NO_2 + 2NH_3 \rightarrow NH_4NO_3 + N_2 + H_2O \qquad (8.1)$$

$$NH_4NO_3 + NO \rightarrow N_2 + NO_2 + 2H_2O \qquad (8.2)$$

Nevertheless, when the catalyst temperature was increased to 180 ℃, no significant $NO_2$ (< 5 ppm) was detected while the SCR catalyst was fed with the exhaust produced at 2 Bar IMEP (low engine load). Notice that the 180 ℃ applied here was matching the exhaust temperature at 2 Bar IMEP, where the DOC's $NO_2$ production was limited. Hence, $H_2$ was also applied to enhance the DOC's performance in NO to $NO_2$ conversion. As shown in Fig. 8.6 (a), enhancing the SCR catalyst's inlet $NO_2$ concentration could result in more pronounced $NO_x$ conversion than only adding hydrogen upstream the SCR. This demonstrated an improved $NH_3$ – SCR resulted by the effective use of the increased $NO_2$ over the SCR catalyst. Shown by Fig. 8.6 (b), when the lowest amount of $H_2$ i.e. 2000 ppm was maintained over the SCR catalyst, the actual NOx conversion

followed closely the stoichiometric prediction at every inlet $NO_2$ concentration. This indicates the NOx conversion was predominantly contributed by the "Fast – SCR" like process.

After the SCR's $H_2$ addition had been increased from 2000 ppm to 4000 ppm, the total NOx conversion further improved (Fig. 8.6(b)). Additionally, in both cases, the increased $NO_2$/NO ratio (i.e. either from 0.10 to 0.35 or from 0.35 to 0.50) seemed to result in similar NOx improvement (Fig. 8.6(b)). This implies that while the DOC was providing the SCR with fixed amounts of $NO_2$ to enhance its performance, the SCR catalyst itself became more active using the increased $H_2$ addition and contributed to those additional NOx conversions (Fig. 8.6 (a) and (b)). Recalling the results shown earlier in Fig. 8.3(c), the $H_2$ improved $NO_2$ formation over the SCR catalyst was believed to be an essential $NO_2$ supplement, which can be involved in the "Fast – SCR" process as an addition to the $NO_2$ produced from the DOC.

From the results presented above, it seems that the NO to $NO_2$ promotion (over the SCR catalyst) as part of the $H_2$ effect was allowed to be achieved by the use of DOC. Hence, the better SCR performance implies the $NH_3$ – SCR is largely determined by the system's $NO_2$ availability. Therefore, the NO's oxidative activation (to $NO_2$) is suggested to be an important step within the overall reaction but which could be limited at low reaction temperature (Fig, 8.3(c)). As $H_2$ is shown to be both a prerequisite and a promotional factors to such $NO_2$ formation, its presence is therefore suggested to indirectly affect the performance of this SCR mechanism

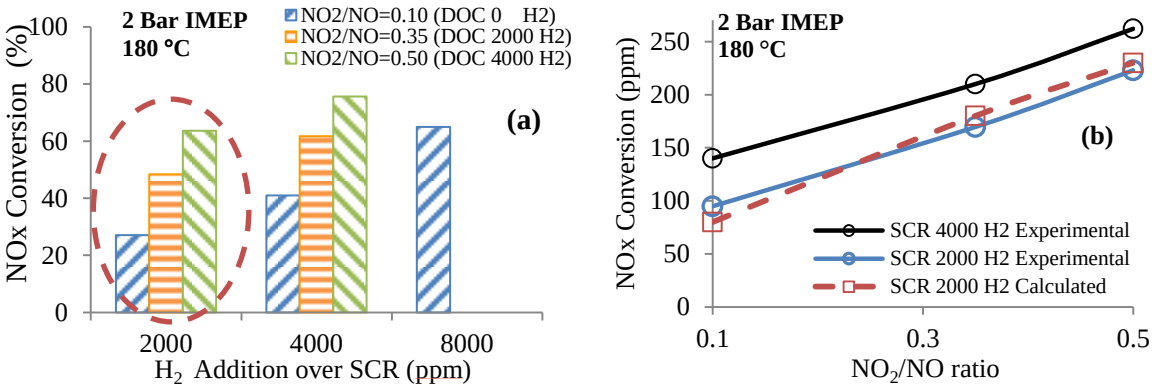


**Figure 8.6:** NOx conversion at 2 Bar IMEP at SCR catalyst inlet temperature of 180 ˚C (a) 2000, 4000 and 8000 ppm $H_2$ addition upstream SCR; (b) experimental and calculated (based on Fast – SCR stoichiometry) NOx conversion at 2000 and 4000 ppm $H_2$ addition.

## 8.5 SCR activity at high reaction temperature with increased $NO_2$ concentration

Shown by Fig. 8.7(a) and the comparison between Fig. 8.6(a) and Fig.8.7(b), the increased catalyst temperature improved the reaction's activity but diminished comparatively the $NO_2$'s promotional effect on the overall NOx conversion. The actual converted NOx and the "Fast – SCR" prediction using the inlet $NO_2$ are plotted in Fig. 8.7(b) for 3 Bar IMEP. It was again observed when 2000 ppm of $H_2$ being applied over the SCR catalyst, the actual NOx conversion was close to the theoretical prediction at 200 ℃. However, further increasing the temperature to 230 ℃ improved the reaction away from the calculated stoichiometry. As shown in Fig. 8.4(a) (at a fixed $H_2$ level), the $NO_2$ formation over the SCR catalyst became well discernable over 200 ℃ and peaked at nearly 300 ℃. This phenomenon implies, as in addition to the $H_2$'s promotional effect on NOx conversion, the temperature is another factor that determines the SCR catalyst's activity: more $NO_2$ becomes available for the NOx conversion when the NO oxidation is

approaching its maximum thermodynamics limit, Fig 8.2 (c) and Fig 8.3 (a). Hence as indicated in Fig. 8.7 (b), the reaction's $H_2$ dependence was largely reduced at increased catalyst temperature, which can be reflected by the smaller slope along the NOx conversion curve at higher temperature i.e. 230 ℃ vs. 200 ℃.

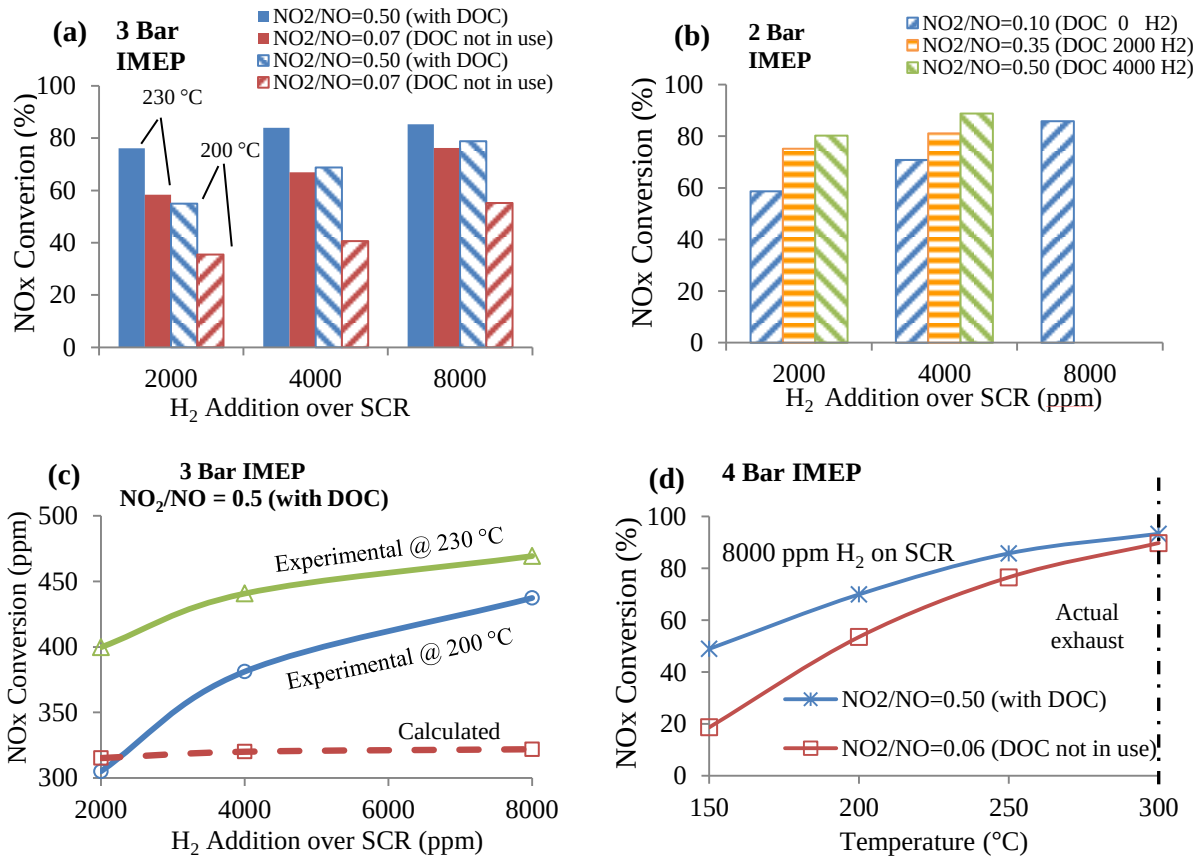


**Figure 8.7** (a) and (b): with different temperature and $NO_2$ level (inlet) over the SCR catalyst, the NOx conversions at (a) 3 Bar IMEP and (b) 2 Bar IMEP; (c) experimental and calculated (based on Fast – SCR stoichiometry) NOx conversion at 3 Bar IMEP, (d) NOx conversion at 4 Bar IMEP

Secondly, the improved NOx conversion (higher than the calculated) may also indicate the "Fast – SCR" like mechanism was not the only reaction occurring at the increased temperature. In the existing literature (Koebel, Madia et al. 2002), the standard SCR (Eq.2.15) is reported to be activated at around 230 – 300 ℃ (30 % to 70% NOx conversion) and its performance becomes sufficiently enough (> 90 % NOx conversion) when temperature is over 350 ℃. This would allow the NOx conversion to improve while increased temperature is applied regardless of the system's $NO_2$ concentration: as indicated in Fig. 8.7(c) and (d).

Apart from that, when the temperature was greater than 275 ℃, the $NO_2/NH_3$ – SCR (Eq. 2.17) could equally happen (Ciardelli, Nova et al. 2007) but which required more $NH_3$ than the "Fast – SCR" to convert the same amount of $NO_x$ i.e. $NO_2$ (Eq. 2.17 vs. Eq. 2.19). Thus even with the enhanced inlet $NO_2$ concentration, the increased occurrence of such reaction would still cause comparatively less improvement in NOx conversion, impairing the $NO_2$'s promotional effect at higher reaction temperature.

Last but not least, although as indicated by Fig. A1 (8.7 Appendix) that the effect of exhaust hydrocarbon on NOx conversion could be largely suppressed when DOC is engaged, at increased temperature (> 230 ℃) and provided the DOC is not in use, the HCs could still contribute to some of the NOx conversion.

Supported by the above reasons, the use of DOC at 4 Bar IMEP was shown to be only necessary at low SCR reaction temperature, Fig. 8.7 (d).

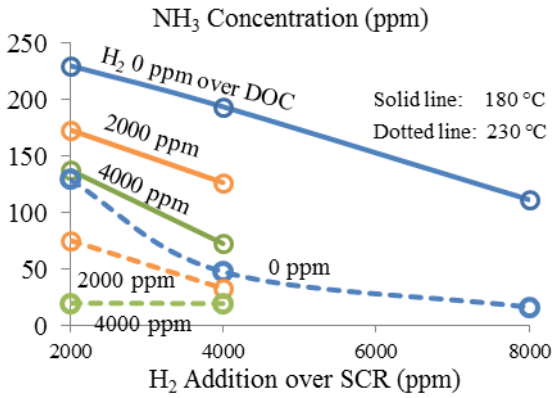


**Figure 8.8:** $NH_3$ detected after the SCR catalyst at 2 Bar IMEP load condition

The detections of the unconverted ammonia downstream the SCR catalyst are plotted in Fig.8.8. All these results are acquired from the 2 Bar IMEP condition. The unconverted $NH_3$, or referred as the "ammonia slippage", expresses a good consistency to the NOx reductions shown in Fig. 6a and Fig. 8.7(c), confirming the increased $NO_2$ concentration was generally more beneficial to the low temperature NOx removal. Since $NH_3$ is toxic in nature, it is necessary to suppress its emission to a very low level. Results here indicate, the $NO_2$ promoted $NH_3$ – SCR not just improved the reaction's low temperature activity, it also achieved quite efficiently the removal of ammonia slippage (< 20 ppm) at comparatively lower $H_2$ promotion.

## 8.6 Summaries

In the study presented, the effect of increased $NO_2$ concentration in affecting the activity of $NH_3$ – SCR was evaluated in diesel lean NOx reduction over an $Ag/Al_2O_3$ catalyst.

NO's conversion to $NO_2$ was observed over the $Ag/Al_2O_3$ with an oxidative promotion from $H_2$. The formed $NO_2$ was suggested to be used in the SCR reaction immediately after its production and with the added $NH_3$. This formed a "Fast – SCR" like process, whose activity at low reaction temperature was shown to be largely determined by the system's $NO_2$ availability. Thus the use of $Pt/Al_2O_3$ based DOC in increasing the exhaust $NO_2$ level was shown to improve significantly the SCR performance, which indicates the DOC simulated or even performed better the function of $H_2$ over the SCR catalyst.

Hence one role of the $H_2$ is confirmed as to promote the NO oxidation and affect indirectly the overall SCR performance at low reaction temperature i.e. around 200 ℃ or less. However, this promotional effect of improved $NO_2$ concentration was shown to be diminished by the increased reaction temperature. Therefore, the SCR reaction's $H_2$ dependence was reduced as well.

In general, the results suggest increasing the $NO_2$ concentration, either in the engine exhaust by means of combustion or from other catalytic aftertreament and/or the $Ag/Al_2O_3$ itself, can improve significantly the $H_2$ – assisted $NH_3$ – SCR in low temperature NOx control and at the same time reduce the system's demand on $H_2$ level.

## 8.7 Appendix

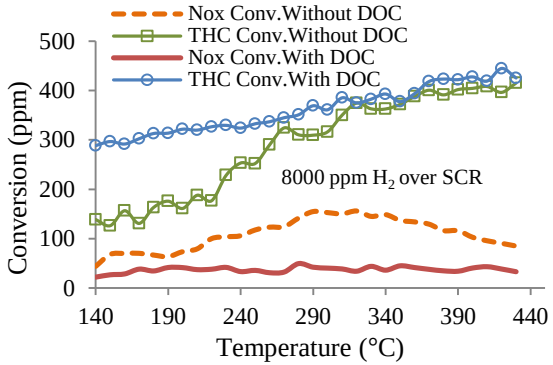


**Figure A8.1:** NOx and exhaust HC conversions over the temperature ramp with and without the DOC being placed in front of the SCR catalyst

**Table A8.1**: Engine conditions and average emissions

| Engine Load (Nm) | IMEP* (bar) | NO (ppm) | $NO_2$ (ppm) | THC** (ppm) | CO (ppm) | $CO_2$ (%) | $O_2$ (%) | $H_2O$ (%) |
|---|---|---|---|---|---|---|---|---|
| 8 | 2 | 320 | 30 | 415 | 160 | 2.53 | 15.6 | 2.54 |
| 16 | 3 | 495 | 40 | 420 | 120 | 3.71 | 15.1 | 3.47 |
| 24 | 4 | 690 | 40 | 435 | 110 | 6.11 | 14.9 | 4.45 |

* IMEP: indicated mean effective pressure

**THC: total hydrocarbon based on $C_1$ emission

**Table A8.2**: Summarise of conditions in each experimental run

| **Type of run** | **Cat. used** | **Engine load (bar IMEP)** | **DOC Temp. (℃)** | **SCR Temp. (℃)** | **$H_2$ on DOC (ppm)** | **$H_2$ on SCR (ppm)** | **$NH_3$ on SCR (ppm)** |
|---|---|---|---|---|---|---|---|
| Steady - state | DOC alone | 2 | 180 (exhaust) | NA | 0, 1000, 2000, 3000, 4000, 6000 | NA | NA |
| | | 3 | 230 (exhaust) | | | | |
| | | 4 | 300 (exhaust) | | | | |
| Transient | SCR alone | 4 | NA | 150 – 500 (ramp) | NA | 8000 | 0, 200, 350, 550 |
| Steady - state | DOC + SCR | 2 | 180 (exhaust) | **180*** (furnace) | 0, 2000, 4000 | 2000, 4000, 8000 | 350 (match exhaust NOx) |
| | | | | 230 (furnace) | | | |
| | | 3 | 230 (exhaust) | 150 (furnace) | 0 | 2000, 4000, 8000 | 530 (match exhaust NOx) |
| | | | | 200 (furnace) | | | |
| | | | | **230*** (furnace) | | | |
| | | 4 | 300 (exhaust) | 150 (furnace) | 0 | 8000 | 730 (match exhaust NOx) |
| | | | | 200 (furnace) | | | |
| | | | | 250 (furnace) | | | |
| | | | | **300*** (furnace) | | | |
| Transient | | 4 | 300 (exhaust) | 150 – 500 (ramp) | 0 | 8000 | 0 |

* SCR inlet temperature matched the exhaust temperature

# CHAPTER 9: CONCLUSIONS

In the studies presented above, ammonia and its various roles in transportation area, namely a hydrogen carrier for vehicle on – board $H_2$ delivering, a carbon – free alternative for fossil fuel substitution, and a catalytic reactant for engine emission control, were assessed in different vehicular applications. In general, the introduction of $NH_3$ in diesel operation, especially after it being reformed into a $H_2$ enriched gas mixture, was demonstrated to cut down significantly the IC engine's greenhouse gas emission i.e. $CO_2$. Simultaneous carbonaceous emissions reduction such as HCs, CO, and PMs were obtained at selected engine conditions. The engine NOx tended to increase due to the nature of $NH_3$ being nitrogen bonded and excessive oxygen availability in the diesel operation. Nevertheless, provided with a silver based SCR system, the emitted $H_2$ and $NH_3$ were capable of working together to reduce the engine NOx. Hence a combination of the reformed $NH_3$ in combustion and catalytic aftertreament was revealed to potentially restrict the NOx and carbon emissions at the same time.

The main findings of the research are summarised in the following sections, whilst some future works are also proposed to extend further the subject areas covered in this thesis.

**a) Ammonia as hydrogen carrier for transportation; investigation of the ammonia exhaust gas fuel reforming**

This study demonstrated, by combining a thermochemical heat recovery of the engine waste heat and an oxidative $NH_3$ decomposition mechanism, a successful $H_2$ production method for the purpose of vehicle on – board hydrogen delivery could be achieved through the reforming of $NH_3$.

This study broadened the application of $NH_3$ from a fertilizer in agricultural industry to a potential hydrogen and energy carrier used in transportation sector, where the $NH_3$'s reformed form, namely a $H_2 – NH_3$ gas mixture, could serve as a carbon – free fuel alternative for improved engine combustion and emission. Apart from that, the reformed $NH_3$ could be also effective in promoting the performance of certain aftertreatment devices, which helped to further expand the application of $NH_3$ in the transportation sector.

Overall, the study presented here reveals that the uses of $NH_3$ in vehicular application can be versatile; benefits in specific engine performance or for the overall energy and environmental concern could be achieved by applying the different roles of $NH_3$ individually or combined.

**b) Combustion of $NH_3$ reformate in diesel operation; the impacts in engine performance and emissions**

In this study, the proposed use of reformed $NH_3$ as partial fuel substitution to decarbonise a diesel engine was presented.

$NH_3$ in its pure form was demonstrated as a less efficient energy carrier (i.e. as compared to diesel) for CI combustion. The combustion of the reformed $NH_3$ was shown to be assisted by its own $H_2$ content and resulted in improved combustion and engine emissions. Therefore, the usefulness of the reformate was shown to be not just carbon – free, it also supported better the role of $NH_3$ to be a viable alternative energy carrier.

In addition, this study also confirmed the necessity of the $NH_3$ reforming process, which was shown to fulfill its function in the vehicle in site carbon reduction that is considered as a major component in the overall life cycle assessment of the vehicle's carbonaceous emissions.

**c) Improved $H_2$ – $NH_3$ reformate combustion for effective diesel engine decarbonisation through use of DGE as an ignition enhancer**

In this research, performance of DGE as an oxygenated fuel blend and ignition improver was assessed in a diesel engine with combustions of the reformed $NH_3$ (simulated) for partial hydrocarbon fuel substitution and engine decarbonisation.

In general, DGE extended the beneficial effect of the reformed $NH_3$ in reduction of the diesel engine carbonaceous emissions.

The DGE is demonstrated to be a suitable diesel blend or individual primary fuel, capable of enhancing the ignition and combustion of the fuels and/or fuel alternatives that are provided with large auto – ignition resistance. Its use even in the "nitrogen – rich" combustion i.e. combustion with $NH_3$ was demonstrated to potentially break the trade – off between the PM and NOx

formation that is usually observed in the combustions of some oxygenated renewable fuels. In addition to that, the DGE's enriched oxygen content and superior ignition properties allowed it to potentially withstand the effect of oxygen dilution after large amount of EGR and/or gaseous fuel being introduced from the air intake. This would imply an EGR operation can be applied to the reformate combustion with the presence of DGE, to help in reducing the NOx formation resulted by the oxidation of $H_2$ and $NH_3$.

**d) $H_2$ – $NH_3$ reformate assisted lean NOx abatement over Silver/Alumina catalyst**

In the above combustion studies, $NH_3$ and $H_2$ emissions were shown as byproducts of the $NH_3$ reformate combustion. Nevertheless, the presence of $NH_3$ and $H_2$ in the exhaust could be beneficial to certain aftertreatment devices i.e. $NH_3$ – SCR, which would utilise the emitted $NH_3$ in further reactions to control the engine NOx emission.

Therefore, an $Ag/Al_2O_3$ - SCR unit was applied with the $NH_3$ exhaust gas reforming system, using the produced $NH_3$ reformate for the purpose of NOx emission control. The combined reformer – SCR system shows successful low temperature NOx reduction under several engine conditions and operation. The completion of this investigation demonstrated the usefulness of $NH_3$ and $NH_3$ exhaust gas reforming in the field of catalytic emission control. This adds another importance to the $NH_3$'s vehicular application, parallel to its role of an effective fuel alternative.

Most importantly, the study presented a possible collaboration between the different roles of $NH_3$, where the $NH_3$'s ability in hydrogen and energy carrier could be first utilised in the

combustion process to perform the engine decarbonisation. Later, its presence in the engine exhaust could be regarded as catalytic reductant to keep favoring the environmental catalyst in further emission abatement.

**e) Increased $NO_2$ concentration in the diesel engine exhaust for improved $H_2 – NH_3 – SCR$ activity over $Ag/Al_2O_3$ catalyst**

While the effectiveness of $NH_3$ reformate in diesel operation was shown to be extended by the presence of DGE, the reformate's performance in the SCR reaction could be also improved with a $H_2 – NO_2$ associated mechanism.

The completion of this study provided an insight into the possible reaction mechanism that explained the low temperature NOx conversion over the $Ag/Al_2O_3$ catalyst. The $H_2$ content was revealed to contribute to the SCR catalyst's in site $NO_2$ formation, which was consumed immediately once the presence of $NH_3$ and NO was made available over the catalyst. Hence the overall SCR reaction at the low temperature region was demonstrated to proceed following a similar route of the Fast – SCR reaction.

It is possible to utilise this reaction feature for better reformate's performance as a catalytic reductant. This reveals that while the performances of $NH_3$ reformate could be limited by its own composition (after reforming) and/or the engine operating conditions, optimisation (e.g. use of DGE and increased $NO_2$) related to the reformate's nature and application (e.g. combustion and catalytic reactions) could be taken to improve the reformate's performance.

**f) Closing Remark and Recommendations**

After a series of investigations, $NH_3$ was demonstrated as a viable carbon – free alternative used in vehicular applications for fossil fuel substitution.

In view of carbon balance within a full life cycle assessment, the use of $NH_3$ in its reformed form i.e. $H_2$ contented reformate implemented effective IC engine decarbonisation, which fulfilled the purpose of decreasing the carbonaceous emissions, e.g. greenhouse gases, from the vehicles' terminal energy consumption.

Provided the $NH_3$ is based on renewable sources such as biomasses, byproduct of food production industry, and animal/human excretions, the benefit of decarbonisation will be further extended within the full life cycle assessment, into the earlier stages of production and refinement processes of $NH_3$ as compared to its industrial method. Overall, this helps to reduce the production load on the current oil wells and refineries, catering partially for the energy demand from transportation and/or stationary power plants, and most importantly reducing the IC engine's negative impacts to the general environment by the ammonia's "cleaner" on – board applications.

In order to improve further the effectiveness of $NH_3$ and its reformate in the vehicular system, future works are recommended after the current studies.

As mentioned in section 5.2, to improve the reforming performance, it is necessary to enhance the thermal management of the reformer's waste heat. It was suggested to use the waste heat generated both during and following the reaction to warm up the $NH_3$ feed before entering the reaction chamber. On the other hand, higher reforming efficiencies can be also achieved at

larger hydrogen output and at decreased reforming temperature i.e. less $NH_3$ is required in the exothermic oxidation and more will be preserved for the $H_2$ production. This could be achieved through optimising the decomposition catalysts.

In terms of the reformate combustion, only basic diesel operation was applied in the current investigation. This was to ensure that the $H_2$ and $NH_3$'s own combustion features could be reflected without being interfered by any other factors. Nevertheless, improved combustion of each of the $H_2$ and $NH_3$ was reported in recent literatures, which were combining different engine strategies such as controlled injection timing, pressurised direct fuel/gas injection, and turbocharged air intake (Reiter and Kong 2008, Reiter and Kong 2011, Liew, Li et al. 2012). These technologies could be equally applied to the combustion of $H_2$ – $NH_3$ mixture to evaluate their impacts on the mixture's combustion pattern and the overall fuel effectiveness.

Apart from the advanced engine strategies, recent studies also demonstrated a use of Reformed EGR or REGR, namely a combination of $H_2$ enriched reformate and regular EGR induction, to break the NOx – PM trade – off. In the current research, it was also shown that the introduction of reformate occupying 5 – 7 % of the engine intake charge could possibly have the same oxygen dilution effect of the normal EGR induction, which tended to suppress the engine NOx formation. Hence, the use of EGR and the $NH_3$ reformate is also recommended to investigate the combustion and emission performance under their combined effects. This study is also recommended to be coupled with the use of DGE, to find out whether DGE's high oxygenation and better ignitability could still power the reformate combustion by counteracting the reduced oxygen concentration and combustion temperature after the EGR operation.

# LIST OF AUTHOR'S PUBLICATION AND AWARDS

## Journal Paper Published/Prepared for Submission

- Wentao Wang, Jose M. Herroros, Athanasios Tsolakis, Andrew P.E. York. Ammonia as hydrogen carrier for transportation; investigation of the ammonia exhaust gas fuel reforming. International Journal of Hydrogen Energy. 2013; 23: 9907-9917

- Wentao Wang, Athanasios Tsolakis, Andrew P.E. York. Ammonia exhaust gas reforming for emission abatement in lean burn engines. Prepared for submission as a research article in Chemical Engineering Journal.

- Wentao Wang, Jose M. Herroros, Athanasios Tsolakis, Andrew P.E. York. Increased $NO_2$ concentration in the diesel engine exhaust for improved $Ag/Al_2O_3$ catalyst $NH_3$ – SCR activity. Prepared for submission as a research article in International Journal of Hydrogen Energy.

- Wentao Wang, Jose M. Herroros, Athanasios Tsolakis. The effects of $H_2$ assisted $NH_3$ combustion in diesel operation for effective engine decarbonisation. Prepared for submission as a research article in Applied Energy.

- Wentao Wang, Jose M. Herroros, Athanasios Tsolakis. Effects of diethyl glycol diethyl ether as an ignition improver on the performance of diesel engine fuelled with $H_2$ and $NH_3$. Prepared for submission as a research article in Environmental Science & Technology.

## Awards

2013: David Brewster Cobb Prize

For school's outstanding research publications, given by the School of Mechanical Engineering, University of Birmingham

2010 – 2013: Department Full PhD Scholarship

3 years of full PhD program funding, given by the School of Mechanical Engineering, University of Birmingham

# REFERENCE


Abu-Jrai, A., A. Tsolakis and A. Megaritis (2007). "The influence of and CO on diesel engine combustion characteristics, exhaust gas emissions, and after treatment selective catalytic reduction." International Journal of Hydrogen Energy **32**(15): 3565-3571.

Ahmed, S. and M. Krumpelt (2001). "Hydrogen from hydrocarbon fuels for fuel cells." International Journal of Hydrogen Energy **26**(4): 291-301.

Al-Baghdadi, M. A. S. (2003). "Hydrogen–ethanol blending as an alternative fuel of spark ignition engines." Renewable Energy **28**(9): 1471-1478.

Alam, M., S. Goto, K. Sugiyama, M. Kajiwara, M. Mori, M. Konno, M. Motohashi and K. Oyama (2001). "Performance and Emissions of a DI Diesel Engine Operated with LPG and Ignition Improving Additives." SAE International 2001-01-3680.

Allansson, R., P. G. Blakeman, B. J. Cooper, H. Hess, P. J. Silcock and A. P. Walker (2002). "Optimising the Low Temperature Performance and Regeneration Efficiency of the Continuously Regenerating Diesel Particulate Filter (CR-DPF) System." SAE International 2002-01-0428.

Andersson, J. and J. Lundgren "Techno-economic analysis of ammonia production via integrated biomass gasification." Applied Energy **130**(1) 484 - 490.

Aneja, V. P., W. H. Schlesinger, D. Nyogi, G. Jennings, W. Gilliam, R. E. Knighton, C. S. Duke, J. Blunden and S. Krishnan (2006). "Emerging national research needs for agricultural air quality." Eos, Transactions American Geophysical Union **87**(3): 25-29.

Atadashi, I. M., M. K. Aroua and A. A. Aziz (2010). "High quality biodiesel and its diesel engine application: A review." Renewable and Sustainable Energy Reviews **14**(7): 1999-2008.

Azis, M. M., H. Härelind and D. Creaser (2013). "Microkinetic modeling of H2-assisted NO oxidation over Ag–Al2O3." Chemical Engineering Journal **221**(0): 382-397.

Bacha, J., L. Blondies, J. Freel, G. Hemighuas, N. Hogue, J. Horn, D. Lesnini, C. McDonald, M. Nikanjam, E. Olsen, B. Scott and M. Sztenderowicz (1998). "Diesel fuels technical review (FTR - 2)." Chevron Products Company, a division of Chevron USA, Inc.

Bika, A. S., L. M. Franklin and D. B. Kittelson (2008). "Emissions Effects of Hydrogen as a Supplemental Fuel with Diesel and Biodiesel." SAE International. Journal of Fuels and Lubricants. **1**(1): 283-292.

Blakeman, P. G., P. J. Andersen, C. Hai-Ying, J. D. Jonsson, P. R. Phillips and M. V. Twigg (2003). "Performance of NOx Adsorber Emissions Control Systems for Diesel Engines." SAE International 2003-03-03.

Bosch, H. and F. Janssen (1988). "Formation and control of nitrogen oxides." Catalysis Today **2**(4): 369-379.

Boubnov, A., S. Dahl, E. Johnson, A. P. Molina, S. B. Simonsen, F. M. Cano, S. Helveg, L. J. Lemus-Yegres and J. D. Grunwaldt (2012). "Structure-activity relationships of Pt/Al 2O 3 catalysts for CO and NO oxidation at diesel exhaust conditions." Applied Catalysis B: Environmental **126**: 315-325.

Brachi, P., R. Chirone, F. Miccio, M. Miccio, A. Picarelli and G. Ruoppolo (2014). "Fluidized bed co-gasification of biomass and polymeric wastes for a flexible end-use of the syngas: Focus on bio-methanol." Fuel **128**(0): 88-98.

Bradford, M. C. J., P. E. Fanning and M. A. Vannice (1997). "Kinetics of NH3Decomposition over Well Dispersed Ru." Journal of Catalysis **172**(2): 479-484.

Brosius, R., K. Arve, M. H. Groothaert and J. A. Martens (2005). "Adsorption chemistry of NOx on Ag/Al2O3 catalyst for selective catalytic reduction of NOx using hydrocarbons." Journal of Catalysis **231**(2): 344-353.

Burch, R., J. P. Breen and F. C. Meunier (2002). "A review of the selective reduction of NOx with hydrocarbons under lean-burn conditions with non-zeolitic oxide and platinum group metal catalysts." Applied Catalysis B: Environmental **39**(4): 283-303.

Burch, R. and M. D. Coleman (2002). "An Investigation of Promoter Effects in the Reduction of NO by H2 under Lean-Burn Conditions." Journal of Catalysis **208**(2): 435-447.

Burch, R., J. A. Sullivan and T. C. Watling (1998). "Mechanistic considerations for the reduction of NOx over Pt/Al2O3 and Al2O3 catalysts under lean-burn conditions." Catalysis Today **42**(1–2): 13-23.

Chansai, S., R. Burch and C. Hardacre (2012). "The use of Short Time on Stream (STOS) transient kinetics to investigate the role of hydrogen in enhancing NOx reduction over silver catalysts." Journal of Catalysis. **295**(0): 223-231.

Chansai, S., R. Burch, C. Hardacre, J. Breen and F. Meunier (2011). "The use of short time-on-stream in situ spectroscopic transient kinetic isotope techniques to investigate the mechanism of hydrocarbon selective catalytic reduction (HC-SCR) of NOx at low temperatures." Journal of Catalysis. **281**(1): 98-105.

Chein, R.-Y., Y.-C. Chen, C.-S. Chang and J. N. Chung (2010). "Numerical modeling of hydrogen production from ammonia decomposition for fuel cell applications." International Journal of Hydrogen Energy **35**(2): 589-597.

Chen, J., Z. H. Zhu, S. Wang, Q. Ma, V. Rudolph and G. Q. Lu (2010). "Effects of nitrogen doping on the structure of carbon nanotubes (CNTs) and activity of Ru/CNTs in ammonia decomposition." Chemical Engineering Journal **156**(2): 404-410.

Chong, J. J., A. Tsolakis, S. S. Gill, K. Theinnoi and S. E. Golunski (2010). "Enhancing the NO2/NOx ratio in compression ignition engines by hydrogen and reformate combustion, for improved aftertreatment performance." International Journal of Hydrogen Energy. **35**(16): 8723-8732.

Christensen, C. H., T. Johannessen, R. Z. Sørensen and J. K. Nørskov (2006). "Towards an ammonia-mediated hydrogen economy?" Catalysis Today **111**(1–2): 140-144.

Ciardelli, C., I. Nova, E. Tronconi, D. Chatterjee, B. Bandl-Konrad, M. Weibel and B. Krutzsch (2007). "Reactivity of NO/NO2–NH3 SCR system for diesel exhaust aftertreatment: Identification of the reaction network as a function of temperature and NO2 feed content." Applied Catalysis B: Environmental **70**(1–4): 80-90.

Deutschmann, O., R. Schwiedernoch, L. I. Maier and D. Chatterjee (2001). Natural gas conversion in monolithic catalysts: Interaction of chemical reactions and transport phenomena. Studies in Surface Science and Catalysis. Elsevier. **136:** 251-258.

Doronkin, D. E., S. Fogel, S. Tamm, L. Olsson, T. S. Khan, T. Bligaard, P. Gabrielsson and S. Dahl (2012). "Study of the "Fast SCR"-like mechanism of H2-assisted SCR of NOx with ammonia over Ag/Al2O3." Applied Catalysis B: Environmental **113–114**(0): 228-236.

Doronkin, D. E., T. S. Khan, T. Bligaard, S. Fogel, P. Gabrielsson and S. Dahl (2012). "Sulfur poisoning and regeneration of the Ag/γ-Al2O3 catalyst for H2-assisted SCR of NOx by ammonia." Applied Catalysis B: Environmental **117–118**(0): 49-58.

Dupont, V. (2007). "Steam reforming of sunflower oil for hydroge gas production." Helia **30**(46): 103-132.

Ehrburger, P., J. F. Brilhac, Y. Drouillot, V. Logie and P. Gilot (2002). "Reactivity of Soot With Nitrogen Oxides in Exhaust Stream." SAE International 2002-01-1683.

Eränen, K., F. Klingstedt, K. Arve, L.-E. Lindfors and D. Y. Murzin (2004). "On the mechanism of the selective catalytic reduction of NO with higher hydrocarbons over a silver/alumina catalyst." Journal of Catalysis **227**(2): 328-343.

FAO (2006). Chapter 3: Livestock's Role in Climate Change and Air Pollutions. Livestock's Long Shadow: Environmental Issues and Options, Food and Agriculture Organization of the United Nations**:** 95-99.

Feitelberg, A. S. and S. M. Correa (2000). "The Role of Carbon Monoxide in NO2 Plume Formation." Journal of Engineering for Gas Turbines and Power**122**(2): 287-292.

Flynn, P. F., R. P. Durrett, G. L. Hunter, A. O. zur Loye, O. C. Akinyemi, J. E. Dec and C. K. Westbrook (1999). "Diesel Combustion: An Integrated View Combining Laser Diagnostics, Chemical Kinetics, And Empirical Validation." SAE International 1999-01-0509.

Fogel, S., D. E. Doronkin, P. Gabrielsson and S. Dahl (2012). "Optimisation of Ag loading and alumina characteristics to give sulphur-tolerant Ag/Al2O3 catalyst for H2-assisted NH3-SCR of NOx." Applied Catalysis B: Environmental **125**(0): 457-464.

Gañán, J., A. Al-Kassir Abdulla, E. M. Cuerda Correa and A. Macías-García (2006). "Energetic exploitation of vine shoot by gasification processes. A preliminary study." Fuel Processing Technology **87**(10): 891-897.

Gañan, J., A. A. K. Abdulla, A. B. Miranda, J. Turegano, S. Correia and E. M. Cuerda (2005). "Energy production by means of gasification process of residuals sourced in Extremadura (Spain)." Renewable Energy **30**(11): 1759-1769.

Ganesan, V. (2008). Internal combustion engines, McGraw-Hill Education (India) Pvt Ltd.

Ganley, J. C., E. G. Seebauer and R. I. Masel (2004). "Development of a microreactor for the production of hydrogen from ammonia." Journal of Power Sources **137**(1): 53-61.

Gao, Z., W. Ma, G. Zhu and M. Roelcke (2013). "Estimating farm-gate ammonia emissions from major animal production systems in China." Atmospheric Environment **79**(0): 20-28.

Gay, S. E. and M. Ehsani (2003). "Ammonia Hydrogen Carrier for Fuel Cell Based Transportation." SAE International 2003-01-2251.

Gilbert, P. and P. Thornley "Energy and Carbon Balance of Ammonia Production From Biomass Gasification." Tyndall Centre, Department of Mechanical, Aerospace and Civil Engineering (University of Manchester) M60 61QD, UK.

Gilbert, P., P. Thornley, S. Alexander and J. Brammer (2009). Biomass gasification for ammonia production. Proc of the International conference on polygeneration Vienna, Austria.

Gill, S. S., G. S. Chatha and A. Tsolakis (2011). "Analysis of reformed EGR on the performance of a diesel particulate filter." International Journal of Hydrogen Energy **36**(16): 10089-10099.

Goto, S., D. Lee, Y. Wakao, H. Honma, M. Mori, Y. Akasaka, K. Hashimoto, M. Motohashi and M. Konno (1999). "Development of an LPG DI Diesel Engine Using Cetane Number Enhancing Additives." SAE International 1999-01-3602.

Graboski, M. S. and R. L. McCormick (1998). "Combustion of fat and vegetable oil derived fuels in diesel engines." Progress in Energy and Combustion Science **24**(2): 125-164.

Grannell, S. M., D. N. Assanis, S. V. Bohac and D. E. Gillespie (2008). "The Fuel Mix Limits and Efficiency of a Stoichiometric, Ammonia, and Gasoline Dual Fueled Spark Ignition Engine." Journal of Engineering for Gas Turbines and Power **130**(4): 042802-042802.

Gross, C. W. and S.-C. Kong (2013). "Performance characteristics of a compression-ignition engine using direct-injection ammonia–DME mixtures." Fuel **103**(0): 1069-1079.

Grossale, A., I. Nova and E. Tronconi (2008). "Study of a Fe–zeolite-based system as NH3-SCR catalyst for diesel exhaust aftertreatment." Catalysis Today **136**(1–2): 18-27.

Grossale, A., I. Nova and E. Tronconi (2009). "Ammonia blocking of the "Fast SCR" reactivity over a commercial Fe-zeolite catalyst for Diesel exhaust aftertreatment." Journal of Catalysis. **265**(2): 141-147.

Gusakov, S. V., P. R. Valjeho Maldonado, I. V. Epifanov and L. Espinosa (2008). "Use of natural gas-dimethyl ether mixture as fuel for HCCI process in internal combustion engines." Chemical and Petroleum Engineering **44**(9-10): 510-513.

Hall-Roberts, V. J., A. N. Hayhurst, D. E. Knight and S. G. Taylor (2000). "The origin of soot in flames: is the nucleus an ion?" Combustion and Flame **120**(4): 578-584.

Hauff, K., U. Tuttlies, G. Eigenberger and U. Nieken (2012). "Platinum oxide formation and reduction during NO oxidation on a diesel oxidation catalyst - Experimental results." Applied Catalysis B: Environmental **123-124**: 107-116.

Heck, R. M. and R. J. Farrauto (2001). "Automobile exhaust catalysts." Applied Catalysis A: General **221**(1–2): 443-457.

Heck, R. M., R. J. Farrauto and S. T. Gulati (2002). Catalytic Air Pollution Control. 2nd Edition Newyork, John Wiley.

Hellman, A. and H. Grönbeck (2009). "First-Principles Studies of NOx Chemistry on Agn/α-Al2O3." The Journal of Physical Chemistry C **113**(9): 3674-3682.

Herreros, J. M., S. S. Gill, I. Lefort, A. Tsolakis, P. Millington and E. Moss (2014). "Enhancing the low temperature oxidation performance over a Pt and a Pt–Pd diesel oxidation catalyst." Applied Catalysis B: Environmental **147**(0): 835-841.

Heywood, J. B. (1988). Internal combustion engine fundamentals New York, Mc Graw - Hill.

Heywood, J. B. (1988). Internal combustion engine fundamentals. Singapore, McGraw-Hill.

Hill, N., T. Hazeldine, V. J. Einem, A. Pridmore and D. Wynn (2009). "EU transport GHG: routes to 2050?" Alternative energy carriers and powertrains to reduce GHG from transport (Paper 2), European Commission

Hori, M., Y. Koshiishi, N. Matsunaga, P. Glaude and N. Marinov (2002). "Temperature dependence of NO to NO2 conversion by n-butane and n-pentane oxidation." Proceedings of the Combustion Institute **29**(2): 2219-2226.

Houel, V., P. Millington, R. Rajaram and A. Tsolakis (2007). "Fuel effects on the activity of silver hydrocarbon-SCR catalysts." Applied Catalysis B: Environmental **73**(1–2): 203-207.

Houel, V., P. Millington, R. Rajaram and A. Tsolakis (2007). "Promoting functions of H2 in diesel-SCR over silver catalysts." Applied Catalysis B: Environmental **77**(1–2): 29-34.

Huff, M., P. M. Torniainen and L. D. Schmidt (1994). "Partial oxidation of alkanes over noble metal coated monoliths." Catalysis Today **21**(1): 113-128.

IFA (2008). 2007 Annual Production and International Trade Statistics Series of statisitical reports on the 2007 production capacity, production and international trade of key fertilizers, raw materials and intermediates, International Fertilizer Industry Association.

Ishimatsu, S., T. Saika and T. Nohara (2004). "Ammonia Fueled Fuel Cell Vehicle:The New Concept of a Hydrogen Supply System." SAE International 2004-01-1925.

Ito, T., M. Ueda, T. Matsumoto, T. Kitamura, J. Senda and H. Fujimoto (2003). "Effects of Ambient Gas Conditions on Ignition and Combustion Process of Oxygenated Fuel Sprays." SAE International 2003-01-1790.

Jiménez-Espadafor, F. J., M. Torres, J. A. Velez, E. Carvajal and J. A. Becerra (2012). "Experimental analysis of low temperature combustion mode with diesel and biodiesel fuels: A method for reducing NOx and soot emissions." Fuel Processing Technology **103**(0): 57-63.

Johnson, T. V. (2004). "Diesel Emission Control Technology 2003 in Review." SAE International 2008-01-0069.

Johnson, T. V. (2008). "Diesel Engine Emission and Their Control". New York, Corning Enviromental, Corning Incorporated**:** 26.

Kaewpanha, M., G. Guan, X. Hao, Z. Wang, Y. Kasai, K. Kusakabe and A. Abudula (2014). "Steam co-gasification of brown seaweed and land-based biomass." Fuel Processing Technology **120**(0): 106-112.

Karabektas, M., G. Ergen and M. Hosoz (2014). "The effects of using diethylether as additive on the performance and emissions of a diesel engine fuelled with CNG." Fuel **115**(0): 855-860.

Katare, S. R., J. E. Patterson and P. M. Laing (2007). "Diesel aftertreatment modeling: A systems approach to NOx control." Industrial and Engineering Chemistry Research **46**(8): 2445-2454.

Khair, M. K. (2003). "A Review of Diesel Particulate Filter Technologies." SAE International 2003-01-2303.

Khair, M. K. and W. A. Majewski (2006). "Diesel emission and their control" SAE International

Kim, J. H. and O. C. Kwon (2011). "A micro reforming system integrated with a heat-recirculating micro-combustor to produce hydrogen from ammonia." International Journal of Hydrogen Energy **36**(3): 1974-1983.

Kim, J. H., D. H. Um and O. C. Kwon (2012). "Hydrogen production from burning and reforming of ammonia in a microreforming system." Energy Conversion and Management **56**(0): 184-191.

Kirwan, J. E., A. A. Quader and M. J. Grieve (1999). "Advanced Engine Management Using On-Board Gasoline Partial Oxidation Reforming for Meeting Super-ULEV (SULEV) Emissions Standards." SAE International 1999-01-2927.

Kittelson, D. B. (1998). "Engines and nanoparticles: a review." Journal of Aerosol Science **29**(5–6): 575-588.

Klingstedt, F., K. Arve, K. Eränen and D. Y. Murzin (2006). "Toward Improved Catalytic Low-Temperature NOx Removal in Diesel-Powered Vehicles." Accounts of Chemical Research **39**(4): 273-282.

Klugman, S., M. Karlsson and B. Moshfegh (2007). "A Scandinavian chemical wood pulp mill. Part 1. Energy audit aiming at efficiency measures." Applied Energy **84**(3): 326-339.

Koebel, M., M. Elsener and M. Kleemann (2000). "Urea-SCR: a promising technique to reduce NOx emissions from automotive diesel engines." Catalysis Today **59**(3–4): 335-345.

Koebel, M., M. Elsener and G. Madia (2000). "Reaction Pathways in the Selective Catalytic Reduction Process with NO and NO2 at Low Temperatures." Industrial & Engineering Chemistry Research **40**(1): 52-59.

Koebel, M., G. Madia and M. Elsener (2002). "Selective catalytic reduction of NO and NO2 at low temperatures." Catalysis Today **73**(3–4): 239-247.

Kondratenko, V. A., U. Bentrup, M. Richter, T. W. Hansen and E. V. Kondratenko (2008). "Mechanistic aspects of N2O and N2 formation in NO reduction by NH3 over Ag/Al2O3: The effect of O2 and H2." Applied Catalysis B: Environmental **84**(3–4): 497-504.

Kuntke, P., K. M. Śmiech, H. Bruning, G. Zeeman, M. Saakes, T. H. J. A. Sleutels, H. V. M. Hamelers and C. J. N. Buisman (2012). "Ammonium recovery and energy production from urine by a microbial fuel cell." Water Research **46**(8): 2627-2636.

Kusaka, J., M. Sueoka, K. Takada, Y. Ohgaa, T. Nagasaki and Y. Daisho (2005). "A basic study on a urea - selective catalytic reduction system for a medium - duty diesel engine." International Journal of Engine Research **6**(1): 11-19.

Kusano, K., Wads, ouml and Ingemar (1971). "Enthalpy of Vaporization of Some Organic Substances at 25.0°C and Test of Calorimeter." Bulletin of the Chemical Society of Japan **44**(6): 1705-1707.

Kwon, O. C. and G. M. Faeth (2001). "Flame/stretch interactions of premixed hydrogen-fueled flames: measurements and predictions." Combustion and Flame **124**(4): 590-610.

Löffler, D. G. and L. D. Schmidt (1976). "Kinetics of NH3 decomposition on iron at high temperatures." Journal of Catalysis **44**(2): 244-258.

Ladommatos, N., S. Adelhalim and H. Zhao (2000). "The effects of exhaust gas recirculation on diesel combustion and emissions." International Journal of Engine Research(1): 107-126.

Ladommatos, N., S. M. Adelhalim, H. Zhao and Z. Hu (1998). "The effects of carbon dioxide in exhaust gas recirculation on diesel engine emissions." Proceedings of the institution of Mechanical Engineers, Part D **212**(1): 25-42.

Lambert, C., R. Hammerle, R. McGill, M. Khair and C. Sharp (2004). "Technical Advantages of Urea SCR for Light-Duty and Heavy-Duty Diesel Vehicle Applications." SAE International 2004-01-1292.

Lapuerta, M., O. Armas and A. Gómez (2003). "Diesel Particle Size Distribution Estimation from Digital Image Analysis." Aerosol Science and Technology **37**(4): 369-381.

Lapuerta, M., O. Armas and J. M. Herreros (2008). "Emissions from a diesel–bioethanol blend in an automotive diesel engine." Fuel **87**(1): 25-31.

Lapuerta, M., O. Armas and J. Rodríguez-Fernández (2008). "Effect of biodiesel fuels on diesel engine emissions." Progress in Energy and Combustion Science **34**(2): 198-223.

Lapuerta, M., J. J. Hernández, A. Pazo and J. López (2008). "Gasification and co-gasification of biomass wastes: Effect of the biomass origin and the gasifier operating conditions." Fuel Processing Technology **89**(9): 828-837.

Larrubia, M. A., G. Ramis and G. Busca (2000). "An FT-IR study of the adsorption of urea and ammonia over V2O5–MoO3–TiO2 SCR catalysts." Applied Catalysis B: Environmental **27**(3): L145-L151.

Lefort, I., J. M. Herreros and A. Tsolakis (2014). "Reduction of Low Temperature Engine Pollutants by Understanding the Exhaust Species Interactions in a Diesel Oxidation Catalyst." Environmental Science & Technology **48**(4): 2361-2367.

Li, J., H. Huang, N. Kobayashi, Z. He and Y. Nagai (2014). "Study on using hydrogen and ammonia as fuels: Combustion characteristics and NOx formation." International Journal of Energy Research: n/a-n/a.

Li, X., Z. Xu, C. Guan and Z. Huang (2014). "Effect of injection timing on particle size distribution from a diesel engine." Fuel **134**(0): 189-195.

Liew, C., H. Li, S. Liu, M. C. Besch, B. Ralston, N. Clark and Y. Huang (2012). "Exhaust emissions of a H2-enriched heavy-duty diesel engine equipped with cooled EGR and variable geometry turbocharger." Fuel **91**(1): 155-163.

Liew, C., H. Li, J. Nuszkowski, S. Liu, T. Gatts, R. Atkinson and N. Clark (2010). "An experimental investigation of the combustion process of a heavy-duty diesel engine enriched with H2." International Journal of Hydrogen Energy **35**(20): 11357-11365.

Lilik, G. K., H. Zhang, J. M. Herreros, D. C. Haworth and A. L. Boehman (2010). "Hydrogen assisted diesel combustion." International Journal of Hydrogen Energy **35**(9): 4382-4398.

Liu, S., H. Li, C. Liew, T. Gatts, S. Wayne, B. Shade and N. Clark (2011). "An experimental investigation of NO2 emission characteristics of a heavy-duty H2-diesel dual fuel engine." International Journal of Hydrogen Energy **36**(18): 12015-12024.

Lyubovsky, M., S. Roychoudhury and R. LaPierre (2005). "Catalytic partial “oxidation of methane to syngas” at elevated pressures." Catalysis Letters **99**(3-4): 113-117.

Mallens, E. P. J., J. H. B. J. Hoebink and G. B. Marin (1997). "The Reaction Mechanism of the Partial Oxidation of Methane to Synthesis Gas: A Transient Kinetic Study over Rhodium and a Comparison with Platinum." Journal of Catalysis **167**(1): 43-56.

Marquevich, M., R. Coll and D. Montané (2000). "Steam Reforming of Sunflower Oil for Hydrogen Production." Industrial & Engineering Chemistry Research **39**(7): 2140-2147.

Marquevich, M., X. Farriol, F. Medina and D. Montané (2001). "Hydrogen Production by Steam Reforming of Vegetable Oils Using Nickel-Based Catalysts." Industrial & Engineering Chemistry Research **40**(22): 4757-4766.

Martin, S. and A. Wörner (2011). "On-board reforming of biodiesel and bioethanol for high temperature PEM fuel cells: Comparison of autothermal reforming and steam reforming." Journal of Power Sources **196**(6): 3163-3171.

Matti Maricq, M. (2007). "Chemical characterization of particulate emissions from diesel engines: A review." Journal of Aerosol Science **38**(11): 1079-1118.

McCormick, R. L., J. D. Ross and M. S. Graboski (1997). "Effect of Several Oxygenates on Regulated Emissions from Heavy-Duty Diesel Engines." Environmental Science & Technology **31**(4): 1144-1150.

Miller Jothi, N. K., G. Nagarajan and S. Renganarayanan (2008). "LPG fueled diesel engine using diethyl ether with exhaust gas recirculation." International Journal of Thermal Sciences **47**(4): 450-457.

Miyamoto, N., H. Ogawa and M. N. Nabi (2000). "Approaches to extremely low emissions and efficient diesel combustion with oxygenated fuels " International Journal of Engine Research **1**(1): 71-85.

Monyem, A. and J. H. Van Gerpen (2001). "The effect of biodiesel oxidation on engine performance and emissions." Biomass and Bioenergy **20**(4): 317-325.

Moore Jr, P. A., T. C. Daniel, D. R. Edwards and D. M. Miller (1995). "Effect of chemical amendments on ammonia volatilization from poultry litter." Journal of Environmental Quality **24**(2): 293-300.

Naber, J. D. and D. L. Siebers (1998). "Hydrogen combustion under diesel engine conditions." International Journal of Hydrogen Energy **23**(5): 363-371.

Nahar, G. A. (2010). "Hydrogen rich gas production by the autothermal reforming of biodiesel (FAME) for utilization in the solid-oxide fuel cells: A thermodynamic analysis." International Journal of Hydrogen Energy **35**(17): 8891-8911.

Neeft, J. P. A., O. P. van Pruissen, M. Makkee and J. A. Moulijn (1997). "Catalysts for the oxidation of soot from diesel exhaust gases II. Contact between soot and catalyst under practical conditions." Applied Catalysis B: Environmental **12**(1): 21-31.

Ng, P. F., Li, S. Wang, Z. Zhu, G. Lu and Z. Yan (2007). "Catalytic Ammonia Decomposition over Industrial-Waste-Supported Ru Catalysts." Environmental Science & Technology **41**(10): 3758-3762.

Nichols, K., L. Thompson and H. Empie (1993). "A review of NOx formation mechanism in recovery furnaces." Tappi Journal **76**(1): 119-139.

Nord, K. E. and D. Haupt (2005). "Reducing the Emission of Particles from a Diesel Engine by Adding an Oxygenate to the Fuel." Environmental Science & Technology **39**(16): 6260-6265.

Pârvulescu, V. I., P. Grange and B. Delmon (1998). "Catalytic removal of NO." Catalysis Today **46**(4): 233-316.

Pandey, P., B. P. Pundir and P. K. Panigrahi (2007). "Hydrogen addition to acetylene–air laminar diffusion flames: Studies on soot formation under different flow arrangements." Combustion and Flame **148**(4): 249-262.

Pearsall, T. J. and C. G. Garabedian (1967). "Combustion of Anhydrous Ammonia in Diesel Engines." SAE International .

Plana, C., S. Armenise, A. Monzón and E. García-Bordejé (2010). "Ni on alumina-coated cordierite monoliths for in situ generation of CO-free H2 from ammonia." Journal of Catalysis **275**(2): 228-235.

Prasad, V., A. M. Karim, A. Arya and D. G. Vlachos (2009). "Assessment of Overall Rate Expressions and Multiscale, Microkinetic Model Uniqueness via Experimental Data Injection: Ammonia Decomposition on Ru/γ-Al2O3 for Hydrogen Production." Industrial & Engineering Chemistry Research **48**(11): 5255-5265.

Reiter, A. J. and S.-C. Kong (2008). "Demonstration of Compression-Ignition Engine Combustion Using Ammonia in Reducing Greenhouse Gas Emissions." Energy & Fuels **22**(5): 2963-2971.

Reiter, A. J. and S.-C. Kong (2011). "Combustion and emissions characteristics of compression-ignition engine using dual ammonia-diesel fuel." Fuel **90**(1): 87-97.

Ribeiro, N. M., A. C. Pinto, C. M. Quintella, G. O. da Rocha, L. S. G. Teixeira, L. L. N. Guarieiro, M. do Carmo Rangel, M. C. C. Veloso, M. J. C. Rezende, R. Serpa da Cruz, A. M. de Oliveira, E. A. Torres and J. B. de Andrade (2007). "The Role of Additives for Diesel and Diesel Blended (Ethanol or Biodiesel) Fuels: A Review." Energy & Fuels **21**(4): 2433-2445.

Richter, H. and J. B. Howard (2000). "Formation of polycyclic aromatic hydrocarbons and their growth to soot—a review of chemical reaction pathways." Progress in Energy and Combustion Science **26**(4–6): 565-608.

Richter, M., U. Bentrup, R. Eckelt, M. Schneider, M. M. Pohl and R. Fricke (2004). "The effect of hydrogen on the selective catalytic reduction of NO in excess oxygen over Ag/Al2O3." Applied Catalysis B: Environmental **51**(4): 261-274.

Richter, M., R. Fricke and R. Eckelt (2004). "Unusual Activity Enhancement of NO Conversion over Ag/Al2O3 by Using a Mixed NH3/H2 Reductant Under Lean Conditions." Catalysis Letters **94**(1-2): 115-118.

Rothrock Jr, M. J., A. A. Szögi and M. B. Vanotti (2013). "Recovery of ammonia from poultry litter using flat gas permeable membranes." Waste Management **33**(6): 1531-1538.

Ryu, K., G. E. Zacharakis-Jutz and S.-C. Kong (2014). "Performance characteristics of compression-ignition engine using high concentration of ammonia mixed with dimethyl ether." Applied Energy **113**(0): 488-499.

Saika, T., M. Nakamura, T. Nohara and S. Ishimatsu (2006). "Study of Hydrogen Supply System with Ammonia Fuel." JSME International Journal Series B Fluids and Thermal Engineering **49**(1): 78-83.

Saito, Y., H. Mitsui, T. Nohara, Y. Aoki and T. Saika (2009). "Hydrogen Generation System with Ammonia Cracking for a Fuel-Cell Electric Vehicle." SAE International 2009-01-1901.

Saravanan, N. and G. Nagarajan (2010). "Performance and emission studies on port injection of hydrogen with varied flow rates with Diesel as an ignition source." Applied Energy **87**(7): 2218-2229.

Saravanan, N., G. Nagarajan, G. Sanjay, C. Dhanasekaran and K. M. Kalaiselvan (2008). "Combustion analysis on a DI diesel engine with hydrogen in dual fuel mode." Fuel **87**(17–18): 3591-3599.

Satterfield, C. N. (1991). Heterogeneous catalysis in industrial practice, 2nd Edition. New York, McGraw-Hill.

Saxena, P. and F. A. Williams (2006). "Testing a small detailed chemical-kinetic mechanism for the combustion of hydrogen and carbon monoxide." Combustion and Flame **145**(1–2): 316-323.

Schlapbach, L. and A. Zuttel (2001). "Hydrogen-storage materials for mobile applications " Nature **114**: 353-358.

Schmidt, L. D. and M. Huff (1994). "Partial oxidation of CH4 and C2H6 over noble metalcoated monoliths." Catalysis Today **21**(2–3): 443-454.

Schott, F. J. P., S. Steigert, S. Zuercher, M. Endisch and S. Kureti (2012). "Reactor design for the evaluation of diesel oxidation catalysts supported by sintered metal filters." Chemical Engineering and Processing: Process Intensification **62**(0): 54-58.

Schriber, T. J. and G. Parravano (1967). "The low temperature oxidation of ammonia over a supported ruthenium catalyst." Chemical Engineering Science **22**(8): 1067-1078.

Seinfeld, J. and S. Pandis (1998). Atmospheric chemistry and physics: from air polution to climate change, John Wiley and Sons, Inc.

Senthil Kumar, M., A. Ramesh and B. Nagalingam (2003). "Use of hydrogen to enhance the performance of a vegetable oil fuelled compression ignition engine." International Journal of Hydrogen Energy **28**(10): 1143-1154.

Shibata, J., K.-i. Shimizu, S. Satokawa, A. Satsuma and T. Hattori (2003). "Promotion effect of hydrogen on surface steps in SCR of NO by propane over alumina-based silver catalyst as examined by transient FT-IR." Phys. Chem. Chem. Phys. **5**(10): 2154-2160.

Shibata, J., K.-i. Shimizu, A. Satsuma and T. Hattori (2002). "Influence of hydrocarbon structure on selective catalytic reduction of NO by hydrocarbons over Cu-Al2O3." Applied Catalysis B: Environmental **37**(3): 197-204.

Shimizu, K.-i. and A. Satsuma (2007). "Reaction Mechanism of H2-Promoted Selective Catalytic Reduction of NO with NH3 over Ag/Al2O3." J. Phys. Chem. C **111**(5): 2259-2264.

Shimizu, K.-i., J. Shibata and A. Satsuma (2006). "Kinetic and in situ infrared studies on SCR of NO with propane by silver–alumina catalyst: Role of H2 on O2 activation and retardation of nitrate poisoning." Journal of Catalysis **239**(2): 402-409.

Shimizu, K.-i., M. Tsuzuki, K. Kato, S. Yokota, K. Okumura and A. Satsuma (2006). "Reductive Activation of O2 with H2-Reduced Silver Clusters as a Key Step in the H2-Promoted Selective Catalytic Reduction of NO with C3H8 over Ag/Al2O3." The Journal of Physical Chemistry C **111**(2): 950-959.

Shudo, T. (2007). "Improving thermal efficiency by reducing cooling losses in hydrogen combustion engines." International Journal of Hydrogen Energy **32**(17): 4285-4293.

Shudo, T., S. Nabetani and Y. Nakajima (2001). "Analysis of the degree of constant volume and cooling loss in a spark ignition engine fuelled with hydrogen " International Journal of Engine Research **2**(1): 81-92.

Siwale, L., L. Kristóf, T. Adam, A. Bereczky, M. Mbarawa, A. Penninger and A. Kolesnikov (2013). "Combustion and emission characteristics of n-butanol/diesel fuel blend in a turbo-charged compression ignition engine." Fuel **107**(0): 409-418.

Smith, B. L., L. S. Ott and T. J. Bruno (2008). "Composition-Explicit Distillation Curves of Diesel Fuel with Glycol Ether and Glycol Ester Oxygenates: Fuel Analysis Metrology to Enable Decreased Particulate Emissions." Environmental Science & Technology **42**(20): 7682-7689.

Starkman, E. S., H. K. Newhall, R. Sutton, T. Maguire and L. Farbar (1966). "Ammonia as a Spark Ignition Engine Fuel: Theory and Application." SAE International.

Stone, R. (1999). Introduction to Internal Combustion Engines, Macmillan press Ltd.

Tamm, S., S. Fogel, P. Gabrielsson, M. Skoglundh and L. Olsson (2013). "The effect of the gas composition on hydrogen-assisted NH3-SCR over Ag/Al2O3." Applied Catalysis B: Environmental **136–137**(0): 168-176.

Tan, P. Q., Z. Y. Hu, K. Y. Deng, J. X. Lu, D. M. Lou and G. Wan (2007). "Particulate matter emission modelling based on soot and SOF from direct injection diesel engines." Energy Conversion and Management **48**(2): 510-518.

Tayyeb Javed, M., N. Irfan and B. M. Gibbs (2007). "Control of combustion-generated nitrogen oxides by selective non-catalytic reduction." Journal of Environmental Management **83**(3): 251-289.

Tennison, P., C. Lambert and M. Levin (2004). "NOx Control Development with Urea SCR on a Diesel Passenger Car." SAE International 2004-01-1291.

Theinnoi, K., S. Sitshebo, V. Houel, R. R. Rajaram and A. Tsolakis (2008). "Hydrogen Promotion of Low-Temperature Passive Hydrocarbon-Selective Catalytic Reduction (SCR) over a Silver Catalyst." Energy & Fuel **22**(6): 4109-4114.

Thomas, J. F., S. A. Lewis, B. G. Bunting, J. M. Storey, R. L. Graves and P. W. Park (2005). "Hydrocarbon Selective Catalytic Reduction Using a Silver-Alumina Catalyst with Light Alcohols and Other Reductants." SAE International 2005-01-1082 .

Traxel, B. E. and K. L. Hohn (2003). "Partial oxidation of methanol at millisecond contact times." Applied Catalysis A: General **244**(1): 129-140.

Tree, D. R. and K. I. Svensson (2007). "Soot processes in compression ignition engines." Progress in Energy and Combustion Science **33**(3): 272-309.

Tsai, W., J. J. Vajo and W. H. Weinberg (1985). "Inhibition by hydrogen of the heterogeneous decomposition of ammonia on platinum." The Journal of Physical Chemistry **89**(23): 4926-4932.

Tsolakis, A. (2006). "Effects on Particle Size Distribution from the Diesel Engine Operating on RME-Biodiesel with EGR." Energy & Fuels **20**(4): 1418-1424.

Tsolakis, A. and S. E. Golunski (2006). "Sensitivity of process efficiency to reaction routes in exhaust-gas reforming of diesel fuel." Chemical Engineering Journal **117**(2): 131-136.

Tsolakis, A. and A. Megaritis (2004). "Catalytic exhaust gas fuel reforming for diesel engines—effects of water addition on hydrogen production and fuel conversion efficiency." International Journal of Hydrogen Energy **29**(13): 1409-1419.

Tsolakis, A., A. Megaritis and S. E. Golunski (2005). "Reaction Profiles during Exhaust-Assisted Reforming of Diesel Engine Fuels." Energy & Fuels **19**(3): 744-752.

Tsolakis, A., A. Megaritis and M. L. Wyszynski (2004). "Low temperature exhaust gas fuel reforming of diesel fuel." Fuel **83**(13): 1837-1845.

Tsolakis, A., A. Megaritis, D. Yap and A. Abu-Jrai (2005). "Combustion Characteristics and Exhaust Gas Emissions of a Diesel Engine Supplied with Reformed EGR." SAE International 2005-01-2087.

Varde, K. S. and G. A. Frame (1983). "Hydrogen aspiration in a direct injection type diesel engine-its effects on smoke and other engine performance parameters." International Journal of Hydrogen Energy **8**(7): 549-555.

Walker, A. P., R. Allansson, P. G. Blakeman, M. Lavenius, S. Erkfeldt, H. Landalv, B. Ball, P. Harrod, D. Manning and L. Bernegger (2003). "The Development and Performance of the Compact SCR-Trap System: A 4-Way Diesel Emission Control System." SAE International 2003-01-0778 .

Wang, D., O. Dewaele, A. M. D. Groote and G. F. Froment (1996). "Reaction Mechanism and Role of the Support in the Partial Oxidation of Methane on Rh/Al2O3." Journal of Catalysis **159**(2): 418-426.

Wang, X., Y. Ge, L. Yu and X. Feng (2013). "Comparison of combustion characteristics and brake thermal efficiency of a heavy-duty diesel engine fueled with diesel and biodiesel at high altitude." Fuel **107**(0): 852-858.

Watanabe, T., K. Kawashima, Y. Tagawa, K. Tashiro, H. Anoda, K. Ichioka, S. Sumiya and G. Zhang (2007). "New DOC for Light Duty Diesel DPF System." SAE International 2007-01-1920.

Webb, J. (2001). "Estimating the potential for ammonia emissions from livestock excreta and manures." Environmental Pollution **111**(3): 395-406.

Westbrook, C. K., W. J. Pitz and H. J. Curran (2006). "Chemical Kinetic Modeling Study of the Effects of Oxygenated Hydrocarbons on Soot Emissions from Diesel Engines†." The Journal of Physical Chemistry A **110**(21): 6912-6922.

White, C. M., R. R. Steeper and A. E. Lutz (2006). "The hydrogen-fueled internal combustion engine: a technical review." International Journal of Hydrogen Energy **31**(10): 1292-1305.

Willand, J., M. Teigeler, F. Wirbeleit, C. Enderle, A. Raab, H. Bockhorn and F. Schmitt (1998). "Selective Non-Catalytic NOx-Reduction in Diesel Engines Using Aqueous Urea." SAE International 982651.

Yamane, K., A. Ueta and Y. Shimamoto (2001). "Influence of physical and chemical properties of biodiesel fuels on injection, combustion and exhuast emission characteristics in a direct injection compression ignition engine." International Journal of Engine Research **2**(4): 249-261.

Yeom, Y. H., M. Li, W. M. H. Sachtler and E. Weitz (2006). "A study of the mechanism for NOx reduction with ethanol on γ-alumina supported silver." Journal of Catalysis **238**(1): 100-110.

Yin, S.-F., Q.-H. Zhang, B.-Q. Xu, W.-X. Zhu, C.-F. Ng and C.-T. Au (2004). "Investigation on the catalysis of COx-free hydrogen generation from ammonia." Journal of Catalysis **224**(2): 384-396.

York, A. P. E., A. Tsolakis, K. H. J. Buschow, W. C. Robert, C. F. Merton, I. Bernard, J. K. Edward, M. Subhash and V. Patrick (2010). Cleaner Vehicle Emissions. Encyclopedia of Material: Science and Technology. Oxford, Elsevier.

Yu, R. and S. Shahed (1981). "Effects of injection timing and exhuast gas recirculation on emission from a DI deisel engine." SAE International **811234**.

Zamfirescu, C. and I. Dincer (2008). "Using ammonia as a sustainable fuel." Journal of Power Sources **185**(1): 459-465.

Zamfirescu, C. and I. Dincer (2009). "Ammonia as a green fuel and hydrogen source for vehicular applications." Fuel Processing Technology **90**(5): 729-737.

Zamfirescu, C. and I. Dincer (2011). "Utilization of hydrogen produced from urea on board to improve performance of vehicles." International Journal of Hydrogen Energy **36**(17): 11425-11432.

Zelenka, P., K. Ostgathe and E. Lox (1990). "Reduction of diesel exhaust emissions by using oxidation catalysts " SAE International **90211**.

Zhang, J., H. Xu and W. Li (2005). "Kinetic study of NH3 decomposition over Ni nanoparticles: The role of La promoter, structure sensitivity and compensation effect." Applied Catalysis A: General **296**(2): 257-267.

Zheng, M., G. T. Reader and J. G. Hawley (2004). "Diesel engine exhaust gas recirculation—a review on advanced and novel concepts." Energy Conversion and Management **45**(6): 883-900.

Zheng, W., J. Zhang, H. Xu and W. Li (2007). "NH3 Decomposition Kinetics on Supported Ru Clusters: Morphology and Particle Size Effect." Catalysis Letters **119**(3-4): 311-318.

Zhuang, J., X. Qiao, J. Bai and Z. Hu (2014). "Effect of injection-strategy on combustion, performance and emission characteristics in a DI-diesel engine fueled with diesel from direct coal liquefaction." Fuel **121**(0): 141-148.